

THE MOLECULAR LANDSCAPE OF G PROTEIN SIGNALING THROUGH THE HUMAN  
LUTEINIZING HORMONE RECEPTOR

by

GENEVA DEMARS

(Under Direction of J. David Puett)

ABSTRACT

The molecular mechanism employed by the human luteinizing hormone receptor (hLHR), a G protein coupled receptor (GPCR) necessary for fertility and reproduction, to couple to its cognate signaling partner, the stimulatory G protein ( $G_s$ ), remains undefined. GPCRs constitute the largest gene family in the human genome (~800-900 genes) yet signal through only a few isoforms of heterotrimeric G proteins. Thus, in general, the translation of activation from GPCR to G protein may exhibit conserved elements that include common points of contact for receptors that activate the same G protein, but unique determinants of the coupling mechanism must define the signaling specificity for each GPCR/G protein pair. This concept challenges the entrenched paradigm of GPCR signaling that was established after experiments with only a few receptor systems. To probe the molecular landscape of hLHR/ $G_s$  signaling, the impact of engineered mutations within the extreme C-terminus (CT) of  $G\alpha_s$ , an area hypothesized as necessary for GPCR/G protein coupling, was tested in a newly-created hLHR<sup>+</sup>/ $G\alpha_s$ <sup>-</sup> model cell system. For comparative purposes, parallel studies were also conducted with the naturally expressed  $\beta_2$ -adrenergic receptor ( $\beta_2$ -AR), a well characterized GPCR. This work initiated the exploration of the  $G\alpha_s$  contribution to the hLHR and  $\beta_2$ -AR signaling interfaces, exposed amino acid residues within the CT of  $G\alpha_s$  that are critical for signal transduction, and characterized these findings within a preliminary mechanism of hLHR/ $G_s$  coupling. In addition, these results support the hypothesis that the network of interactions that define GPCR/G protein coupling is distinctive for each singular relationship. The physiochemical nature

of hLHR limited attempts to further characterize its signaling properties, additionally suggesting that although this homologous family of proteins evolved within a structural constraint to maintain signaling integrity, traits of the individual GPCR may have diverged significantly from those of its cohort. The pharmacological relevance of this work thus extends beyond the potential design of drugs that more precisely treat abnormalities of hLHR signaling to prompt the pharmaceutical industry to target the GPCR/G protein interface as a viable, and perhaps preferred, candidate for drug development to improve the specificity of engineered therapeutics.

THE MOLECULAR LANDSCAPE OF G PROTEIN SIGNALING THROUGH THE HUMAN  
LUTEINIZING HORMONE RECEPTOR

by

GENEVA DEMARS

B.S., The University of Virginia, 1997

A Dissertation Submitted to the Graduate Faculty of The University of Georgia in Partial Fulfillment of  
the Requirements for the Degree

DOCTOR OF PHILOSOPHY

ATHENS, GEORGIA

2010

© 2010

Geneva DeMars

All Rights Reserved



THE MOLECULAR LANDSCAPE OF G PROTEIN SIGNALING THROUGH THE HUMAN  
LUTEINIZING HORMONE RECEPTOR

by

GENEVA DEMARS

Major Professor: J. David Puett

Committee: Shelley Hooks  
Prema Narayan  
Walter Schmidt

Electronic Version Approved:

Maureen Grasso  
Dean of the Graduate School  
The University of Georgia  
May 2010

## TABLE OF CONTENTS

	Page
INTRODUCTION .....	1
RESEARCH GOALS .....	3
CHAPTER	
1 LITERATURE REVIEW .....	4
The biological roles of the luteinizing hormone receptor .....	4
The LHR protein is a G protein coupled receptor.....	9
The molecular structure and function of the LHR protein.....	17
GPCR/G protein coupling and G protein activation .....	28
2 THE EXTREME C-TERMINAL REGION OF $G\alpha_s$ DIFFERENTIALLY COUPLES TO THE HUMAN LUTEINIZING HORMONE AND THE $\beta_2$ -ADRENERGIC RECEPTORS.....	35
Abstract .....	36
Introduction.....	36
Experimental procedures.....	38
Results.....	42
Discussion .....	52
3 THE HUMAN LUTEINIZING HORMONE RECEPTOR EXHIBITS PARTICULAR PHYSIOCHEMICAL PROPERTIES THAT IMPAIR THE CHARACTERIZATION OF ITS SIGNALING ENVIRONMENT.....	60
The use of Förster Resonance Energy Transfer (FRET) to probe the molecular environment proximal to hLHR.....	61
$G\alpha_s$ does not specifically co-immunoprecipitate with hLHR from HEK-293 cells.....	73

The expression of $G\alpha_s$ C-terminal minigenes does not diminish the hLHR signaling response in HEK-293 cells.....	79
A peptide corresponding to the second intracellular loop of hLHR does not inhibit hLHR activity.....	85
The trypsin-protection assay does not discriminate between hLHR-activated and spontaneously –active G protein $\alpha$ subunits .....	90
Non-specific effects of $G\alpha_s$ -targeted RNAi preclude its use to dissect hLHR/ $G_s$ signaling.....	96
Conclusions.....	99
CONCLUSIONS.....	100
REFERENCES .....	102
APPENDIX.....	118

## INTRODUCTION

Cell-surface receptors that signal through G proteins, the G protein coupled receptors (GPCRs), constitute the largest gene family in the human genome as well as a valuable group of pharmacological targets. Evolutionary selection chose the GPCR template to mediate numerous yet diverse physiological functions such as sensory responses, cardiac and vascular activity, neurotransmission, metabolism, pain control, and endocrine signaling; thus, the malfunction of GPCRs disrupts vital biological systems (1). The pathophysiological relevance of this protein group emphasizes the need for a thorough description of GPCR behavior to facilitate rational drug design. Whereas the molecular relationship between GPCRs and their external stimuli has been the focus of much research and pharmacological therapy, the overlooked GPCR/G protein interface is emerging as a promising area for pharmaceutical attention (2). For example, highly homologous GPCRs that bind the same ligand may stimulate different G protein pathways (2,3), and therefore drugs engineered to act at the extracellular or transmembrane domains of the receptor may produce off-target effects. The interactions that compose the contour of each GPCR/G protein association must thus tailor a distinct interface that, when targeted, offers the promise of greater control over drug specificity.

The human luteinizing hormone receptor (hLHR), a GPCR, is essential for fertility and reproduction as hLHR stimulation acutely enhances steroidogenesis and up-regulates the expression of enzymes that are required for the continued synthesis of sex steroid hormones. Therefore, aberrant hLHR signaling leads to reproductive pathologies that may impair sexual differentiation and/or fertility. Gain-of- or loss-of-function mutations within the receptor may release its activity from the control of the hypothalamic-pituitary-gonadal axis and thus cause hLHR malfunction (4-8). The existing treatments for many of the ensuing pathologies include the administration of aromatase inhibitors and anti-androgens (9) to regulate the system and thus do not directly act upon the mutant receptors. Although these therapies are

adequate, a thorough description of the molecular environment of hLHR signaling should permit the translation of this basic scientific information to support the design of more effective treatments for diseases resulting from abnormal or absent hLHR activity. Specifically, the interface between the receptor and its cognate signaling partner, the stimulatory G protein,  $G_s$ , may provide an appropriate platform for pharmaceutical intervention.

This document chronicles efforts to elucidate more detailed, basic scientific information about the molecular environment of hLHR signaling to encourage its translation to clinical utility. An introductory review of the relevant literature presents the appropriate context for analysis and interpretation of the studies. It discusses the general properties of GPCR function and the evidence that GPCR activity occurs within ‘receptosomes’, the biological roles of the hLHR and the influence the hLHR structure asserts over its function, and the molecular details of GPCR/G protein coupling and the proposed mechanisms for G protein activation. The second chapter describes novel work that explored the contribution of  $G\alpha_s$  to the hLHR/ $G_s$  signaling interface and reported noteworthy differences between the mechanisms of hLHR/ $G_s$  and  $\beta_2$ -adrenergic receptor/ $G_s$  coupling. These results imply that the GPCR/G protein interface may be unique for each GPCR/G protein pair, an idea that underlies a paradigm shift from the accepted view of GPCR/G protein coupling.

The third chapter documents the resistance of hLHR to analysis with published techniques that probe the proximal signaling environment of GPCRs. The observations raise the possibility that certain physiochemical properties render hLHR unsuitable for these types of evaluation with the current methodologies and suggest caution when considering the extrapolation of findings from one GPCR system to another. Although G protein signaling pathways were selected, and thus preserved, to govern numerous, different, and vital physiological systems, the heterogeneity acquired within the conservation of the GPCR architecture may have generated an unanticipated diversity of GPCR character. This chapter is followed by a general conclusion that unites the mutual themes described in this document and addresses the future implications of the work.

## RESEARCH GOALS

- 1) to identify residues within  $G\alpha_s$  that are important for coupling to hLHR
- 2) to determine how implicated residues of  $G\alpha_s$  associate with hLHR prior to and during activation
- 3) to determine how residues of hLHR identified as important for  $G_s$  coupling impact the association of hLHR with  $G\alpha_s$
- 4) to monitor the self-association of hLHR with itself prior to and during activation
- 5) to determine the relevance of hLHR self-association with  $G_s$  coupling
- 6) to describe a mechanism that details the coupling of hLHR and  $G_s$

## CHAPTER 1

### LITERATURE REVIEW

#### *The biological roles of the luteinizing hormone receptor*

The luteinizing hormone receptor (LHR) is necessary for human reproduction because it preserves the homeostasis of the hypothalamic-pituitary-gonadal (HPG) axis, a complex and tightly-regulated endocrine network. Specifically, LHR signaling contributes to male sexual differentiation, the onset and progression of puberty, gonadal function (including gametogenesis and steroidogenesis), and the maintenance of the first trimester of pregnancy. Therefore, malfunction of the LHR signaling pathway may cause infertility and/or other serious reproductive pathologies (4-7).

The LHR protein is primarily expressed upon the surface of the Leydig cells of the testes and the theca, granulosa, and cororal luteal cells of the ovary. The LHR binds two gonadotropin hormones with high affinity: luteinizing hormone (LH) derived from the pituitary, and choriogonadotropin (CG) secreted by the trophoblasts of the developing placenta (10). When activated, LHR signaling through the stimulatory G protein  $G_s$  then triggers acute steroidogenesis and the expression of key steroidogenic enzymes in the gonads that produce sex steroid hormones. These androgens, estrogens, and progestins then circulate throughout the body to induce physiological response, and importantly, they also act to regulate the HPG axis through feedback mechanisms (6).

This section briefly summarizes the biological importance of the LHR; a plenary and sapient understanding of human reproductive physiology, however, appropriately threads the specific contributions of LHR activity within the tapestry of molecular and physiological events essential for human fertility and reproduction.

### *Sexual differentiation and LHR*

LHR activity is essential for the sexual differentiation of 46XY individuals. The process of sexual development begins during the seventh week of pregnancy (11). In the following week, human choriogonadotropin (hCG) secreted by the placenta circulates to the 46XY fetus and binds to LHRs expressed upon the surface of fetal Leydig cells. LHR signaling then generates the high concentrations of androgens in the fetal serum necessary to stimulate testicular development, and later, the development of male external genitalia (12,13).

If, during this critical period of gestation, LHR activity is absent or greatly reduced, the high serum levels of androgens necessary for virilization are absent. Subsequently, the feminizing process is not suppressed, and by default, the individual displays some feminine secondary sex characteristics and is infertile (5-7,11). Individuals with Leydig cell hypoplasia harbor two copies of the LHR gene with mutations that impair or completely inhibit LHR activity and, therefore, they exhibit this phenotype, which may range in severity from very mild undervirilization to complete pseudohermaphroditism. One wild-type copy of the LHR gene is sufficient to produce a normal phenotype, and thus this disease displays a recessive inheritance pattern (5,7). Impaired or abrogated LHR activity in these individuals interrupts normal sexual differentiation *in utero* as well as, later, normal pubertal development and gonadal function (14).

### *Puberty and LHR*

In children, the feedback inhibition exerted upon the HPG axis by circulating sex steroids suppresses the blood levels of the pituitary gonadotropins LH and FSH (follicle stimulating hormone). The absence of high LH and FSH concentrations prevents the induction of gonadal function and thus the onset of puberty. The pre-pubertal rise in the blood concentration of these gonadotropins results from changes in the sensitivity of the HPG axis to stimuli. As children approach puberty, the restraints of the feedback inhibition weaken as the hypothalamus becomes less sensitive to the sex steroid hormones. It then secretes more gonadotropin-releasing hormone (GnRH) to stimulate an increasingly GnRH-sensitive



pituitary gland to produce more LH and FSH. The affinity of LHR for LH is high, and LHR responds quickly to the increased availability of its ligand. In concert with other newly-activated pathways, LHR signaling directs the gonads to produce the high levels of estrogens, androgens, and other hormones necessary to stimulate pubertal changes which include the maturation of the gonads and accessory structures, menarche and ovulation in females, the development of secondary sexual characteristics, and the growth of bones and muscle (11,15,16).

Therefore, mutations within the LHR gene that affect its activity may disturb normal pubertal development. An absence of LHR activity in 46XY individuals, as described above, disrupts fetal sexual differentiation, and not surprisingly, these individuals do not progress through recognizable stages of pubescent development. For 46XX females expressing two copies of LHR with inactivating mutations, a milder phenotype results. The primary and secondary sexual characteristics of these individuals are approximately normal, although some irregularities in the structure and function of some organs and bones are observed and are attributable to a decreased presence of estrogen. Importantly, menarche is never reached, and as normal LHR function is essential for ovulation and menstruation (see below), the amenorrhea observed in these individuals signifies infertility. Again, one wild-type copy of the LHR gene is sufficient to produce normal phenotypes in all individuals harboring this type of mutated gene (5,7,14).

46XY individuals bearing mutations in LHR that cause constitutive activity display a dramatic phenotype known as a pituitary-independent precocious puberty, or familial male-limited precocious puberty (FMPP). These mutations release LHR from the grip of the HPG axis, and the premature and unchecked production of near adult-like levels of androgens stimulates the developmental changes associated with puberty in affected children at very young ages (three to four years). FMPP follows an autosomal-dominant inheritance pattern as one copy of a constitutively-activated LHR suffices to produce the phenotype. Interestingly, 46XX individuals with constitutively-activating LHR mutations appear to progress normally towards and through puberty, suggesting that the onset of puberty in genotypic males is more sensitive to LHR activity than for females (5,7,14).

### *Gondal function, including gametogenesis, and LHR*

Small arteries and capillaries feed the interstitial spaces between the seminiferous tubules of the testes and deliver circulating LH to LHRs expressed upon the surface of Leydig cells. Leydig cells, after LHR stimulation, synthesize and secrete 95% of androgens in the adult human male, and a small network of veins in the interstitial spaces absorb the hormones for delivery throughout the body. Importantly, testosterone also diffuses through the basement membranes of the seminiferous epithelium into the tubule lumen. The availability of testosterone to the immature male germ cells and Sertoli cells that line the tubule interior initiates spermatogenesis. After spermatogonia mature to sperm and spermatogenesis is complete, the release of mature sperm heads from the bed of Sertoli cells, or spermiation, requires testosterone. Because LH release from the male pituitary remains relatively constant, sperm production is continuous (11,17).

The periodic rise and fall of circulating LH levels in the adult female regulates the menstrual cycle and ovulation. During the early- to mid-follicular stage of the cycle, theca cells of growing follicles express LH receptors that bind LH and signal the upregulation of the steroidogenic  $\Delta^5$  pathway for androgen synthesis. Neighboring granulosa cells convert these androgens to estradiol and other estrogens. As theca cells multiply within growing follicles and as the levels of circulating LH increase, more estrogens are produced. The rising levels of estrogens initiate physiological change throughout the body and promote the growth, development, selection, and atresia of follicles in the ovary (11,18-20).

In the mid- to late-follicular stage, granulosa cells of tertiary and Graafian follicles begin to express LHR, and LHR activity primes the oocyte for ovulation. The hypothalamus and pituitary react to a peak of estradiol levels to produce a surge in circulating LH at day 12-13 after menstruation. 9-12 hours after the LH surge, ovulation occurs and the granulosa cells of the ruptured follicle begin to luteinize as the follicle transforms into a corpus luteum (CL) (11,18-20).

During the luteal phase, stimulated LHR receptors on the luteal cells of the CL initiate the  $\Delta^4$  pathway of steroidogenesis to produce a very high level of progesterone and a moderate amount of

estradiol. These hormones stimulate the uterine endometrium to prepare for the implantation of an embryo. If fertilization does not occur, the CL degenerates, sex steroid levels fall, and the cycle begins anew with the menstrual phase (11,18,21).

#### *Pregnancy and LHR*

If, however, the oocyte is fertilized and the embryo implants into the uterine wall, protracted, elevated progesterone levels are critical for the maintenance of the nascent pregnancy, and thus luteolysis must be avoided. LHR signaling rescues the CL by binding an alternate ligand, hCG, secreted by the trophoblasts of the embryo and developing placenta. The CL is then able to generate enough progesterone to maintain the pregnancy until the placenta can supplant this function of the CL at approximately week 7 of fetal development, after which, the CL undergoes luteolysis (11,22).

#### *Ovarian cancer and LHR*

After menopause and the cessation of ovarian function, circulating levels of LH and FSH are released from the feedback regulation imposed by the HPG axis, and the serum concentrations of the pituitary hormones rise to 3-4 and 10-20 fold, respectively, of those measured during the proliferative phase of the menstrual cycle (23). The Gonadotropin Theory of ovarian epithelial cancer (OEC) pathogenesis suggests that the concomitant elevation of gonadotropin serum levels and the significantly increased occurrence of OEC in post-menopausal women may be related (24-26). Although genetic mutations of LHR and FSHR (FSH receptor) are not implicated in ovarian tumorigenesis (27), a relationship between the expression of the gonadotropin receptors and the development of ovarian cancer may exist (24,28). The very high levels of LH and FSH may facilitate neoplastic transformation by eliciting an inflammatory-like response from the ovarian epithelium, not unlike that observed during ovulation (26). The Incessant Ovulation and Inflammatory Theories of OEC etiology also implicate an inflammatory microenvironment for the ovarian epithelium but do not emphasize a role for post-menopausal gonadotropin signaling. Nevertheless, none of the proposed hypotheses for OEC

pathogenesis reconcile all of the molecular and epidemiological data, and therefore evidence supporting the Gonadotropin Theory remains germane to ovarian cancer research (24,26).

### ***The LHR protein is a G protein coupled receptor***

#### *The relevance of GPCRs*

The LHR protein is a member of one of the largest and most versatile protein families encoded within the human genome, the superfamily of G protein coupled receptors (GPCRs) (10,29,30). GPCR proteins appeared before the separation of plants, animals, and fungi, and the evolutionary preference for the GPCR signaling paradigm has encouraged enormous sequence diversity for these proteins within the constraint of a highly-conserved structural motif (29,31). Thus, the GPCR family recognizes an assortment of ligand types (such as photons, ions, organic odorants, nucleotides, amines, peptides, proteins, lipids, and proteases) and regulates a variety of physiological systems, including sensory stimulation, cardiac and vascular function, neurotransmitter signaling, metabolism, pain control, and endocrine signaling (1,30). Because of this nearly ubiquitous participation in human physiology and the extensive pathophysiological relevance of this protein family, GPCRs represent a significant portion (some reports claim as much as 50%) of pharmaceutical targets (32-35).

#### *The general molecular structure of GPCRs*

Seven transmembrane-spanning alpha helices are the defining structural characteristic that led researchers to uncover the existence of the GPCR superfamily (1). Three extracellular and three intracellular loops link the helices, and a network of hydrogen bonds and salt bridges, strengthened within the hydrophobic membrane milieu, stabilize the helices counter-clockwise into a tightly-packed bundle (30,31). A recent, more sophisticated phylogenetic analysis of GPCR transmembrane domains updated the classical categorization of this superfamily (classes A (rhodopsin-like), B (secretin-like), and C (glutamate-like)) and identified five groups, termed GRAFS (for glutamate, rhodopsin, adhesion, frizzled and secretin) (29). An evaluation that included all domains of GPCR sequences revealed that the

extracellular N-terminal length, the third intracellular loop, and the intracellular C-terminus exhibit the most sequence diversity between receptors (31). Upon stimulation, all GPCRs, regardless of GRAFS classification and of ligand type, shift the helical bundle from an inactive conformation to one that translates activation to apposing signaling partners (1,30,31).

### *The molecular landscape of GPCR signaling*

Historically, the heterotrimeric guanine-nucleotide binding proteins, the G proteins, were accepted as the cognate signaling partners of GPCRs. The simple assertion, however, that ‘a GPCR acts through a G protein to generate a signal’ masks the underlying complexity that is necessary for the intricate signaling specificity of this large protein family. For example, when GPCRs activate G proteins, both  $G\alpha$  and  $G\beta\gamma$  subunits may stimulate effectors for response. Also, the discovery that GPCRs may activate multiple families of G proteins and that certain ligands exploit this pleiotropy to selectively generate specific responses exposed the GPCR/G protein relationship as a tightly-regulated network rather than a straightforward linear pathway (36-39).

In fact, this network contains numerous types of molecular species besides G proteins. These ligands, signaling partners, and various GPCR interacting proteins (GIPs) such as GPCR kinases (GRKs), arrestins, Src-family tyrosine kinases, PDZ domain containing proteins, chaperones, and receptor activity modifying proteins (RAMPs), may affect GPCR conformation and/or localization and thus may significantly affect GPCR activity (40-43). Importantly, it is now known that GPCRs may also activate G protein independent signaling pathways (such as the MAP kinase cascade) which has prompted a change in nomenclature for this family from ‘G protein coupled receptors (GPCRs)’ to ‘Seven Transmembrane Receptors (7TMRs)’ to emphasize the common structural motif rather than an isolated behavioral characteristic of the protein family<sup>1</sup> (1,29,44-46). In addition, to diversify their pharmacologic

---

<sup>1</sup> This document uses the canonical GPCR designation because its focus is the interaction of LHR with its preferred signaling partner, the stimulatory G protein,  $G_s$ .

responses, certain GPCRs (e.g. glutamate-like) traffic and function as obligate homo- and heterodimers, and some may signal as higher-order oligomers. Evidence suggests that all GPCRs may self-associate, but conflicting data indicates that this ‘blanket’ conclusion for the entire GPCR family may be misguided. The physiological relevance of self-association is also disputed in many cases (31,47).

The molecular landscape of GPCR signaling is densely populated with molecules that may impose allosteric influence, link GPCR activation with other signaling pathways, and/or affect receptor expression, trafficking, and/or desensitization. Ultimately, this complex environment, under strict spatial and temporal regulation, empowers GPCRs to appropriately recognize extracellular stimuli and translate this signaling information across the cellular membrane for intracellular evaluation and response (30,41).

### *Models of GPCR signaling*

After decades of study, researchers have yet to define a model to characterize the molecular landscape of GPCR signaling that satisfies the empirical data as well as principles of pharmacologic theory (48,49). The Classical (Two-State) Model (Figure 1.1A) for ligand-induced receptor activation—that receptors are “active” (agonist-bound) or “inactive” (empty)—could not explain the low- and high-affinity agonist-binding GPCR states identified by researchers. Scientists then determined that the intracellular GPCR signaling partner, the G protein, may directly influence the affinity of the receptor for agonist. The Ternary Complex Model (TCM) (Figure 1.1B) was constructed to recognize that a coupled receptor/G protein pair may bind agonist with higher affinity than an uncoupled receptor (48,50). Later, using over-expression cellular systems, researchers measured basal levels of GPCR activity that correlated with receptor density and discovered ligands that act as inverse agonists, a phenomenon not defined by the TCM. The TCM was edited in the Extended Ternary Complex Model (ECM) (Figure 1.1C) to suggest that receptors may spontaneously switch between “inactive” and “active” conformations without external stimuli, and thus this model explains activity in a ‘resting’ system. Also, inverse agonists are viewed within the ECM to shift the equilibrium of the system towards the inactive state

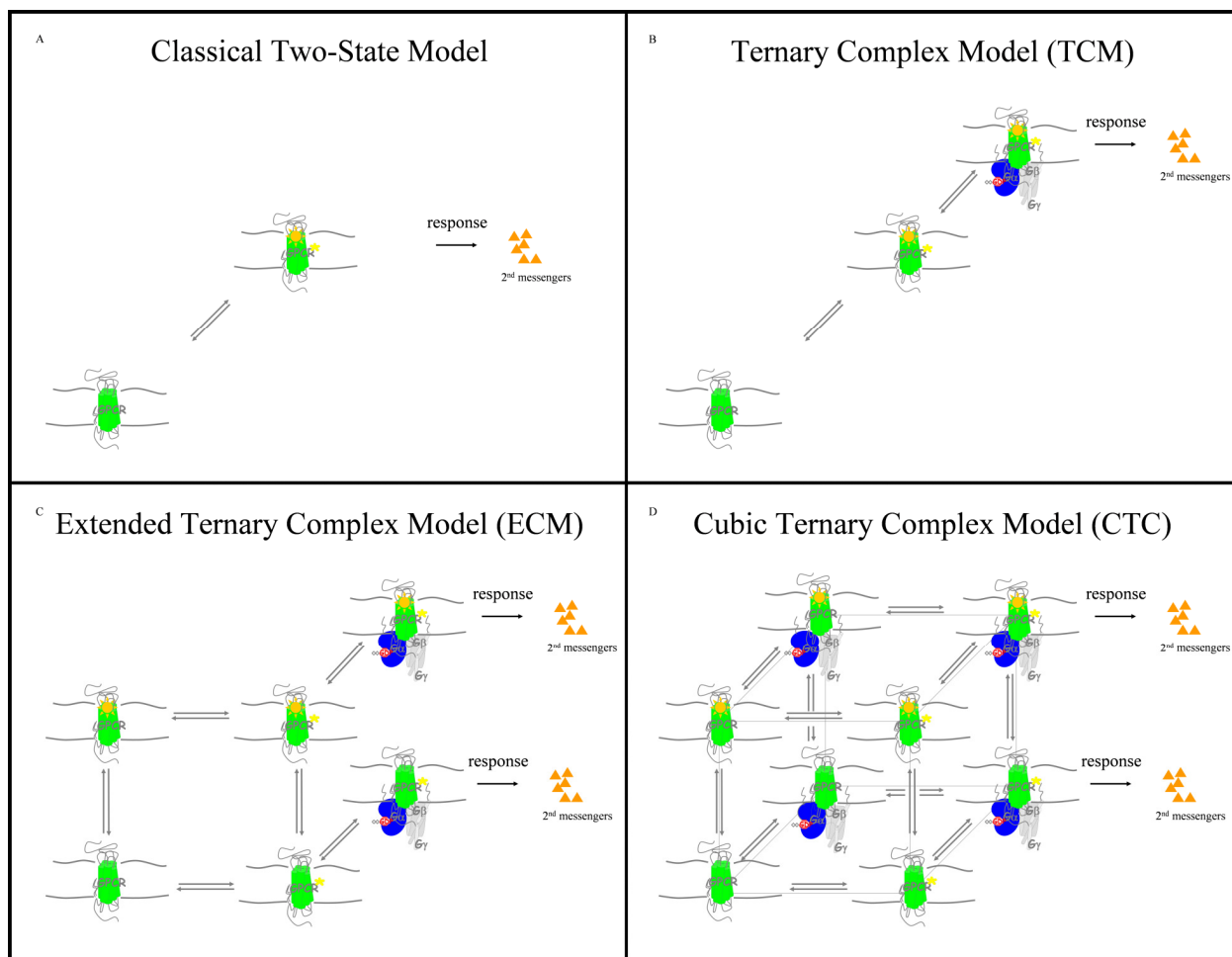


**Figure 1.1.** Cartoons represent the two-state model of GPCR signaling and its variants. The green seven transmembrane helical bundle represents the **GPCR**, the orange sun represents **ligand**, the yellow star represents an **active GPCR**, orange triangles represent the signaling **response** as measured by second messengers, and the blue (the **G $\alpha$  subunit**, with an associated red **GDP** molecule) and gray (the **G $\beta\gamma$  subunits**) cartoons represent the heterotrimeric G protein. For simplicity, affinity and allosteric constants that describe the relationships between complexes are not included. **A.** The classical representation of a two-state model of receptor activation defines inactive and active receptor states. **B.** The Ternary Complex Model (TCM) expands the classical model by suggesting that the G protein signaling partner affects the receptor affinity for ligand. **C.** The Extended Ternary Complex Model (ECM) explains basal receptor activity. **D.** The Cubic Ternary Complex Model (CTC) presents more complete relationships between receptor, ligand, and G protein. Adapted from (48) and (51).

(48,52). The Cubic Ternary Complex Model (CTC) (Figure 1.1D) is a later refinement of the ECM that addresses the thermodynamic relationships between ligand, inactive receptor, active receptor, and G protein (48,53).

These models, however, do not reflect the structural plasticity of the GPCR proteins: they recognize only two conformations of receptor, “active” and “inactive”. It is now generally accepted that GPCRs may sample a spectrum of conformational states (54); therefore, an interaction with ligand, signaling partner, associated protein, and/or another receptor may distinctly bias the distribution of receptor states within the conformational space. This probabilistic view of GPCR complexation reflects the behavioral dimensionality of GPCRs and the allosteric influence other molecules may exert upon GPCR activity (48,49,55).

Receptor theory once confined the components of and mechanisms underlying GPCR signaling to an ill-defined molecular “black box”, but, during the last 25 years, researchers have applied increasingly sophisticated molecular biology tools to dissect these fundamental yet complex phenomena of GPCR functionality. Because this work has yet to exhaustively describe the molecular landscape of GPCR activity, any models of the processes remain incomplete (48,49,55).

#### *The advantages and flaws of rhodopsin as a representative GPCR*

Although aware of functional similarities (G protein coupling, e.g.), rhodopsin was not viewed as a receptor during the early years of its study, and therefore was not considered a GPCR until sequence analysis suggested that the protein exhibits the hallmark seven transmembrane-spanning alpha helices of GPCRs. This discovery exposed an overlooked wealth of information for researchers. Because the rod outer membranes of the bovine retina contain an abundance of nearly homogeneous rhodopsin, scientists have exploited this natural source to perform many biochemical and structural analyses unavailable to other GPCR systems that are limited by the amount of available purified material. Rhodopsin became the template and namesake for the family of homologous GPCRs (the largest of the GPCR classes), and GPCR scientists have often since assumed that ‘as rhodopsin goes, so goes the GPCR’. Rhodopsin studies have thus illuminated much about GPCR function, but accumulating, conflicting evidence has prompted researchers to question the validity of rhodopsin-based models for the behavior of homologous GPCRs (1,56).



For example, together, the crystal ‘snapshots’ of the structures of native, dark-adapted rhodopsin, its subsequent refinements, its photo-responsive intermediates, and active forms depict a molecular progression of rhodopsin activation. These data strongly suggest that very slight rearrangements of the chromophore binding site lead to pronounced functional changes (57). Until the recent solution of the recombinant turkey  $\beta_1$ -adrenergic, human  $\beta_2$ -adrenergic, and the human A2A-adenosine receptor structures, rhodopsin was the only available template for GPCR homology modeling (57-61). Although the RMSDs of the alignment between rhodopsin and the other GPCR structures are notably low ( $< 4.5\text{\AA}$ ), subtle but relevant differences exist. The global architecture of these proteins appears quite similar, but importantly, the sites for ligand recognition reveal distinct topologies that dictate ligand specificity. These comparisons emphasize the need for reliable and precise structural data for individual GPCRs, preferably isolated from native tissue, to guide effective, rational drug design (57,62,63).

Purified rhodopsin and transducin ( $G_t$ ) dissociate upon rhodopsin activation *in vitro* (as do the transducin  $\alpha$  and  $\beta\gamma$  subunits from each other) (64,65). This is the evidence underlying the textbook model of GPCR/G protein activation. Although G protein dissociation may occur under extreme experimental conditions, these proteins may behave differently in a physiological environment. Notably, contradictory biochemical data exist to repudiate this “dissociation” model (66,67), including kinetic data that suggest the proteins are tightly associated throughout signal transduction, as inferred from the 1<sup>st</sup>-order kinetics of effector activation—dissociation of the proteins (heterotrimeric G protein from GPCR and  $G\alpha$  from  $G\beta\gamma$ ) should produce a complex kinetic pattern that is not observed (68-71). Recent evidence from resonance energy transfer experiments with live cells and from *in vitro* co-immunoprecipitation experiments complements the older, contrary data to suggest that the entrenched paradigm should undergo revision to represent a mechanism that does not depict protein dissociation. The discrepancies that exist, however, between the results from different GPCR/G protein pairs will delay any immediate changes to the accepted model; perhaps a precise description of the spectrum of GPCR/G protein signaling should encompass more than one mechanism of activation (72-78).

Biochemical experiments with light-activated rhodopsin suggest a two-step mechanism for the coupling of transducin that begins with an initial recognition of the farnesylated G $\gamma$  C-terminus (CT) which then aligns the G $\alpha_t$  CT within proximity of the coupling interface of the receptor. The association of rhodopsin with the G $\alpha_t$  CT then triggers the conformational rearrangement of the G $\alpha_t$  subunit which in turn promotes the release of GDP and the ensuing nucleotide exchange event that denotes G protein activation (79,80). The crystal structures of G $\alpha$  reveal a 'kink' in the middle of the  $\alpha 5$  helix of G $\alpha_s$  (absent in G $\alpha_t$  and other G $\alpha_{i/o}$  isoforms) that may expose its extreme CT for receptor recognition and thus obviate the need for G $\beta\gamma$ -mediated presentation of the G $\alpha_s$  CT (81). Therefore, the two-step mechanism of activation may not be universal for the GPCR family. Also, the N-terminus (NT) of G $\alpha_t$  interacts with rhodopsin, but the NT of G $\alpha_s$  is not part of the receptor-coupling interface (82-85). In addition, the G $\alpha_t$   $\alpha 4$ - $\beta 6$  loop is a site of rhodopsin contact, but the homologous region in G $\alpha_s$  does not participate in  $\beta_2$ -AR receptor signaling (83,86-89).

Importantly, the analysis of native bovine rod outer-segment disk membranes with atomic force microscopy suggests that dimers of rhodopsin organize in a uniform pattern (90) but reconstitution experiments demonstrate that a monomer of rhodopsin is sufficient to activate a single heterotrimeric transducin complex (91). A model of heterotrimeric transducin docked to dimeric rhodopsin fits the biochemical observations of receptor/G protein contact, but the stoichiometry of the physiologically active, supramolecular rhodopsin:transducin complex remains the subject of debate (81,91-93).

The studies with the rhodopsin/transducin system have supplied structural information about the transition of a GPCR during signal transduction as well as mechanistic descriptions of receptor and G protein activation. Often, no other explanations of this GPCR behavior existed. The accumulation of data that suggest rhodopsin-like receptors, however, do not always function like rhodopsin cautions researchers to carefully examine the validity of any inferences drawn from rhodopsin research and applied to other receptor systems.

### *The $\beta_2$ -adrenergic receptor ( $\beta_2$ -AR): a foil for rhodopsin*

Early pharmacologists studied the adrenergic system as a model to examine the response of tissues to chemical stimulation (94). Modern-day relevance complements the historical significance of this receptor family as biochemists continue to tackle basic scientific questions that concern general GPCR functionality with adrenergic ‘tools’. Both the availability of numerous ligands for the  $\beta_2$  isoform as well as its cardiovascular value led to its selection as a  $G_s$ -coupled standard for the analysis of GPCR behavior (1).

Notably, the TCM of GPCR signaling emerged from the investigation of  $\beta_2$ -AR/ $G_s$  coupling (50). In addition, the discovery that the non-visual arrestins mediate the desensitization of the  $\beta_2$ -AR paralleled work with rhodopsin and, because arrestins were later shown to also coordinate non-canonical, ‘7TMR’ signaling pathways, this study of the  $\beta_2$ -AR exposed a previously-unappreciated yet fundamental capacity of the GPCR/7TMR family to influence cellular responses (95).  $\beta_2$ -AR behavior often contrasts that of rhodopsin, and therefore the  $\beta_2$ -AR serves as an important foil for rhodopsin during the interpretation of data that concerns GPCR/G protein coupling (83,85,96), receptor trafficking (97), and dimerization (98). Importantly, the recently-solved crystal structures of the  $\beta_2$ -AR provided the research community with alternative templates for GPCR homology modeling and reminded investigators of the abundant diversity encompassed within the GPCR family (63,99).

### *The outlook for GPCR research*

The emerging portrait of GPCR behavior is richly textured. Because GPCRs are components of cardiovascular, metabolic, neurodegenerative, psychiatric, cancer, and infectious disease pathophysiology, the molecular exposition of all GPCR activity has social, therapeutic, and economic relevance. Therefore, a comprehensive knowledge of GPCR biology should guide more specific, and thus more effective, advanced drug-discovery applications that employ combinatorial library design, structural biology, molecular informatics, and advanced screening technologies (100). Specifically,

approximately 140 *endo*-GPCRs (receptors with expected endogenous ligands) await deorphanization, and the resolution of the ‘receptosome’ networks of GIPs is highly anticipated (41-43,101).

### ***The molecular structure and function of the LHR protein***

#### *The glycoprotein hormone receptor family*

The FSHR and the thyroid stimulating hormone receptor (TSHR) share the most sequence homology (~40%) with LHR, and together, they constitute the glycoprotein hormone receptor (GpHR) family, so named because the receptors bind the glycoprotein hormones. These heterodimeric hormones (LH, CG, FSH, and TSH) are also very similar to each other; in fact, they share a common  $\alpha$ -subunit that associates with distinct yet homologous  $\beta$ -subunits that confer specificity. The  $\beta$ -subunits are derived from paralogous genes, and the families of glycoprotein hormones and their cognate receptors are thought to have co-evolved (102). Researchers have exploited these sequence similarities in biochemical experiments with chimeric hormones and receptors to determine the patterns of recognition (or repulsion) that dictate ligand/receptor specificity (103-109). Because the GpHRs activate the same cognate signaling partner,  $G_s$ , the sequence homology held between these receptors has also offered insight into the molecular mechanisms of GpHR signal transduction (110-113).

The GpHRs are a subset of the eight-member leucine-rich repeat (LRR) containing GPCR (LGR) family. The other LGRs are divided into two families, the relaxin-binding receptors (LGR7, LGR8) and a set of orphan receptors, LGR4, LGR5, and LGR6, that are emerging as essential for development. The sequence homology between GpHRs and the other LGR proteins is relevant only to studies regarding LGR genetic and structural evolution<sup>2</sup> (114).

---

<sup>2</sup>See Appendix

### *The molecular domains of LHR*

Unlike other rhodopsin-like GPCRs, the extracellular domain (ECD) of LHR is large (~340 amino acid residues) and is necessary and sufficient for high-affinity ligand binding (10,115-118). In this domain, two cysteine-rich domains flank nine leucine-rich repeat (LRR) sequence motifs and are thought to 'cap' the hydrophobic, leucine-rich, centers of the extended, slightly-curved, tubular structure formed by this kind of sequence motif (119-121). The ECD contains six putative N-linked consensus sites for glycosylation, and although the predicted molecular weight of the human LHR protein is ~75 kDa, the mature form of the receptor that localizes to the cell surface is susceptible to glycosidase treatment and resolves as an ~85-95 kDa protein during electrophoresis (10,122). Much research has focused upon the molecular interaction between the LHR ECD and its ligands, hCG and LH (102,103,123-125). Recent crystallographic structures of a truncated FSHR ECD in complex with its ligand and the TSHR ECD bound to the M antibody suggest that the hormones associate with the concave,  $\beta$ -strand surface of the receptors in the fashion of a 'hand-clasp' (119,126).

Figure 1.2 depicts a model of the LHR ECD bound to hCG in such a manner (120). Although glycosylation of the receptor is dispensable for high-affinity ligand binding (127), the presence of a carbohydrate moiety on the common  $\alpha$ -subunit of hCG is required (128,129). Alternate models of LHR/ligand interaction that do not disregard potential carbohydrate modifications argue that the crystal structures may not represent a native relationship of the receptor/hormone complex (125,130). Therefore, the docked model of hCG and the hLHR ECD in Figure 1.2 accounts for the glycosylation of the proteins.

Another cysteine-rich region of the ECD 'caps' the LRR domain and links it to the transmembrane domain (TMD). The fold of this C-terminal cysteine-rich region (CCR) accommodates a "constellation" of disulfide bridges and is not homologous to that of any known protein structure (131-133). Therefore, the CCR may be relatively flexible in solution, free to direct a hormone-occupied ECD towards the TMD to translate activation. (The theory that the ligand-less ECD acts as an inverse agonist

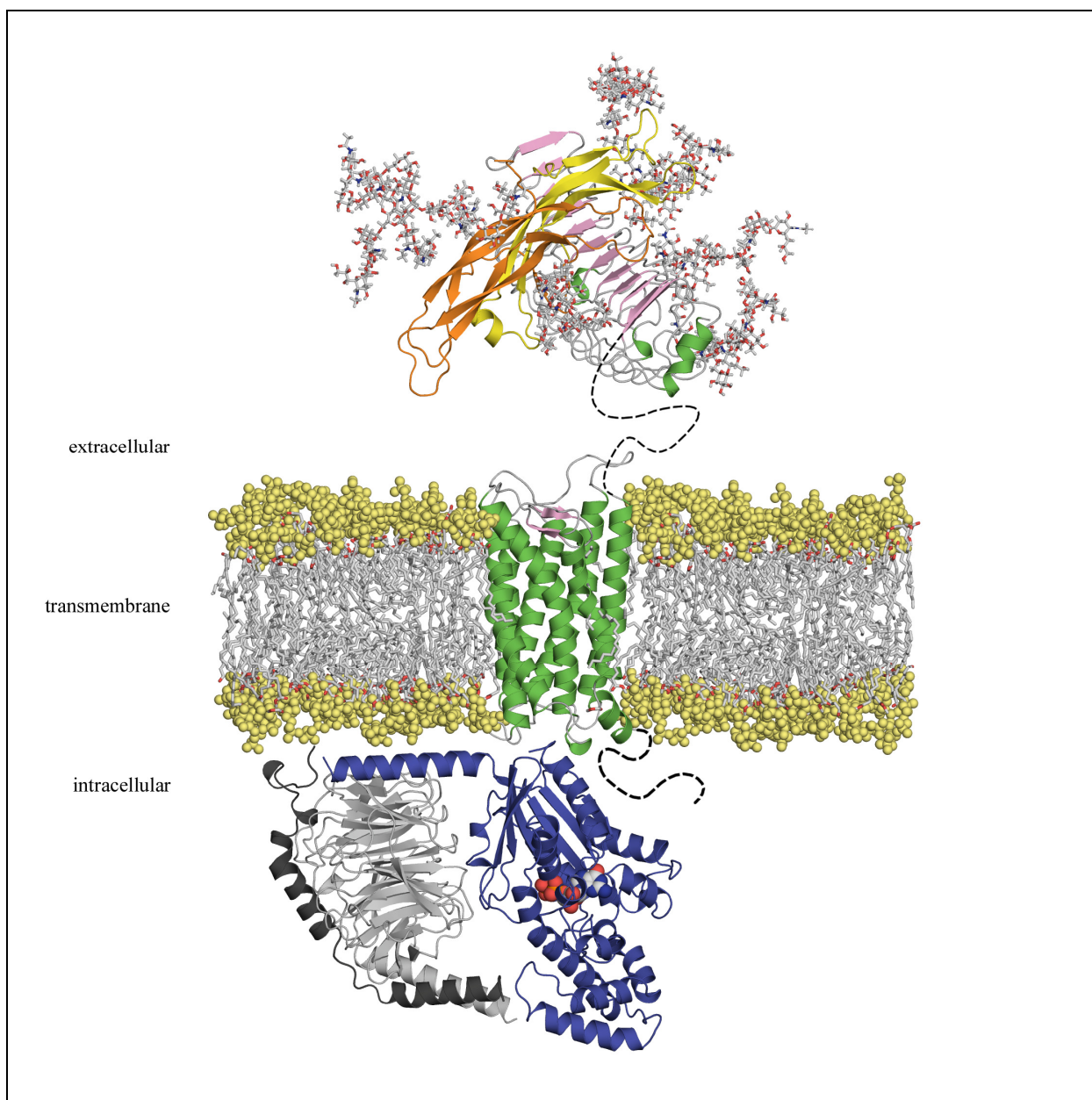


**Figure 1.2.** A structural representation of agonist (hCG), receptor (hLHR), and G protein ( $G\alpha_{i1}\beta_1\gamma_1$ ) in a membrane-oriented topology features proposed models of agonist/ECD association and TMD helical bundling. The crystal structure (PDB 1HCN) (134) of dimeric hCG (**hCG $\alpha$** , **hCG $\beta$** ) was docked to the hLHR **ECD** (120). Glycosyl residues are modeled as ball-and-stick structures and are meant only to illustrate the sites of modification. The CCR and cytosolic C-terminal tail of hLHR are represented as dotted black lines to emphasize the lack of structural information and presumed flexibility of these regions. The hLHR **TMD** domain was modeled with the rhodopsin TMD as a template (135). Membranous lipids are represented by a network of dipalmitoylphosphatidylcholine phospholipids. The crystal structure of heterotrimeric G protein (**G $\alpha_{i1}\beta_1\gamma_1$** ) (PDB 1GOT) (136) with bound nucleotide (spheres) was used because a heterotrimeric  $G_s$  structure is unavailable. The placement of G protein in proximity to hLHR is arbitrary and does not represent an experimentally docked complex. All images were created with Pymol (DeLano Scientific, LLC).

that associates with the TMD to inhibit activation has lost favor (137-139)). Interestingly, two residues of the CRR, D330 and Y331, are essential for hormone-induced receptor activation; this and other evidence suggest that not only does the CCR stabilize the LRR of the ECD but that the CCR is necessary for effective signal transduction (131-133).

Most GPCRs bind small ligands within the helical bundle of the transmembrane domain. The helices must then rearrange its complex network of molecular interactions to accommodate an induced fit of the ligand (1,140); LHR, however, binds its large glycoprotein hormone ligands with its ECD ‘arm’ (10,115-118). In a mechanism whose definition has eluded researchers, the agonist-occupied LHR ECD in tandem with the CCR somehow translates activation to the LHR TMD, which then, like its familial counterparts, rearranges its helical bundle to an ‘active’ conformation (102). Computer modeling of the inactive as well as mutated forms of the LHR TMD has outlined many of the molecular relationships that may define activation, although these contacts may not exist in an agonist-stimulated conformation of the receptor. Regardless, experiments with constitutively-active LHRs agree that the positioning of helices III, VI, and VII is significantly different than in an inactive state, possibly due to rigid body movements of helices II, III, IV, and VI that may change the packing interactions between the cytosolic halves of helices II/VII, II/III, III/VI, and VI/VII and importantly, the highly-conserved NPxxY motif in helix VII. These rearrangements are thought to increase the solvent-accessibility of the receptor’s cytosolic surface (58,59,141,142).

The helical extensions of the third and sixth transmembrane helices as well as the second and third intracellular loops of the hLHR TMD couple to G<sub>s</sub>, its preferred signaling partner (143-147). Biochemical experiments complemented by *in silico* modeling suggest that hydrogen bonding between residues E463, R464 (of the highly-conserved D-R-Y motif of rhodopsin-like GPCRs in the helical extension of helix III), and D564 (in the helical extension of helix VI) restricts the receptor to an inactive conformation (141). The crystal structure of dark-adapted rhodopsin reveals the presence of a salt bridge at this locus (148) which is supported by biochemical data (149). Models for other receptors place a similar restriction upon receptor activation (150-153). This constraint is thought to be absent in an active

receptor: a relaxed interaction between the cytosolic ends of helices III and VI and, therefore, the second and third intracellular loops, increases the surface area exposed to solvent, and thus, presumably, to  $G_s$  (141,143,146,147,154).

The cytosolic C-terminal tail of LHR contains residues that regulate the post-endocytotic trafficking patterns of the receptor. To internalize, many GPCRs associate with the non-visual arrestins after phosphorylation of serine or threonine residues in the intracellular loops; the hLHR, however, does not require phosphorylation of T561 (located in the cytosolic extension of helix VI) for arrestin association or internalization, although mutation to residues other than alanine impairs receptor internalization (155). Residues S635, S639, S649, and S652 (in the cytosolic C-terminal tail) become phosphorylated upon receptor activation (156), but arrestin-3 association with hLHR is dependent only upon receptor activation and not receptor phosphorylation (157). Receptor phosphorylation, however, is necessary for the uncoupling of hLHR from its effector, adenylate cyclase, as well as endocytosis of the receptor/hormone complex (158). Two residues in the C-terminal tail of hLHR, L683 and C699, influence both the recycling of ligand and the maintenance of a relatively constant presence of receptors on the cell surface (159). An association between hLHR and GAIP-interacting protein C terminus (GIPC) requires C699, and similarly, L683 may be a contact site for interaction with a protein or proteins involved in the recycling pathway (160).

#### *Naturally-occurring mutations in the human LHR*

Because the normal function of the LHR is necessary for human reproduction, naturally-occurring mutations of LHR are rarely inherited and propagated. A few mutations are genetically linked, however, and some occur spontaneously (see ref. (5,7,8)). Figure 1.3 illustrates the position of naturally-occurring mutations within the primary sequence of the human LHR protein. Mutations may impair the function of the receptor, or in some cases, increase its basal activity. Inactivating mutations include both nonsense and missense mutations: these prohibit the mature expression and localization of the protein. In



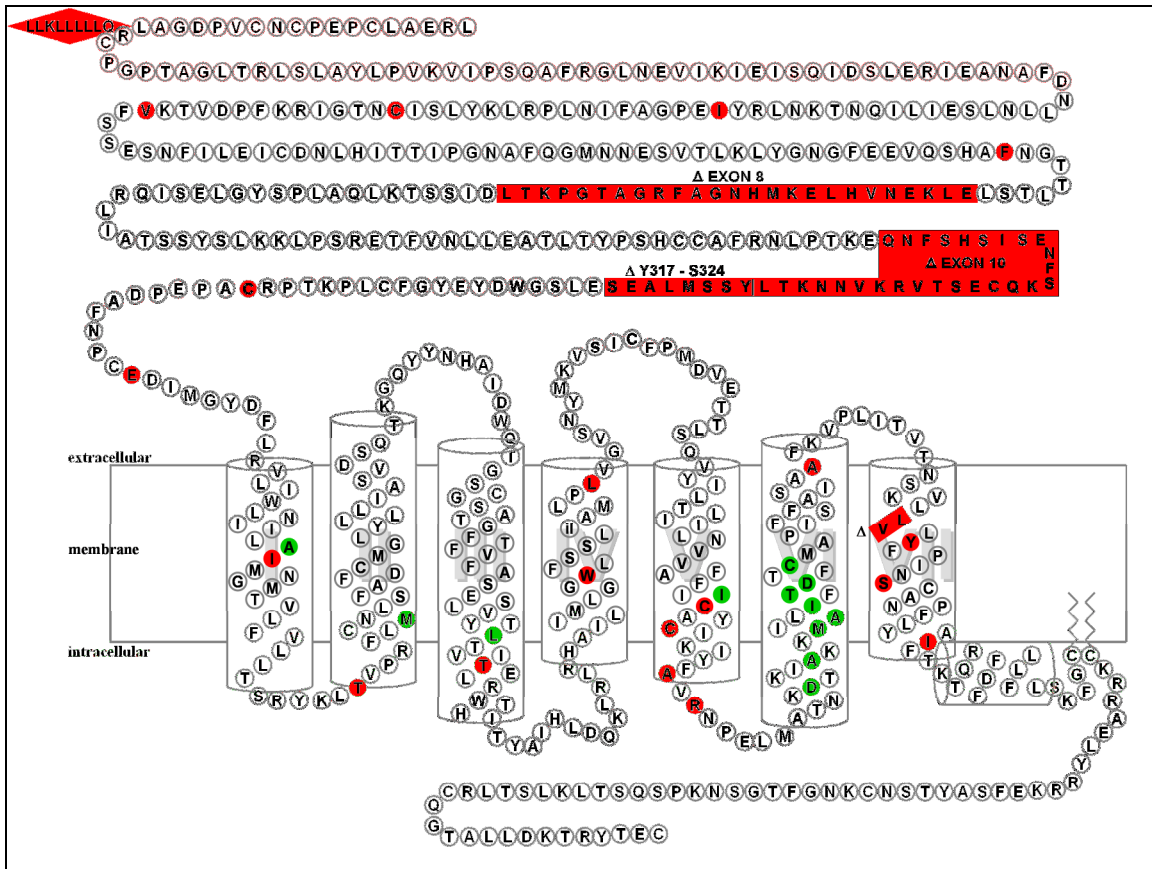


**Figure 1.3.** A snake diagram of the primary amino acid sequence of the human LHR protein represents the extracellular, membrane-spanning, and intracellular domains. The large N-terminal extracellular domain is followed by the hallmark seven transmembrane helical passes of the GPCR family. The dual palmitoylation of adjacent cysteine residues anchors the beginning of the intracellular domain in the membrane, thus creating a ‘fourth’ loop that may form a helical secondary structure. The positions of naturally-occurring mutations are represented in color. Mutations that impair or inactivate LHR function are **red** and mutations that cause constitutive activation of LHR are **green**. The sequence ‘LLKLLLLLQ’ is a rare insertion, and  $\Delta$  indicates a deletion. Adapted from (5,7,8)

addition, some missense mutations inhibit the binding of hormone—not surprisingly, most of these are found in the LHR ECD. Many missense mutations within the TMD prevent the receptor from shifting to an active conformation upon the binding of agonist, while other TMD missense mutations promote an active conformation of the receptor in the absence of ligand.

Interestingly, many of the constitutively-activating mutations are found in the sixth transmembrane helix, suggesting that this area of the receptor governs both the suppression and induction of LHR activation. The discovery of this ‘hot spot’ of naturally-occurring mutagenesis directed researchers to dissect the physiochemical relationships between the resident and neighboring amino acids

to assess the molecular nature of LHR activation (145,161-165). Some constitutively-active receptors lose responsiveness to agonist stimulation, but others may adjust their signaling selectivity from  $G_s$  to  $G_q$  (see the following discussion in *Signaling pathways of LHR*), a pathway that is activated by wild-type hLHR only at high concentrations of receptor and agonist (10,166). This capacity of LHR to form multiple, distinct, active conformations emphasizes the inherent plasticity within and pleiotropy of the human LHR protein. Because many naturally-occurring mutations have prompted GpHR researchers to engineer an abundance of mutant GpHRs, the GRIS (glycoprotein hormone receptor information system) database (<http://gris.ulb.ac.be/>) was created in 2006 to extract and organize GpHR mutagenesis data (both engineered and naturally-occurring) from the literature into a standardized, freely-accessible format (167). An alternate database on the glycoprotein hormone receptors, recently updated, is also available (<http://www.ssfa-gphr.de>).

### *Signaling pathways of LHR*

Although the preferred signaling partner of LHR is considered to be  $G_s$  due to the large cAMP increase upon agonist stimulation, many studies have implicated other heterotrimeric G protein signaling pathways as targets of LHR activation. The production of inositol phosphates after stimulation with high levels of ligand and/or receptor indicates that an active LHR may initiate a PLC-mediated cascade of second messenger production. Evidence exists to suggest that both  $G\alpha_q$  as well as  $G\beta\gamma$  liberated from activated  $G\alpha_i$  may stimulate PLC activity (10,165,168,169). The direct analysis of activated  $G\alpha$  subunits suggests that LHR may couple with  $G\alpha_s$ ,  $G\alpha_q$ ,  $G\alpha_{i/o}$ , and  $G\alpha_{13}$ , but the reports do not always agree (10,112,163,165,169-174). The method of detection and the sensitivity of the assays may contribute to the conflicting results (10). Certain constitutively-activating mutations of hLHR, such as L457R and D578H, were originally thought to exhibit a different pattern of G protein activation than wild-type (170,173), but this has since been refuted (174). The cell type, the species of LHR derivation,

ligand concentration, and receptor density do, however, appear to affect the signaling response of wild-type LHR (10,166,175).

An examination of LHR signaling within a physiological context explains much of the discrepancy found in the literature. LHR activity should not be characterized as a singular, static action—endocrine cells receive signals from LHR within a dynamic pattern of stimuli that derive from multiple sources and subsequently, the cells elicit a response that meets the needs of the system at that particular time and place. For example, during granulosa cell differentiation, the increasing expression levels of LHR and FSHR influence the selection process of follicles with the production of  $\Delta^5$ -pathway hormones (175) but during the luteal transition of granulosa cells, LHR signaling upregulates the  $\Delta^4$ -mediated production of progesterone (11,175,176).

Interestingly, some patients with Leydig cell adenomas exhibit a somatic D578H mutation, but patients with a substitution at this position to a tyrosine residue lack tumors and demonstrate diffuse Leydig cell hyperplasia (162,170,177). It is tempting to suggest that a change in signaling preference of the D578H hLHR may facilitate the neoplastic transformation (170), but both receptors appear to activate the same combination of G $\alpha$  isoforms (174). Perhaps the disparate phenotypes develop from a subtle shift in the production of second messengers that is beyond the sensitivity of current assays but not beyond the sensitivity of the Leydig cell response to signaling information. The precise nature of this signaling information, however, remains elusive. What is evident, nonetheless, is that the architectural difference between the D578H and D578Y receptors is sufficient to expose a pleiotropic disposition of the hLHR signaling repertoire.

Although non-heterotrimeric G protein signaling may occur through the MAPK pathway (46), studies indicate that LHR activates the MAPK pathway predominantly in a G protein-dependent manner (154,178-184). Specifically, the cAMP response elicited from G<sub>s</sub> activation appears to, through PKA, stimulate intracellular Ras-mediated ERK1/2 phosphorylation in a Leydig cell model (182,185). GPCRs may also signal through non-receptor tyrosine kinase pathways, either via  $\beta$ -arrestin-mediated activity,

EGF or integrin receptor-mediated transactivation, the direct binding of G $\alpha$  proteins, and/or by PKA- or PKC-mediated phosphorylation (95,186-193). In Leydig cells, LHR appears to activate the Src-family kinases Fyn and Yes, possibly via G<sub>q</sub> (194,195) or through arrestin-3 (196), to engage an intercellular network that is dependent upon EGFR activity to phosphorylate downstream ERK1/2 (185,195,197). Therefore, two distinct and independent pathways activate ERK1/2 to promote Leydig cell proliferation and anti-apoptosis (184,185,198).

In immature rat granulosa cells, the hCG-stimulated, G<sub>q</sub>-mediated, EGFR-transactivated ERK1/2 activity induces epiregulin release and negatively regulates aromatase expression (195,199). In the ovary, LH stimulates a JAK2 pathway (which includes phosphorylation of STAT-1, STAT-5b, IRS-1, and Shc signaling molecules) as well as the phosphorylation of AKT/PKB and ERK1/2. These signaling patterns may influence cell survival (200). In the early- to mid-follicular phase of granulosa cell development, LH mobilizes the expression of EGF members that, in a paracrine fashion, stimulate EGFR to activate the MAPK pathway which initiates cumulus cell expansion and oocyte maturation. Although this induction of MAPK signaling is cAMP-dependent, additional, non-G protein pathways may influence this inflammatory-like response that characterizes ovulation (201,202). After ovulation, human granulosa/lutein cells require ERK1/2 activation for progesterone production (180). Considerable work remains to exhaustively describe the molecular interplay between the signaling networks of tissue microenvironments that effect the biology of LHR activity.

### *LHR dimerization*

As with other facets of GPCR behavior, the question of dimer/oligomerization most likely will be answered within a long discussion that addresses the comparable and contrasting aspects between individual receptors rather than within a neat, concise ‘cartoon’ that encapsulates a simple model of pairwise receptor activity for all GPCRs (for extensive reviews, see ref. (31,47)). The examination of GPCR dimerization must consider biological relevance and cannot ignore the possibility of experimental artifact that may be introduced by the methods to detect dimerization—results gathered from co-

immunoprecipitation, resonance energy transfer, and membrane compartmentalization approaches are controversial (203-206). That a GPCR must remain either solitary or paired throughout its functional lifetime is another assumption that should be challenged. It is well-accepted that receptors of the glutamate-like family homo- and heterodimerize to traffic, bind ligand, signal, and internalize (207), and, interestingly, this work suggests that a singular transmembrane domain of a receptor protomer is sufficient to couple to G proteins and that other domains of receptors mediate dimerization. How these ideas pertain to rhodopsin-like GPCR activity, however, is unresolved. In addition, even the term “dimer” is ambiguous because GPCR-GPCR association can be transient (on the scale of nanoseconds) or quite stable (mediated by intermolecular disulfide bonds) (31,47).

These caveats must be considered when analyzing the data that suggests LHR not only exists but also functions as a homodimer. The results of studies employing equilibrium sedimentation and radiation inactivation of LHRs first proposed that the receptor assembles into higher-order self-associations (208,209). Subsequently, fluorescent resonance energy transfer (FRET) experiments demonstrated cell-surface LHR dimerization as well as self-association during desensitization (210-212). The demonstration of functional complementation further strengthened the argument for LHR dimerization when the co-expression of ligand binding-incompetent and signaling-defective LHR mutants were shown to rescue LHR activity (138,139). Researchers were also able to co-immunoprecipitate differentially-tagged hLHRs and measured an increase of this self-association after ligand stimulation; they did, however, describe a dependence of their results upon receptor concentration and localization. Importantly, they claimed an influence of the over-expression system upon their results (213).

Both bioluminescent resonance energy transfer (BRET) and BRET(2) signals were measured for LHR (214,215). Together, the BRET(2) data and results from hormone desorption assays that measured an allosteric modulation indicative of dimerization suggested that self-association of hLHR occurs during trafficking, persists during cell-surface expression, is a functional characteristic of hLHR behavior, and is not regulated by the activation state of hLHR (215). In another study, cell surface wild-type and constitutively-active receptor signaling was attenuated when co-expressed with certain signaling-

defective hLHR mutants that traffic properly to the membrane. Because a BRET(2) signal implied heterodimerization of the two receptor types, the signaling-defective mutants in this report were thought to either sequester the signaling-competent receptors from G<sub>s</sub> or to act as inverse agonists to allosterically impose a less-efficient conformation of the signaling-competent protomers (216). These signaling-defective mutants, however, were laboratory-engineered; in fact, all known naturally-occurring inactivating mutations of hLHR induce misfolding and mislocalization, and therefore, although these results describe a susceptibility of hLHR activity to its oligomeric state, its physiological relevance is speculative.

The transmembrane domains (TMDs) of rhodopsin-like receptors are thought to govern inter-protomer interactions, and the conclusions from computational modeling of hLHR self-association agree with this hypothesis. This work implicated helices IV, V, and VI (and specifically identified residue W491 in helix IV) as agents of dimerization. Notably, the models in this study were of the LHR TMD and extracellular/intracellular loops only (217). The crystal structure of FSH bound to a truncated FSHR ECD suggested that Y110 (within the FSHR ECD) mediates FSHR dimerization through the ECD (119), but BRET(2) signals did not differ between dimerized wild-type and mutant Y110 FSHRs. This work did propose, however, that as yet unidentified residues within both the TMD and ECD moderate FSHR dimerization (218).

Although some attempts were made to explain the functional relevance of LHR self-association, these studies as a whole do not escape from the general critique of GPCR dimer/oligomerization research which emphasizes that the capacity of most GPCRs to self-associate does not necessarily imply a biological imperative to do so.

#### *The outlook for LHR research*

Despite careful work that has extensively researched the interaction between LHR and its ligands, the precise maps of hCG and LH bound to LHR in a physiologically-relevant fashion await elucidation through the continuation of study that includes both the biochemical analysis of mutant and GpHR-

chimeric proteins as well as the structural examination of full-length, glycosylated molecules. Certainly the contribution of the CCR to LHR activity requires clarification, and the appeal to unravel the intricate choreography necessary for the TMD residues to coordinate the fluid, molecular ‘dance’ of the helical bundle during receptor activation is compelling. The terpsichorean repertoire of LHR grants a selection of signaling responses that poises the receptor within an orchestra of transmission that researchers are only beginning to decipher (219). The molecular landscape of LHR is flexible and dynamic and therefore must be defined according to the stages of its lifetime. Researchers should reconcile the influence of associated proteins such as chaperones and heterotrimeric G proteins upon LHR expression and trafficking, explain the physiological purpose of self-association, search for partners of LHR within its ‘receptosome’, further investigate LHR behavior upon desensitization and internalization, and importantly, should interpret their results within a biological context that perpetually regards LHR as an instrument of endocrine function.

### ***GPCR/G protein coupling and G protein activation***

#### *The structure of heterotrimeric G proteins*

Crystal structures revealed that guanine nucleotides bind in a cleft that forms between the GTPase domain (homologous to the fold of small G proteins) and the helical bundle of  $G\alpha$  (Fig. 1.2, 1.4) (136,220). A comparison between heterotrimeric G protein complexes and monomeric, activated forms of  $G\alpha$  suggests that three areas of the  $G\alpha$  GTPase domain, designated ‘switch I’, ‘switch II’, and ‘switch III’, significantly restructure when bound to a face of the  $G\beta$  propeller, and that the N-terminus (NT) of  $G\alpha$  contacts the top of  $G\beta$  (136,220). The coiled-coil association between the  $G\beta$  NT and  $G\gamma$  places the  $G\gamma$  N-terminal helix proximal to the helical bundle of  $G\alpha$ . The small  $G\gamma$  subunit wraps around  $G\beta$  placing its C-terminus near that of  $G\alpha$ . Heterotrimeric G proteins are membrane-associated proteins because post-translational lipid modifications at the C-termini of  $G\alpha$  and  $G\gamma$  and the NT of  $G\alpha$  anchor the

complex into the membrane (221-223). These modifications orient the proteins to the membrane as depicted in Figures 1.2 and 1.4. This orientation places the nucleotide-binding pocket approximately 35Å from a membrane-embedded receptor and limits the areas of Gα that are available for direct receptor contact.

Crystal structures complement biochemical analyses and suggest new hypotheses, and the G protein structures have served as fruitful templates to test many theories that concern the mechanisms of GPCR/G protein coupling and G protein activation.

### *The GPCR/G protein interface*

References (224) and (225) discuss the GPCR domains that have been identified as responsible for G protein coupling. Together, the implicated areas include any region of the receptor that may access the cytosol: specifically, extensions of transmembrane helices, intracellular loops, and the C-terminal tail. Individual receptors select from these regions to expose a unique arrangement of residues for association with G proteins. Defined patterns of residues most likely also characterize the coupling specificity of each Gα isoform to form multiple and distinct domains for receptor association (88).

The G<sub>i/o</sub> family appears to generally present the Gα N- and C-termini and α2-β4 and α4-β6 loops for receptor recognition (2,86,226-229), although researchers have noted subtle differences within the family, and remarkably, between highly homologous receptor isoforms (88,230,231). The α3-β5 loop and C-terminus are important for G<sub>s</sub>-coupling to the β<sub>2</sub>-AR (83,96,232), as is the Gα<sub>q</sub> CT to cognate receptors (233,234). The removal or substitution of the non-conserved Gα<sub>q</sub> N-terminal extension appears to permit promiscuous coupling; thus, this region constrains the coupling selectivity of Gα<sub>q</sub> (235). Direct association between Gβγ and receptors has been measured, but the precise contribution(s) to the coupling event for the heterodimer remains undefined (81,228,236-239). No crystal structure of a GPCR/G protein complex yet exists, and the biochemical examination of the interface relies upon creative approaches to



implicate the areas that mediate association. Therefore, the relief of the GPCR/G protein coupling ‘map’ is missing many details and contours (2).

A survey of the literature discerns that the G $\alpha$  CT is well-accepted as necessary for receptor coupling to isoforms of G $\alpha$ . For example, pertussis toxin targets the cysteine at position -4 from the CT of G $\alpha_{i/o}$  and the addition of an ADP-ribosyl moiety to this residue uncouples G $\alpha$  from its cognate receptors (240). Also, antibodies that target the CT of G $\alpha$  block signaling (227), chimeric substitutions within the CT are sufficient to switch the coupling of G proteins to non-cognate receptors (226,233,234), and extensive deletion and mutagenesis of Scg1/Gpa1 (homologous to the G $\alpha_{i/o}$  proteins) in a yeast model revealed the native CT to be required for mating and the pheromone response pathway (241,242). The addition of peptides corresponding to the G $\alpha$  CT impair signaling (243-247) or stabilize the active forms of receptors (85,87,248); one such example includes the recently-solved structure of opsin in complex with a G $\alpha_t$  CT peptide (249). Importantly, *in silico* docking studies with hLHR and G $\alpha_s$  suggest that the CT is important for coupling (144). Albeit necessary, the G $\alpha$  CT is not, however, always sufficient to substitute for full-length G $\alpha$  within the GPCR interface.

That the G $\beta\gamma$  heterodimer may contribute to the GPCR/G protein coupling interface encourages a ‘pentameric’ model of association in which a dimeric receptor associates with a heterotrimeric G protein. The size of the heterotrimer matches that of a dimeric receptor and is easily docked onto the receptor oligomer, which may be the functional unit of GPCR signaling (93,250); nevertheless, a thorough examination of the biochemical and biophysical data suggests that a monomeric receptor is sufficient to associate with a single heterotrimeric G protein to transduce signaling information (92). The analysis of GPCR/G protein coupling is also beset by controversy that concerns the lifetime of the receptor/G protein complex as factions either support a transient relationship between receptors and G proteins (251,252) or endorse a stable association between the proteins that rearranges upon activation (66,67,73,78,253,254).

### *A mechanism for the translation of activation from receptor to G protein*

As discussed previously, studies of rhodopsin behavior have been extremely insightful but limited in scope. The elegant and powerful application of site-directed spin labeling (SDSL) observed with electron paramagnetic resonance (EPR) to measure the association between rhodopsin and  $G\alpha_{t1}$  before and after exposure to light, however, has provided a molecular mechanism that describes (in more detail than presented by previous models) the translation of activation from a GPCR to a G protein (89,255). The validity of this mechanism to represent the behavior of all GPCRs is questionable, however, as no single mechanism to define GPCR/G protein coupling satisfies all of the experimental results that examine this relationship (2,88), but it does encompass a description of the changes that radiate from the receptor interface through  $\sim 35\text{\AA}$  of the  $G\alpha$  subunit to direct the nucleotide exchange event. This molecular relay may be conserved for  $G\alpha$  isoforms (89,255).

This mechanism suggests that i) the extreme C-terminus of  $G\alpha$  binds to a solvent-exposed pocket within active rhodopsin to ii) induce a rigid-body rotation and translation of the  $G\alpha$   $\alpha 5$  helix that iii) destabilizes the  $\beta 6$ - $\alpha 5$  loop that contacts the guanine nucleotide (Fig. 1.4A). A naturally-occurring mutation (A366S) in this loop was found to decrease the affinity of  $G\alpha_s$  for GDP and thus cause constitutive production of cAMP in Leydig cells. Patients with this mutation exhibit testotoxicosis (256). Another SDSL/EPR study identified a receptor-mediated instability of the switch I- $\alpha F$  helix region during activation that may trigger the opening of the interdomain cleft to release the nucleotide. This work proposed that receptor association may influence movements at the  $G\alpha/G\beta$  interface (within the switch I domain) to subsequently displace residues either along the  $\alpha 5$ - $\beta 6$  loop, down the  $\beta 2$  strand from the  $\beta 2$ - $\beta 3$  loop, or within  $G\beta$  to open the ‘portal doors’ ( $\alpha 5$ - $\beta 6$  loop and  $\alpha F$  helix) for nucleotide release (Fig. 1.4B).

Together, these studies implicate  $G\alpha$  residues that may translate the necessary conformational changes through the domains surrounding the nucleotide-binding pocket of  $G\alpha$  to promote GDP release.

Interestingly, they do not, however, provide evidence to preferentially support or refute any of the three general models that have been proposed to explain receptor-mediated G protein activation.

*The 'lever-arm' versus the 'gear-shift' versus the 'sequential-fit' models of G protein activation*

Three general models, each backed by some experimental evidence, describe possible mechanisms of GDP release by G $\alpha$  (257-259). The first, the 'lever-arm' model, integrates biochemical data that was extracted from studies with the rhodopsin/transducin system (Fig. 1.4C) (258). The second, the 'gear-shift' model, is also rhodopsin-based but, in addition, considers the similarities between heterotrimeric G protein activation and the activation scheme of the small G proteins by their guanine nucleotide exchange factors (GEFs) as well as that of the related GTP-binding elongation factors and their GEFs (Fig. 1.4D) (257). Studies with a receptor-mimetic peptide of the D<sub>2</sub>-dopamine receptor suggested the third, 'sequential-fit', model and dispenses with the necessity of the G $\alpha$  NT for G protein activation (259).

In the 'lever-arm' model, an activated receptor associates with the G $\alpha$  N-and C-termini to leverage the G $\alpha$  NT as an arm that, in lateral contact with G $\beta\gamma$ , tilts G $\beta\gamma$  away from the G $\alpha$  GTPase domain. Switch I and II remain tightly associated with G $\beta$  and extend with its movement to open the 'lips' covering the nucleotide binding pocket, promoting nucleotide release (Fig. 1.4C). The linker between the G $\alpha$  NT and the GTPase domain is flexible and is thus able to function as a 'hinge' within this model.

The 'gear-shift' model also defines an important role for the G $\alpha$  NT, but rather than moving away from the GTPase domain, the G $\alpha$  NT is proposed to rotate  $\sim 10^\circ$  to pull G $\beta\gamma$  towards the G $\alpha$  core. This small change translates into a large movement of the coiled-coil G $\beta$  and G $\gamma$  N-termini which causes the G $\gamma$  NT to then 'hook' into the helical domain of G $\alpha$  near helices  $\alpha A$  and  $\alpha B$ . The novel interaction of G $\gamma$  with the helical domain disturbs the nucleotide-binding site and promotes GDP release (Fig. 1.4D). In this model, the close-packing of G $\beta$  with the switch regions of G $\alpha$  is similar to the mechanism of GEF

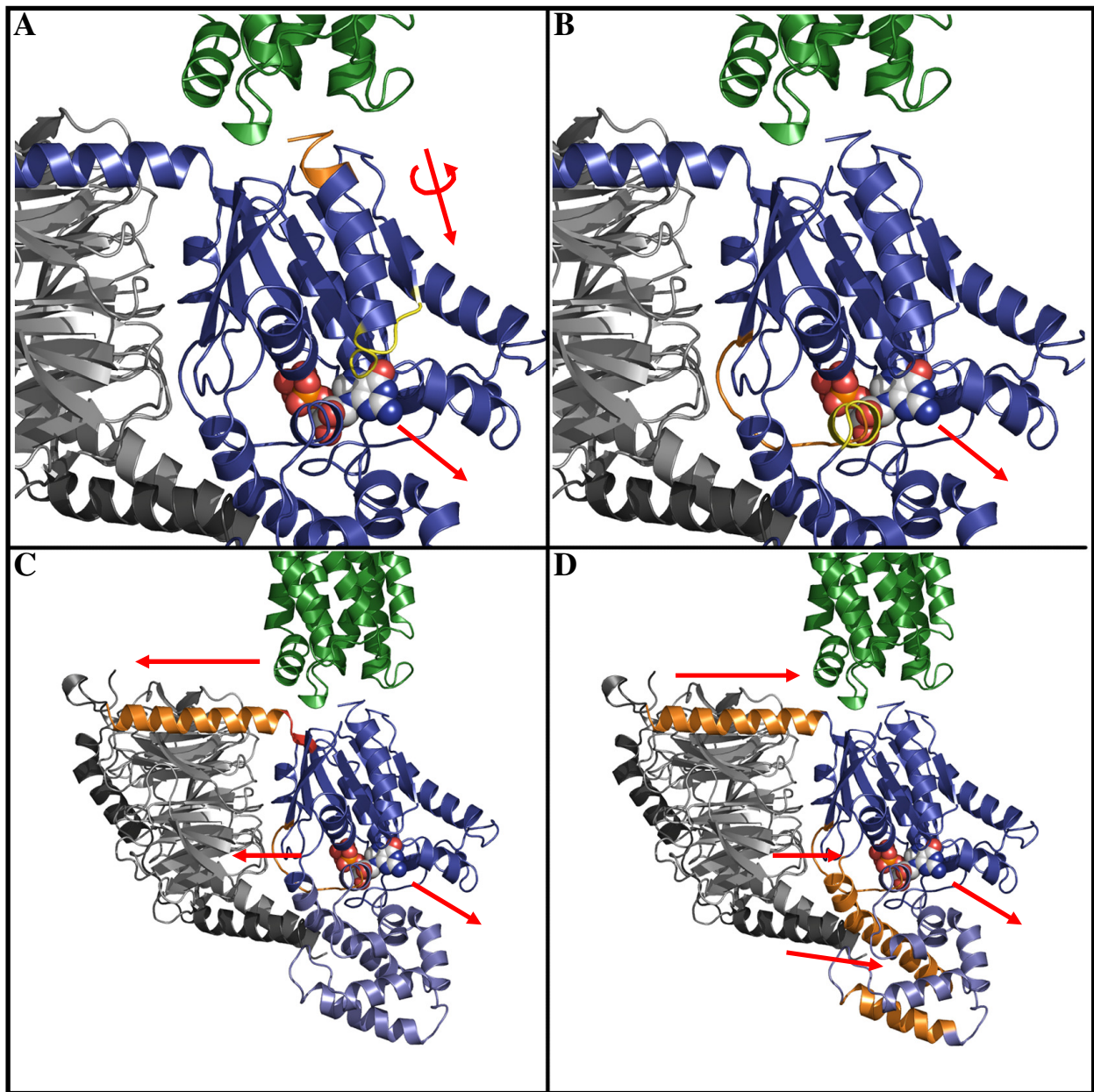


**Figure 1.4.** GPCR/G protein coupling and heterotrimeric G protein activation. **A.** A SDSL/EPR study suggested that an **activated receptor** binds to the **extreme C-terminus** of **Gα**. This association induces a rigid-body rotation and translation of the  $\alpha 5$  helix (represented by the **red arrows**) that destabilizes the  **$\beta 6$ - $\alpha 5$  loop** to cause GDP (spheres) release (**arrow**). **B.** Another SDSL/EPR study complements that of (A) to indicate that changes in **Gβ** affect the **Gα switch I region** to prompt the  **$\alpha F$  helix** of **Gα** to permit the dissociation of GDP (spheres) (**arrow**). **C.** The ‘lever-arm’ model of G protein activation proposes that the **linker** between the **Gα NT** and the **GTPase domain** acts as a hinge for the arm of the **Gα NT** to extend both **Gβγ** and the **switch I region** away from the **GTPase domain**. This disturbance opens the cleft between the **GTPase domain** and the **helical bundle** for GDP (spheres) release (**arrow**). **D.** The ‘gear-shift’ model suggests that the **Gα NT** pulls **Gβγ** toward the **Gα core** to permit the **Gγ NT** to ‘hook’ into the  **$\alpha A$  and  $\alpha B$  helices** of **Gα**. This novel interaction opens the nucleotide pocket for GDP (spheres) release (**arrow**). The images of the PDB file 1GOT were drawn with Pymol (DeLano Scientific, LLC).

association with small GTPases, and the interaction of  $G\gamma$  with the helical domain is reminiscent of the binding between related GRP-binding elongation factors and their GEFs.

In the 'sequential-fit' model, the receptor first binds to  $G\beta$  which then presents the CT of  $G\alpha$  to the newly-exposed, solvent-accessible G protein binding pocket of the activated receptor. This model is minimalistic because it suggests that the receptor only requires contact with the  $G\alpha$  CT to translate activation to the nucleotide cleft and that  $G\beta\gamma$  is only necessary for the initial association of the receptor with the heterotrimer.

The three models propose general mechanisms for G protein activation which are not necessarily mutually exclusive. The biochemical data that support these models, however, all derive from  $G_{i/o}$ -coupled receptor systems. Although the models present exciting theories for how GPCRs activate G proteins, they most likely do not accurately represent the complete mechanisms of  $G_s$ -,  $G_q$ - and  $G_{12/13}$ -coupled receptor activation.

## CHAPTER 2

# THE EXTREME C-TERMINAL REGION OF $G\alpha_s$ DIFFERENTIALLY COUPLES TO THE HUMAN LUTEINIZING HORMONE AND THE $\beta_2$ -ADRENERGIC RECEPTORS<sup>1</sup>

---

<sup>1</sup> DeMars, G., Fanelli, F., and D. Puett. To be submitted to *Journal of Biological Chemistry*.

## ***Abstract***

Many reports have implicated the extreme C-terminus (CT) of G protein  $\alpha$ -subunits as important for association with G protein coupled receptors (GPCRs). However, since GPCRs with little sequence homology activate the same G protein isoform, the mechanism for G-protein interaction appears to differ between GPCRs that signal through different isoforms of  $G\alpha$ , and this relationship has been tested for only a few GPCR/G protein partners. Therefore, the coupling processes for GPCRs may share general characteristics, such as a requirement for the  $G\alpha$  CT, but also may require specific interactions unique for each GPCR/G protein partnership. Hypothesizing that the extreme CT of  $G\alpha_s$  is a relevant part of the molecular landscape of the GPCR, human luteinizing hormone receptor (hLHR), a model cell system was created to allow the expression and manipulation of  $G\alpha_s$  subunits in hLHR<sup>+</sup> s49 cells that lack endogenous  $G\alpha_s$ . For comparative purposes, parallel studies were performed on the naturally expressed  $\beta_2$ -adrenergic receptor ( $\beta_2$ -AR). Based on studies involving truncations and mutations in the extreme CT of  $G\alpha_s$ , the  $G\alpha_s$  CT was found to be necessary for hLHR and  $\beta_2$ -AR signaling. Overall, some general similarities were found for the responses of the two receptors, including the importance of E392 in maintaining  $G\alpha_s$  in an inactive form and the functional effects of certain replacements. The data also indicate that significant differences exist between the coupling mechanisms of hLHR/ $G_s$  and  $\beta_2$ -AR/ $G_s$ , including the observation that L394 is not required for hCG-mediated activation of hLHR, but is for isoprenaline-induced  $\beta_2$ -AR signaling.

## ***Introduction***

G protein coupled receptors (GPCRs) constitute the largest gene family in the human genome and mediate a variety of physiologic functions including, but not limited to, sensory stimulation, cardiac and vascular function, neurotransmitter signaling, metabolism, pain control, and endocrine signaling (1). Therefore, the physiological and pathophysiological relevance of this family justifies studies to identify

the general similarities and dissect the specific differences of the GPCR signaling mechanisms that have evolved to impart such divergent physiological functions (2).

Active GPCRs directly associate with G proteins to transfer signals across the cell membrane. No sequence homology exists to define the coupling of GPCRs to specific G protein isoforms, although ~800-900 GPCRs signal through only four families of G proteins (2,29). This suggests that charge and conformation are more important than primary sequence identity for the specificity of G protein coupling (2,29). Prediction algorithms have matched GPCRs to their cognate G protein signaling partners with 70-90% accuracy, but these programs often failed to recognize the promiscuity of many GPCRs that signal through multiple G protein families (260,261). Biochemical approaches have determined regions as well as individual amino acid residues of GPCRs and G proteins that are important for coupling to one another, although their influence upon the coupling relationship may not be direct (140,224).

Generally, these studies have identified the cytosolic regions of GPCRs, specifically residues in the second and third intracellular loops, as well as residues in the surrounding cytosolic helical extensions. Many receptors have been individually examined to define the precise residues involved in G protein coupling (140,224). A smaller number of studies have investigated the G protein contribution to the coupling relationship. The extreme C-terminus (CT) of G $\alpha$  subunits is often recognized as important for coupling, but this conclusion has not been defined for many receptor systems (2). The partnerships between rhodopsin and transducin (G<sub>t</sub>) and the  $\beta_2$ -adrenergic receptor ( $\beta_2$ -AR)/G<sub>s</sub> pair were investigated and share some similarities, such as the importance of the G $\alpha$  CT to the coupling relationship, but, importantly, exhibit significant differences (80,83,86,96). Therefore, the mechanisms for GPCR/G protein coupling may vary between receptors that couple to different G protein isoforms (88).

The human luteinizing hormone receptor (hLHR) is a GPCR essential for reproduction, normal male sex differentiation, the onset of puberty, gametogenesis, gonadal steroidogenesis, ovulation, and the maintenance of early pregnancy. Persons with naturally-occurring mutations of the hLHR protein may suffer from infertility and/or other serious reproductive pathologies (123). The insight provided by these



mutations and an array of laboratory-engineered mutations has led to a better understanding of the many dynamic molecular relationships between the hLHR residues that define receptor function (167). In particular, residues important for coupling to  $G_s$  were found in the cytosolic extensions of helices III and IV as well as in the second and third intracellular loops (14). Nothing, however, is known about the  $G\alpha_s$  contribution to the hLHR/ $G_s$  coupling interface.

To test the hypothesis that the extreme C-terminus is important in LHR signaling, a model system was created to answer the following questions: i) Does hLHR require the extreme C-terminal region of  $G\alpha_s$  for activity? and ii) Does the  $\beta_2$ -AR associate with  $G\alpha_s$  in the same manner? The system permitted the introduction of  $G\alpha_s$  variants with engineered mutations at the extreme C-terminus, and therefore allowed the measurement of a functional response between the variants and hLHR or  $\beta_2$ -AR. The results suggested that the C-terminus is indeed important for coupling to both hLHR and  $\beta_2$ -AR. Interestingly, the two receptors responded differently to certain  $G\alpha_s$  variants, suggesting that the mechanisms of coupling not only differ between GPCRs that signal through different families of G proteins but may also vary between receptors that signal through the same G protein isoforms.

## ***Experimental Procedures***

### ***Materials***

s49 ck (cyc<sup>-</sup> kin<sup>-</sup>) cells were obtained from the University of California, San Francisco Cell Culture Facility, San Francisco, CA (262). The Virapower Lentivirus Expression System, HEK293FT cells, and Lipofectamine 2000 were from Invitrogen (Carlsbad, CA). Dulbecco's Modified Eagle Medium (DMEM) and Weymouth's medium were products of Cellgro Mediatech Inc. (Herndon, VA). PBS, HEPES, MEM non-essential amino acids, hexadimethrine bromide (Polybrene), purified hCG, crude hCG, isoprenaline, BSA, and isobutylmethylxanthine (IBMX) were purchased from Sigma (St. Louis, MO). Iodo-Gen was from Pierce Biotechnology (Rockford, IL). Heat-inactivated horse serum, fetal bovine serum (FBS), and OPTI-MEM were obtained from Gibco (Carlsbad, CA). Blasticidin and

puromycin were products of Invivogen (San Diego, CA). PSF (penicillin, streptomycin, and amphotericin B) and EDTA-free trypsin were from Life Science Technologies, (Gaithersburg, MD), and cholera toxin was from Calbiochem (Gibbstown, NJ).

#### *cDNA Plasmids*

The long splice variant of human  $G\alpha_s$  cDNA was purchased from ATCC (Manassas, VA). The insertions of the internal 6x-histidine tag into the long splice variant of  $G\alpha_s$  (after codon 76) and the N-terminal c-myc epitope tag (EQKLISEEDL) into hLHR (after codon 24) were prepared via the method of overlap PCR (263). The final PCR products were ligated into the pLenti6 Topo vector as recommended (Invitrogen). The c-myc\_hLHR/pLenti6 vector was modified to replace the EM7 promoter and the blasticidin-resistance cDNA with the cDNA encoding puromycin resistance using standard molecular cloning techniques. An AgeI site was introduced upstream of the  $P_{SV40}$  sequence in the puromycin cassette (pRS vector from Origene, Rockville, MD), and the replacement was performed utilizing AgeI and KpnI sites. Single site-directed mutations were created using the Stratagene QuikChange method (La Jolla, CA). The entire reading frames of manipulated cDNAs were sequenced (Sequencing and Synthesis Facility, University of Georgia, Athens, GA; Genewiz, South Plainfield, NJ).

#### *Cell Culture*

s49 cells (262,264) were maintained in a stationary suspension of DMEM supplemented with 10% (v/v) heat-inactivated horse serum at 37°C in 10% CO<sub>2</sub> as described (265). Conditioned medium for s49 cells variants was produced as described (265) by seeding growth medium at a density of  $1 \times 10^5$  cells/mL and harvesting the supernatant after 48 h. HEK293FT cells were maintained in DMEM supplemented with 10% (v/v) fetal bovine serum, 2 mM L-glutamate, 5 mM MEM non-essential amino acids, and PSF at 37°C in 5% CO<sub>2</sub>.

### *Lentiviral Production, Viral Transduction of s49 ck cells, and Selection of Stable Transformants*

Lentivirus production in HEK293FT cells was performed according to the ViraPower Lentivirus Expression System protocol (Invitrogen) in 10 cm dishes. Virus-containing medium was removed and filtered 60-72 h after transfection. Immediately after harvesting, transduction was performed in the presence of 6 µg/mL hexadimethrine bromide (Polybrene). HEK293 cells at 40% confluency in 6-well plates were transduced for viral titering according to the manufacturer's protocol.

For each transduction of s49 ck cells,  $5 \times 10^5$  s49 cells were resuspended in 2 mL virus-containing medium (average titer of  $5 \times 10^5$  transducing units/mL) and plated in a 6-well plate. After 6 h the cells were pelleted and resuspended in fresh growth medium. Then, 48 h after transduction, the cells were resuspended in 2 mL growth medium supplemented with 50 µg/mL blastidicin or 2.5 µg/mL puromycin. Two weeks after the addition of selective medium, the population of transformed cells was diluted to a density of 1 cell/200 µL conditioned and selective medium/well in 96 well plates for clonal selection. After two weeks, clonal lines were expanded and assayed for recombinant protein expression.

### *<sup>125</sup>I-hCG Saturation Binding*

Radioiodination of hCG was performed following the manufacturer's instructions with the Iodo-Gen reagent (Pierce Biotechnology) using [Na<sup>125</sup>I] (GE LifeSciences, Piscataway, NJ). Transformed s49 ck cells were washed twice in assay buffer (Weymouth's medium supplemented with 0.1%, w/v, BSA). Cells were resuspended in assay buffer with increasing amounts of <sup>125</sup>I-hCG with or without 100 IU of crude hCG at a density of  $4 \times 10^6$  cells/mL. 0.5 mL was plated per well in 12 well plates and the cells were incubated at 37°C for 5 h. Cells were washed twice with 0.5 mL PBS, lysed in 1 mL 1 N NaOH, and counts were measured in a γ-counter (PerkinElmer, Waltham, MA). Prism v. 3.0 (GraphPad Software, Inc., La Jolla, CA) was used to analyze saturation binding data using non-linear regression curve fitting.

### *Cholera Toxin (CTX) cAMP Assay*

Transformed s49 ck cells were pelleted and washed twice with cAMP medium (Weymouth's medium supplemented with 0.1% BSA). Cells ( $4 \times 10^6$ ) were added to 0.5 mL of cAMP medium supplemented with 0.8mM IBMX per well of a 12-well plate at 37°C. After 15 min, medium was replaced with cAMP medium plus 0.8 mM IBMX with or without 2  $\mu$ L/mL CTX. The cells were incubated for 2 h at 37°C and then stored in 0.5 mL/well 100% ethanol at -20°C overnight. The samples were dried in a SpeedVac (ThermoFisher, Waltham, MA) and resuspended in 200  $\mu$ L cAMP buffer. The  $^{125}$ I-cAMP radioimmunoassay (RIA) was performed according to manufacturer's protocol (PerkinElmer). cAMP values from non-stimulated cells were subtracted from the values for stimulated cells to represent the amount of cAMP produced solely from the CTX treatment. Prism v.3.0 (GraphPad Software, Inc.) was used to analyze the data using one-way ANOVA followed by Dunnett's post-test.

### *Collection of Cellular Membranes, SDS-PAGE, and Western Blotting*

$4 \times 10^8$  transformed s49 ck cells were pelleted, washed twice with 50 mL cold PBS, frozen at -80°C, and thawed in 10 mL cold membrane buffer (50 mM Tris-Cl pH 7.4, 250 mM sucrose, 1 mM PMSF, 5 nM N-ethylmaleimide, and 2 mM EDTA, pH 8.0). All subsequent steps were performed on ice or at 4°C (266). The suspension was homogenized with a Tekmar instrument for 2 min using the small probe with a power level of 25 and then centrifuged at 1,000g for 5 min. The supernatant was collected and the pellet was resuspended and homogenized again. The combined supernatants were centrifuged at 48,000g for 45 min at 4°C. The membrane-containing pellet was suspended in membrane buffer without glucose and frozen at -80°C. Protein concentrations were determined using the Bradford method (BioRad).

Crude membranes (100  $\mu$ g) in reducing Laemmli sample buffer were resolved on 4-20% Tris-Cl denaturing gels (BioRad, Hercules, CA) and transferred to Immobilon PVDF membranes (Millipore, Billerica, MA). Western blotting was performed in 5% blocking buffer (20 mM Tris-Cl, pH 7.4, 150 mM

NaCl, 0.05% Tween-20, 5% non-fat milk). Antibody dilutions were as follows in 1.5% blocking buffer: 10,000x for anti-6xHistidine (6219-1, BD Biosciences, San Jose, CA), 50x for anti-actin (sc-1616, Santa Cruz Biotechnologies, Santa Cruz, CA), 10,000x for sheep anti-mouse (GE Lifesciences), and 20,000x for donkey anti-goat HRP (Santa Cruz). Incubations for primary antibodies were performed at 4°C overnight, and the incubation for secondary antibodies was 1 h at room temperature. The Western Lightning ECL kit was used to visualize chemiluminescence (PerkinElmer).

#### *Dose-response cAMP assays*

cAMP assays were performed as described above. After 15 min, the medium was replaced with 0.5 mL/well cAMP medium plus 0.8 mM IBMX supplemented with the appropriate concentration of purified hCG or isoprenaline at 37°C. After 30 min, the medium was replaced with 0.5 mL/well 100% ethanol (PharmcoAAPER, Shelbyville, KY) and the plates were stored at -20°C overnight. The samples were dried, resuspended, measured, and analyzed using non-linear regression curve fitting in Prism v.3.0. One-way ANOVA followed by Dunnett's post-test was performed for the comparison of basal cAMP levels.

## **Results**

#### *Creation and Characterization of hLHR<sup>+</sup> and hLHR<sup>+</sup>/Gα<sub>s</sub><sup>+</sup> s49 ck Cell*

The lack of Gα<sub>s</sub> mRNA transcription and an inactivating mutation of protein kinase A define the s49 ck (s49 cyc<sup>-</sup> kin<sup>-</sup>) murine lymphoma cell line (262,264). s49 ck cells were transduced with a lentivirus containing hLHR cDNA and puromycin resistance. A stable, clonal line was isolated, expanded, and characterized for hLHR expression by <sup>125</sup>I-hCG saturation binding analysis (Fig. 2.1A). Specific and saturable binding of the transformed cells was measured, and the K<sub>d</sub> and B<sub>max</sub> were determined to be 4.5 nM and 24 x 10<sup>3</sup> receptors/cell, respectively, for the hLHR<sup>+</sup>/hGα<sub>s</sub><sup>+</sup> line.

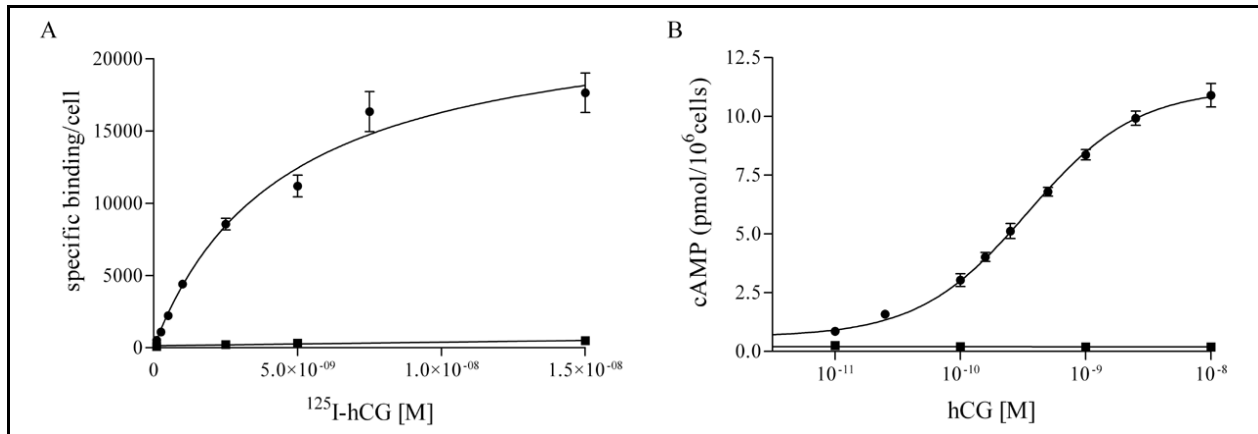


**Figure 2.1.** Characterization of the model system of transformed s49 ck cell lines. *A.* Saturation-binding curve. Specific binding was measured after a 5 h incubation with  $^{125}\text{I}$ -hCG at  $37^\circ\text{C}$  for the mock (■) and hLHR $^+$  s49 ck (●) cells, and the derived  $K_d$  and  $B_{\max}$  values for the hLHR $^+$  cells are  $4.5 \pm 0.4$  nM and  $(24 \pm 1.2) \times 10^3$  receptors/cell, respectively. *B.* Dose-response curve. The cAMP response was measured after a 30 min incubation with hCG ( $37^\circ\text{C}$ ) of the hLHR $^+$ /mock (■) and hLHR $^+$ / $G\alpha_s^+$  (●) transformed cell lines, and the values found for  $EC_{50}$  and  $R_{\max}$  for the hLHR $^+$ / $G\alpha_s^+$  cell line are  $0.34 \pm 0.1$  nM and  $11.2 \pm 0.2$  pmol/ $10^6$  cells, respectively. Data are presented as mean  $\pm$  SEM.

The clonal hLHR $^+$  s49 ck cell line was then transduced with lentiviral constructs containing blasticidin resistance as well as the long splice-variant cDNA of the human  $G\alpha_s$  or an empty vector as a mock control. In order to characterize the model cell, hLHR $^+$ /mock and hLHR $^+$ /wild-type  $G\alpha_s^+$  cells were incubated with increasing concentrations of hCG and the resulting cAMP response was measured (Fig. 2.1B). No response was generated from the hLHR $^+$ /mock cells, but the hLHR $^+$ / $G\alpha_s^+$  cells responded with cAMP production. The  $EC_{50}$  and  $R_{\max}$  were 0.34 nM and 11.2 pmol/ $10^6$  cells, respectively, for the hLHR $^+$ / $G\alpha_s^+$  line.

#### *Design and expression levels of wild-type and mutant forms of $G\alpha_s$ .*

Having established a suitable model cell system, sequential C-terminal truncations were made at positions -1 through -4 (391-394), and Ala scanning mutagenesis was done for each amino acid residue in the -6 through the -1 (389-394) region. The results suggested the design of additional mutations in this portion of  $G\alpha_s$  for functional characterization. In all, a total of 26 cell lines were prepared and characterized (Fig. 2.2A). Figures 2.2B and 2.2C highlight the targeted positions within the crystal

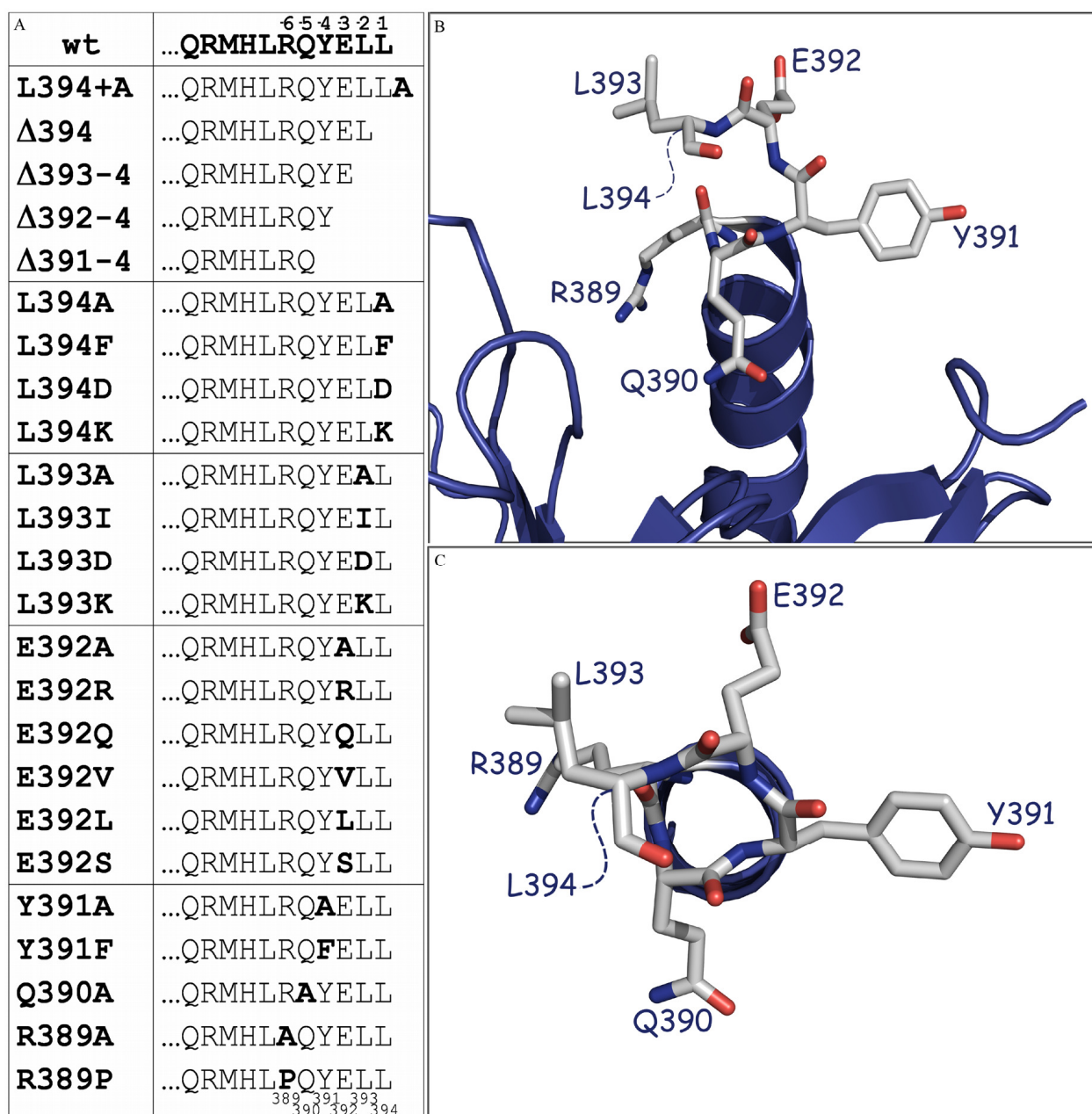


**Figure 2.2.**  $G\alpha_s$  C-terminal targets of experimental manipulation. **A.** List of the last eleven amino-acid residues of the wild-type and manipulated  $G\alpha_s$  variants. The variants are grouped according to residue position. The position of the residues with regard to the C-terminus (-1 to -6) is indicated at the top of the chart and the residue number corresponding to the long-splice variant sequence of human  $G\alpha_s$  (389-394) is depicted at the bottom. **B.** Cartoon representation of the  $G\alpha_s$  subunit in the 1AZS PDB file with the five terminal residues illustrated in ball-and-stick mode, with the final residue, L394, disordered in the structure, represented by a dotted line. **C.** Same representation as (B) but turned 90° towards the reader in a helical-wheel fashion. The images in (B) and (C) were created with Pymol (DeLano Scientific, LLC).

structure of  $G\alpha_s$ -GTP $\gamma$ S (1AZS) (267). The perspective in Figure 2.2C emphasizes the helical orientation of the last amino acids of the protein and places the terminal residue (L394, disordered in the structure) at the forefront of the image.

To monitor  $G\alpha_s$  expression, crude membranes from each cell line were probed and the resultant Western blots are presented in Figure 2.3. The Western blots indicated that all of the deletion and replacement mutants were expressed; however, the apparent levels were variable. To better gauge the biological activity of the introduced proteins, each of the cell lines was incubated with CTX in order to estimate the expression level of functional protein (Fig. 2.4A). The extreme C-terminus of  $G\alpha_s$  has not been implicated in the binding to and activation of the effector enzyme, adenylate cyclase, and therefore manipulation of this area is assumed not to affect the impact of cholera toxin stimulation of  $G\alpha_s$  (20). Each of the mutated  $G\alpha_s$  proteins responded to CTX stimulation, indicating that the alterations made at the C-terminus do not abrogate  $G\alpha_s$  activity. However, the biological activity for the mutants was also variable. Most fall within about 2-2.5-fold that of wild-type  $G\alpha_s$ ; only E392A/V/L and Y391F exhibit apparent lower expression.

#### *Functional analysis of $hLHR^+/G\alpha_s^+$ ck cells expressing engineered forms of $G\alpha_s$*

Basal cAMP values were determined for wild-type and  $G\alpha_s$  mutants, and only those replacing E392 exhibited constitutive activity (Fig. 2.4B). These findings indicate that a negatively charged side chain at position -3 (392) is required to maintain the protein in an inactive form.

Figure 2.5 shows the dose-response curves of the various cell lines with increasing concentrations of hCG. Table 2.1 gives the efficiency,  $EC_{50}$ , and efficacy,  $R_{max}$ , of signaling for each. The efficiency of each falls within 2-2.5-fold that of wild type  $G\alpha_s$ , but the efficacy varies somewhat. Extension of the protein at the C-terminus by addition of an Ala ( $G\alpha_s$  L394+A) or deletion of L394 ( $\Delta$ 394) did not reduce the efficacy (Fig.4A). Extension of the protein at the C-terminus by addition of an



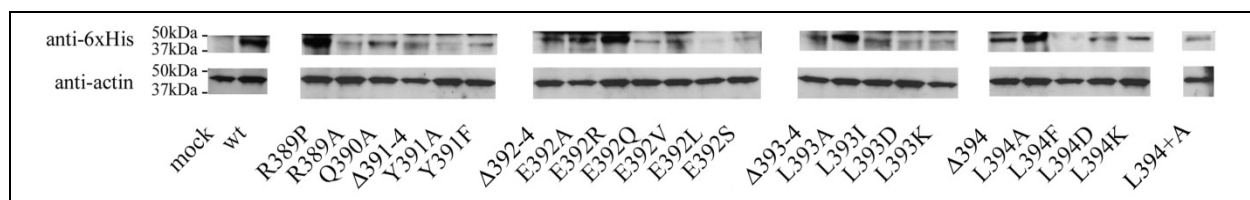


**Figure 2.3.** Western blots of membrane protein from the  $G\alpha_s$ -transformed cell lines. As an estimate of total LHR expression, 100  $\mu$ g crude membrane protein was probed with anti-6xHis (top panels), along with an anti-actin probe to serve as a control for protein recovery and loading (bottom panels).

Ala ( $G\alpha_s$  L394+A) or deletion of L394 ( $\Delta$ 394) did not reduce the efficacy (Fig. 2.5A). Thus, neither the location of the  $\alpha$ -carboxyl group nor the presence of the Leu at position 394 is essential for signaling.

Further truncation to give  $G\alpha_s$   $\Delta$ 393-394,  $\Delta$ 392-394, and  $\Delta$ 391-394 (Fig. 2.5A) abolished signaling, suggesting that the extreme C-terminus of  $G\alpha_s$ , but not L394, is necessary for coupling to hLHR. Ala scanning mutagenesis at each of the positions -6 through -1 (389-394) illustrated that signaling was abrogated with Ala at position 393 (Fig. 2.5C) and reduced with replacements at positions 392 and 391 (Fig. 2.5D,E). The mutants L394A, Q390A, and R389A signaled similarly to wild-type  $G\alpha_s$ . In order to further characterize the nature of the side chains required for bioactivity at these positions, additional mutations were made at residues 392-394. Also, the R389P variant (identified in the s49 unc<sup>-</sup> line) was included as a negative control because this mutation is known to ‘uncouple’ the G protein from the  $\beta_2$ -AR (268). The results are presented in Figure 2.5 B-E and summarized in Table 2.1.

Since Ala scanning mutagenesis suggested that the L394A mutant signaled similar to wild-type, the impact of aromatic (L394F) and charged (L394D and L394K) residues were probed (Fig. 2.5B, Table 2.1). The L394K mutant exhibited a slight reduction in signaling efficacy, while the F and D replacements gave apparent increases in efficacy compared to wild-type protein. hLHR signaling thus appears to tolerate various amino acids at the -1 position of  $G\alpha_s$ . Since an Ala replacement at position -2 (residue #393) abrogated signaling, a larger hydrophobic side chain, I, was tested and found to yield an apparently higher efficacy, compared to wild-type protein; however, replacements with ionizable side chains, D and

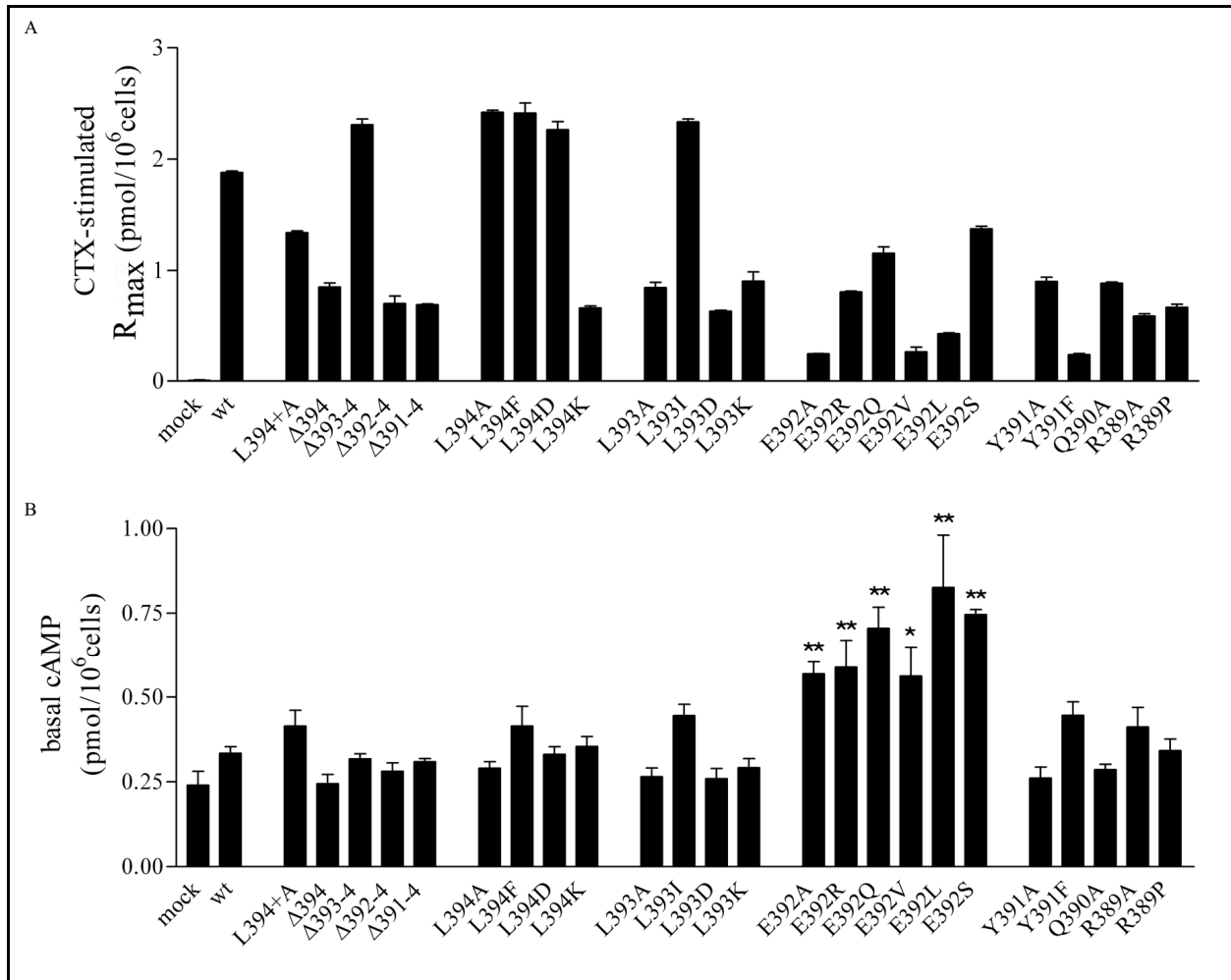


**Figure 2.4.** A. Maximal cAMP production ( $R_{\max}$ ) of hLHR<sup>+</sup>/G $\alpha_s$ <sup>+</sup> wild-type and variant cells stimulated with CTX. Measurements were made after incubating cells for 2 h (37°C) with 2  $\mu$ g/mL CTX, and the results are given as mean  $\pm$  SEM. One-way ANOVA followed by Dunnett's post-test was used for statistical analysis, and all samples were found to be significantly different than wild-type G $\alpha_s$  ( $p < 0.001$ ). B. Basal cAMP values of the transformed s49 ck cells. The cells were incubated for 30 min, and One-way ANOVA followed by Dunnett's post-test was used for the statistical analysis of significance compared to wild-type (wt) (\*  $p < 0.05$ , \*\*  $p < 0.001$ ). Experiments were performed in quadruplicate,  $n = 3$ .

K, abolished signaling. Thus, a relatively large hydrophobic side chain appears to be required at position -2 (#393) for wild-type-like signaling (Fig. 2.5C, Table 2.1).

Because replacement with Ala at position -3 (#392) was somewhat tolerated, a series of replacements at this position were probed (Fig. 2.5D, Table 2.1). Although the efficacies of the mutant proteins appeared to be affected, none of the replacements entirely abrogated signaling through hLHR. Figure 2.5E and Table 2.1 show the dose-response results for the mutations at positions -6 through -4

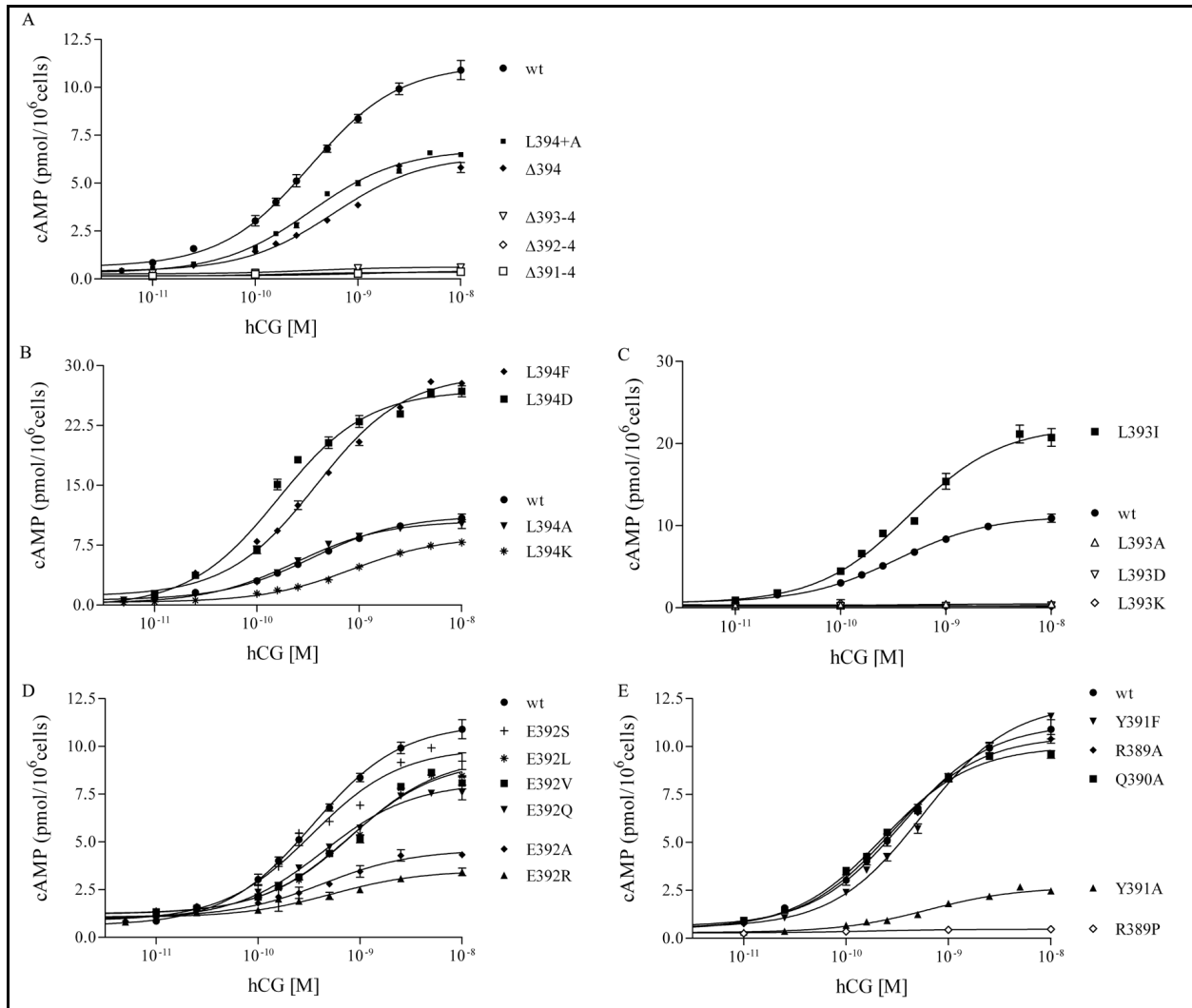


**Figure 2.5.** Dose-response isotherms of cAMP concentrations following hCG stimulation of LHR in the transformed s49 ck cell lines. All panels include data from hLHR<sup>+</sup>/G $\alpha_s$ <sup>+</sup> wild-type cells. Data from the C-terminal Ala extension, L394+A, and the truncation mutations are presented in panel A, while panels B-E present data from the point mutations at positions -1 (#394), -2 (#393), -3 (#392), and -4/-5/-6 (#391/#390/#389), respectively. The results show mean  $\pm$  SEM; the numerical values are given in Table 2.1. Results from samples  $\Delta$ 393-4,  $\Delta$ 392-4, and  $\Delta$ 391-4 in panel A and from L393A, L393D, and L393K in panel C are superimposed.

(#s389-391). Replacement of Y391 with F was tolerated, although the efficacy of Y391A was reduced, and R389P was, as expected from studies with the  $\beta_2$ -AR (21), devoid of signaling.

The s49 ck cells endogenously express  $\beta_2$ -AR, and the cAMP responses to the agonist isoprenaline ( $\pm$  isoproterenol) of engineered cells expressing wild-type and variant forms of G $\alpha_s$  were determined (Fig. 2.6, Table 2.1). The results for the C-terminal extension and truncations are given in

**Table 2.1.** Summary of EC<sub>50</sub> and R<sub>max</sub> values.

	hCG		isoprenaline	
	EC <sub>50</sub> (nM)	R <sub>max</sub> (pmol/10 <sup>6</sup> cells)	EC <sub>50</sub> (μM)	R <sub>max</sub> (pmol/10 <sup>6</sup> cells)
mock	-- <sup>a</sup>	0.19 ± 0.06 <sup>**</sup>	-- <sup>a</sup>	0.14 ± 0.01 <sup>**</sup>
wt	0.34 ± 0.11	11.2 ± 0.2	5.7 ± 1.1	3.44 ± 0.07
L394+A	0.35 ± 0.11	6.76 ± 0.08 <sup>**</sup>	5.8 ± 1.1	1.15 ± 0.02 <sup>**</sup>
Δ394	0.58 ± 0.11	6.44 ± 0.17 <sup>**</sup>	-- <sup>a</sup>	0.30 ± 0.000 <sup>**</sup>
Δ393-4	-- <sup>a</sup>	0.63 ± 0.03 <sup>**</sup>	-- <sup>a</sup>	0.21 ± 0.01 <sup>**</sup>
Δ392-4	-- <sup>a</sup>	0.42 ± 0.02 <sup>**</sup>	-- <sup>a</sup>	0.22 ± 0.00 <sup>**</sup>
Δ391-4	-- <sup>a</sup>	0.35 ± 0.03 <sup>**</sup>	-- <sup>a</sup>	0.23 ± 0.01 <sup>**</sup>
L394A	0.24 ± 0.11	10.5 ± 0.24	6.7 ± 1.1	0.89 ± 0.01 <sup>**</sup>
L394F	0.38 ± 0.11	28.9 ± 0.3 <sup>**</sup>	8.6 ± 1.2 <sup>**</sup>	3.09 ± 0.04 <sup>**</sup>
L394D	0.16 ± 0.11	27 ± 0.88 <sup>**</sup>	8.1 ± 1.1 <sup>*</sup>	1.37 ± 0.03 <sup>**</sup>
L394K	0.84 ± 0.10 <sup>**</sup>	8.54 ± 0.09 <sup>*</sup>	6.1 ± 1.1	0.73 ± 0.01 <sup>**</sup>
L393A	-- <sup>a</sup>	0.47 ± 0.05 <sup>**</sup>	-- <sup>a</sup>	0.22 ± 0.00 <sup>**</sup>
L393I	0.45 ± 0.11	22.1 ± 0.5 <sup>**</sup>	5.4 ± 1.0	2.85 ± 0.03 <sup>**</sup>
L393D	-- <sup>a</sup>	0.30 ± 0.05 <sup>**</sup>	-- <sup>a</sup>	0.27 ± 0.00 <sup>**</sup>
L393K	-- <sup>a</sup>	0.15 ± 0.39 <sup>**</sup>	-- <sup>a</sup>	0.22 ± 0.01 <sup>**</sup>
E392A	0.74 ± 0.12	5.38 ± 0.25 <sup>**</sup>	11 ± 1.1 <sup>**</sup>	1.28 ± 0.01 <sup>**</sup>
E392R	0.75 ± 0.12 <sup>*</sup>	3.50 ± 0.14 <sup>**</sup>	9.5 ± 1.1 <sup>**</sup>	1.36 ± 0.03 <sup>**</sup>
E392Q	0.44 ± 0.11	8.09 ± 0.13 <sup>**</sup>	7.2 ± 1.1	2.13 ± 0.02 <sup>**</sup>
E392V	0.80 ± 0.11 <sup>*</sup>	9.29 ± 0.19 <sup>*</sup>	--	0.77 ± 0.00 <sup>**</sup>
E392L	0.83 ± 0.11 <sup>*</sup>	9.44 ± 0.12 <sup>*</sup>	5.0 ± 1.1	1.30 ± 0.01 <sup>**</sup>
E392S	0.21 ± 0.15	9.94 ± 0.76	3.8 ± 1.0	1.92 ± 0.01 <sup>**</sup>
Y391A	0.62 ± 0.11	2.66 ± 0.06 <sup>**</sup>	12 ± 1.1 <sup>**</sup>	0.82 ± 0.01 <sup>**</sup>
Y391F	0.55 ± 0.11	12.3 ± 0.2	5.2 ± 1.1	1.11 ± 0.02 <sup>**</sup>
Q390A	0.23 ± 0.11	10.0 ± 0.1	5.4 ± 1.1	3.18 ± 0.06 <sup>**</sup>
R389A	0.28 ± 0.11	10.6 ± 0.1	4.8 ± 1.1	2.66 ± 0.05 <sup>**</sup>
R389P	-- <sup>a</sup>	0.47 ± 0.04 <sup>**</sup>	-- <sup>a</sup>	0.13 ± 0.01 <sup>**</sup>

<sup>a</sup> indicates a zero or insufficient response to ligand for determination of EC<sub>50</sub>  
<sup>\*</sup> p < 0.05, <sup>\*\*</sup> p < 0.001 compared to wild-type (wt)

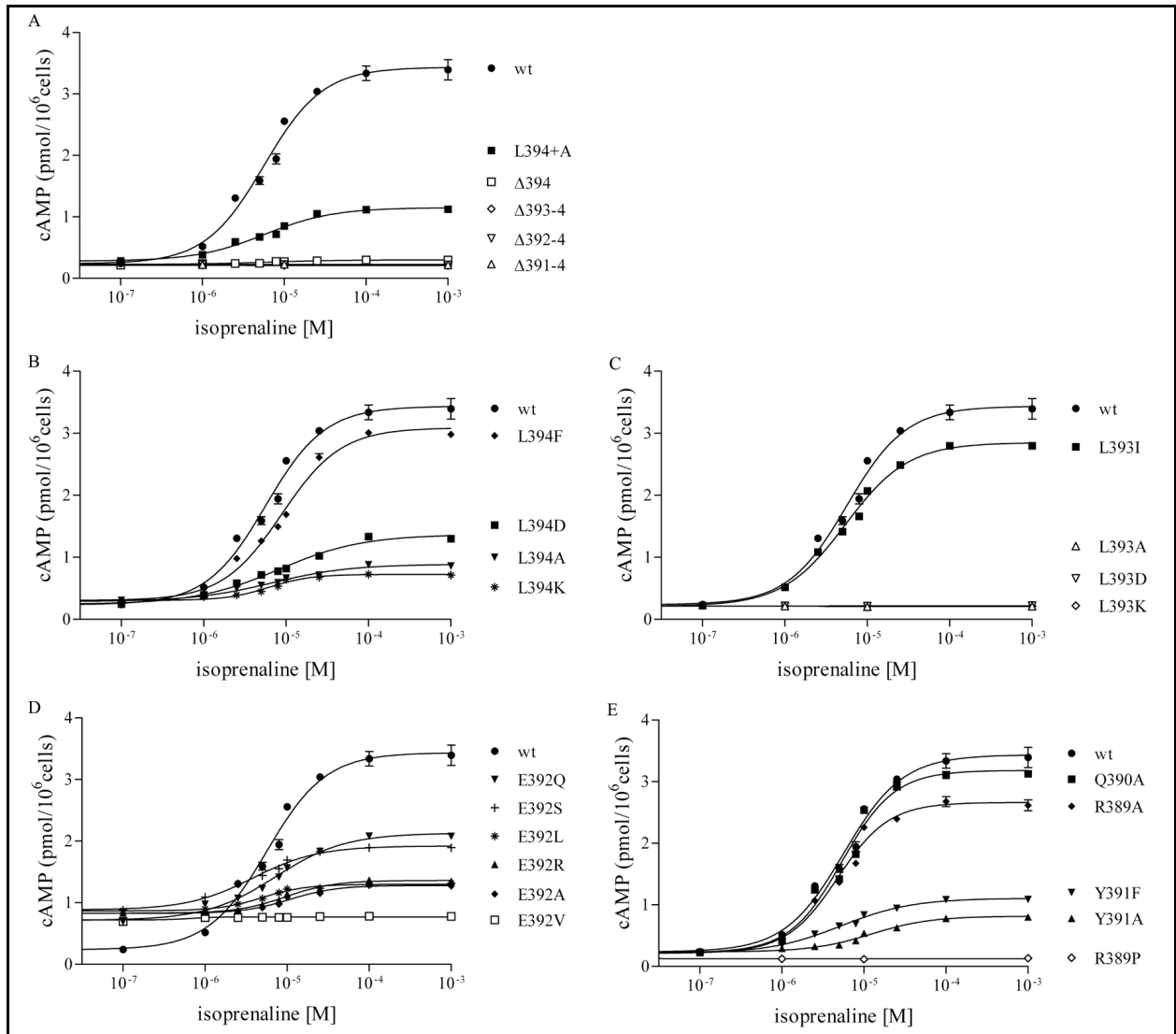


**Figure 2.6.** Dose-response isotherms of cAMP concentrations following isoprenaline stimulation of LHR in the transformed s49 cell lines. All panels include data from hLHR<sup>+</sup>/G $\alpha_s$ <sup>+</sup> wild-type cells. Data from the C-terminal Ala extension, L394+A, and the truncation mutations are presented in panel A, while panels B-E present data from the mutations positions -1 (#394), -2 (#393), -3 (#392), and -4/-5/-6 (#391/#390/#389), respectively. The results show mean  $\pm$  SEM; the numerical values are given in Table 2.1. The results from samples  $\Delta$ 394,  $\Delta$ 393-4,  $\Delta$ 392-4, and  $\Delta$ 391-4 in panel A and from L393A, L393D, and L393K in panel C are superimposed.

Figure 2.6A and Table 2.1. The  $\beta_2$ -AR functionally coupled to G $\alpha_s$  upon extending the C-terminus with an Ala residue (Fig. 2.6A). However, truncation of G $\alpha_s$ , e.g. G $\alpha_s$   $\Delta$ 394,  $\Delta$ 393-394,  $\Delta$ 392-394, and  $\Delta$ 391-394, abrogated  $\beta_2$ -AR signaling. Thus, unlike LHR coupling, the  $\beta_2$ -AR has a requirement for the G $\alpha_s$  C-terminal Leu.

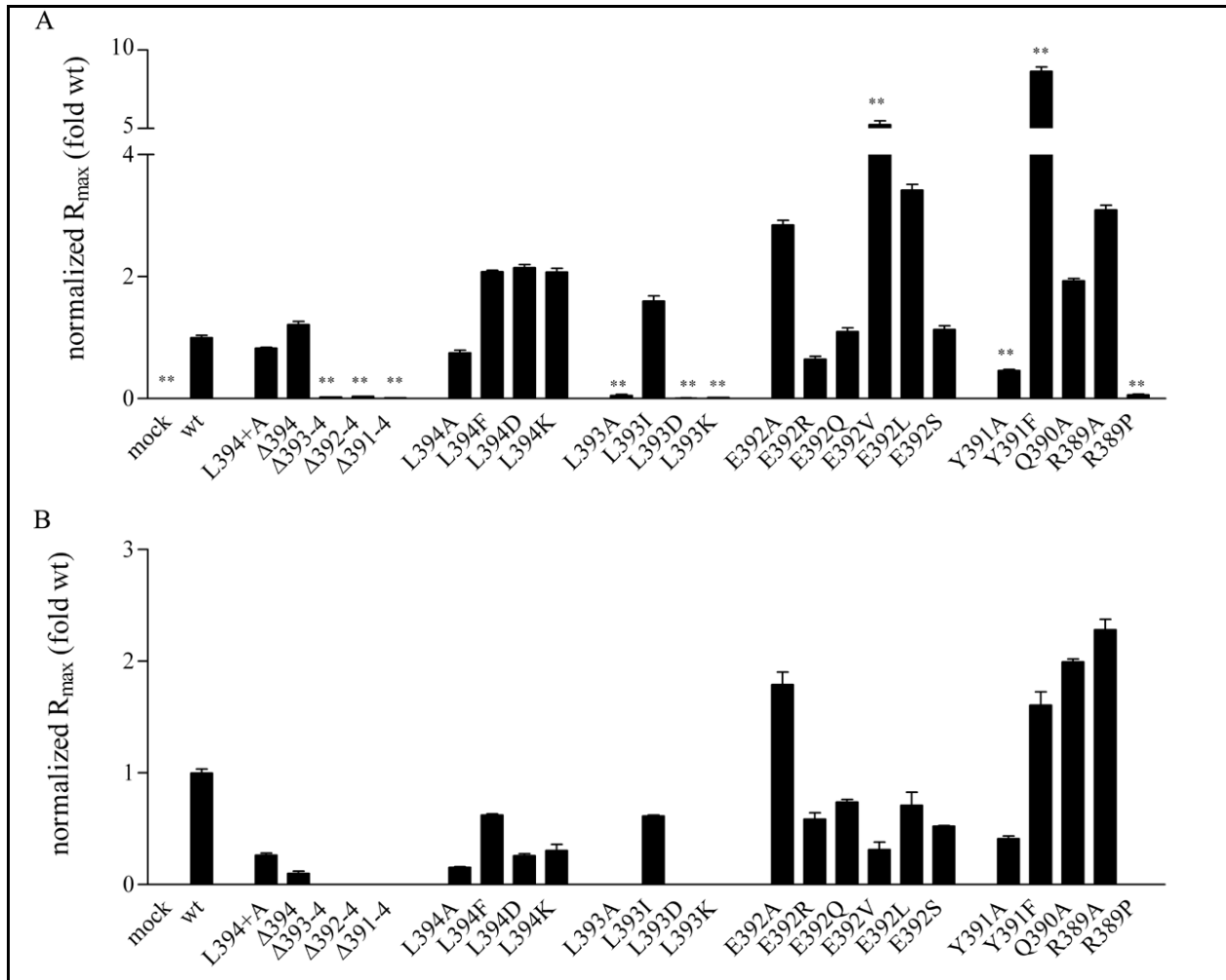


**Figure 2.7.** Efficacy of the transformed s49 ck cell lines corrected for cholera toxin stimulation (indirect assessment of functional protein expressed) and normalized to that of wild-type  $G\alpha_s$ . Normalized, adjusted  $R_{max}$  values are presented for hCG-stimulated cells (A) and for isoprenaline-stimulated cells (B). One-way ANOVA followed by Dunnett's post-test was used for statistical analysis of significance compared to wild-type (wt) (\*\*  $p < 0.001$ ), and all values in (B) are significantly different from wild-type  $G\alpha_s$  (\*\*  $p < 0.001$ ). No signal was detected from samples  $\Delta$ 393-4,  $\Delta$ 392-4,  $\Delta$ 391-4, L393A, L393D, L393K, and R389P.

The substitutions at position -1 (#394) were tolerated, but signaling efficacy was reduced. At position -2 (#393), the L393I mutant was functional, but substitutions with A, D, and K abrogated signaling (Fig. 2.6C). At position -3 (#392), the replacement E392V abolished a response above basal levels, while the other replacements were tolerated (Fig. 2.6D). Probing further into the protein, the Y391A and Y391F replacements were functional, the Q390A and R389A replacements had a minimal effect on signaling, and the R389P mutant, as expected (21), abolished signaling (Fig. 2.6E).

The results from the dose-response curves suggest differences in magnitude of the efficacies between the two receptors, perhaps reflecting expression levels, but there are many similarities when comparing the impact of single replacements between residues 389-393. The major difference between the two receptors appears to occur at L394,  $\beta_2$ -AR being, in general, much more sensitive than LHR to deletion, addition to, and replacement of the C-terminal residue.

In an effort to obtain at least a semi-quantitative comparison of the  $R_{\max}$  values, the following approach was taken. The hCG-mediated  $R_{\max}$  values in Table 2.1 were normalized to that of wild type LHR, and the CTX-mediated  $R_{\max}$  values from Figure 2.4A were also normalized to that of wild type LHR. The ratios of  $(R_{\max})_{\text{hCG}}/(R_{\max})_{\text{CTX}}$  are shown in Figure 2.7A for each of the mutants. The ratios are within 2-2.5-fold that of wild type LHR in all cases except for the mutants E392A,V,L, Y391F, and perhaps R389A, which was just on the borderline. With the exception of R389A, the others are the same mutants that exhibited lower expression as ascertained from CTX stimulation. A similar analysis for  $\beta_2$ -AR, using the data in Table 2.1 and in Figure 2.4A, was also done, but the apparent lower expression of  $\beta_2$ -AR, as judged by the reduced magnitudes of  $R_{\max}$  (Table 2.1), compromised some of the numbers. Yet, the results shown in Figure 2.7B indicate that the majority of the  $(R_{\max})_{\text{iso}}/(R_{\max})_{\text{CTX}}$  values fell within a 2-2.5-fold range except those that obviously expressed poorly, these being  $\Delta 393$ -4,  $\Delta 392$ -4,  $\Delta 391$ -4, L393A,D,K, Y391F, and R389A,P. Thus, most of the values are similar to and thus validate the uncorrected data, particularly for LHR. Due caution will be exercised in interpreting the results from the poorly expressing  $G\alpha_s$  mutants.

## **Discussion**

*The extreme C-terminus of  $G\alpha$  is likely to couple to GPCRs during activation.*

In the structural snapshots of  $G\alpha_s$  (1AZT, 1AZS) and other isoforms of the  $G\alpha$  subunit (1TAG, 1GOT, 2BCJ), the C-termini are adjacent to the N-termini which contain the necessary lipid modifications for membrane association (136,220,267,269,270). From this perspective, the extreme C-terminus may contribute to a membrane-proximal face available for receptor contact (Fig. 2.2B).

Biochemical studies have indicated that the coupling of many G protein isoforms to GPCRs involves the extreme C-terminus of G $\alpha$  subunits (2). Only a few C-terminal residues (eleven or less) were sufficient to confer recognition and/or inhibition by G $_{i/o}$ - and G $_q$ -coupled GPCRs (243,244,271), but many more G $\alpha_s$  residues were required for similar outcomes (85,233,272-275). The evidence suggests that GPCR-G protein interactions may rely upon the G $\alpha$  C-terminus, but this region is not always sufficient for the coupling of all GPCR-G protein systems (2,226). For example, the  $\alpha$ 3- $\beta$ 5 loop of G $\alpha_s$  may contribute to  $\beta_2$ -AR coupling (83). Therefore, the mechanisms of GPCR/G protein coupling may vary between receptors that signal through different families of G proteins.

*s49 ck cells are a suitable platform to measure GPCR/G protein coupling.*

For these studies, hLHR was successfully incorporated into s49 ck cells where it functioned appropriately as judged by cAMP production. The major advantage of this system to study GPCR/G $\alpha_s$  coupling is a lack of endogenous G $\alpha_s$  activity (262,264). Clonal hLHR<sup>+</sup> s49 ck cells expressed approximately 24,000 receptors/cell and exhibited a similar K $_d$  (4.5 nM) for the agonist hCG as reported in the literature (276). Because the EC $_{50}$  (0.34 nM) of the wild type G $\alpha_s$ -transformed hLHR<sup>+</sup> cells is also within reported ranges for hCG-stimulated hLHR activity (10), these experiments suggested that the s49 ck cells tolerated the introduction of hLHR and G $\alpha_s$  proteins and served as an acceptable model system to monitor the coupling of the hLHR to G $\alpha_s$  as measured by cAMP production after agonist stimulation. Also, this system allowed comparison of hLHR/G $_s$  signaling to that of the G $_s$ -coupled, endogenously-expressed  $\beta_2$ -AR, often viewed as a model G $_s$ -coupled GPCR.

*hLHR and  $\beta_2$ -AR require the extreme C-terminal region of G $\alpha_s$  for coupling.*

Truncations at positions -4 (#391), -3 (#392), and -2 (#393), but not -1 (#394) abrogated hCG-stimulated hLHR signaling. These variant G $\alpha_s$  proteins were able to function independently from



$G\alpha_s$	$G\alpha_{s(\text{long})}$	...QRMHLRQYELL	394
	$G\alpha_{s(\text{short})}$	...QRMHLRQYELL	380
	$G\alpha_{\text{olf}}$	...QRMHLKQYELL	381
$G\alpha_{i/o}$	$G\alpha_{t1}$	...IKENLKDCGLF	349
	$G\alpha_{t2}$	...IKENLKDCGLF	353
	$G\alpha_{i1}$	...IKNNLKDCGLF	353
	$G\alpha_{i2}$	...IKNNLKDCGLF	354
	$G\alpha_{i3}$	...IKNNLKECGLY	353
	$G\alpha_{o1}$	...IANNLRGCGLY	353
	$G\alpha_{o2}$	...IAKNLRGCGLY	353
	Gpalp	...IQQNLKKIGII	471
$G\alpha_{q/11}$	$G\alpha_z$	...IQNNLKYIGLC	354
	$G\alpha_q$	...LQLNLKEYNAV	353
	$G\alpha_{11}$	...LQLNLKEYNLV	359
	$G\alpha_{14}$	...LQLNLREFNLV	355
	$G\alpha_{15}$	...LARYLDEINLL	374
$G\alpha_{12/13}$	$G\alpha_{12}$	...LQENLKDIMLQ	380
	$G\alpha_{13}$	...LHDNLKQLMLQ	377

**Figure 2.8.** CLUSTALW alignment of the last eleven amino acids of the human isoforms of the  $G\alpha$  protein and the *S. cerevisiae* Gpalp homolog. The highly-conserved leucine at position -2 is highlighted in light gray. The isoforms are grouped into families according to sequence homology, and the position of the terminal amino acids are indicated to the right of the sequences (277,278).

receptor stimulation, so therefore, most of the extreme C-terminus of  $G\alpha_s$  is necessary for coupling to hLHR. In this model system, the  $\beta_2$ -AR also required this region for functionality, which agrees with previous research (85,279).

*The mechanisms for GPCR/ $G_s$  protein coupling may share some common determinants but appear to differ in general between different  $G_s$ -coupled receptors.*

Since signaling efficiencies are within about 2-2.5-fold that of wild type LHR and  $\beta_2$ -AR, the Discussion will, for purposes of consistency, focus on differences in signaling efficacies. Neither the loss of the C-terminal Leu residue nor the displacement of the C-terminal  $\alpha$ -carboxylate to the anterior position by Ala addition disrupted hLHR signaling, indicating that the hydrophobic side chain and the  $\alpha$ -carboxylate at the -1 position, i.e. the C-terminus (L394), contribute little, if any, to hLHR signaling. As supporting evidence, the A/F/D/K substitutions for L394 also did not alter efficacy. In contrast, the  $\beta_2$ -AR did not tolerate the loss of the terminal residue ( $\Delta$ 394) nor the Ala addition (L394+A) as well as

hLHR, indicating that the chemical nature of the last residue as well as the placement of the terminal  $\alpha$ -carboxylate may be more important for  $\beta_2$ -AR signaling than for hLHR signaling.

The L393A, L393D, and L393K variants were unable to couple to either the hLHR or the  $\beta_2$ -AR, but the L393I protein rescued cAMP production upon agonist stimulation. These results suggest that, for effective coupling, the -2 position (L393) of  $G\alpha_s$  may require a residue with a long, hydrophobic side-chain and does not tolerate substitutions with radically different side-chains. Importantly, the Leu at this position is highly conserved within the family of human  $G\alpha$  proteins (Fig. 2.8). A study monitoring the inhibition of  $A_{2A}$ -adenosine receptor signaling with dominant-negative  $G\alpha_s$  C-terminal synthetic peptides also found the -2 position to be sensitive to substitutions (280). The  $\beta_2$ -AR exhibited similar responses with the variants at position #393 in this study which suggests that the constraint upon this  $G\alpha_s$  residue may be common, and thus necessary, for all  $G_s$ -receptor coupling.

At position -3 (#392), a charged or polar residue (R, Q, or S) does not alter hLHR efficacy, but substitution with hydrophobic residues (A, V, L) increases apparent efficacy, although these mutants exhibited relatively low expression. E392 may thus 'restrict' the hLHR signaling response. Conversely, the substitutions at -3 (#392) had less of an apparent effect upon  $\beta_2$ -AR efficacy, and thus this position may not be as important a determinant for  $\beta_2$ -AR/ $G_s$  coupling. The  $\beta_2$ -AR did not signal through  $G\alpha_s$  E392V, although hLHR did. Therefore, even though the receptors seem to share some requirements for effective  $G_s$ -coupling, the entire set of determinants for coupling may differ for the two receptors, suggesting that each GPCR/ $G_s$  pair may utilize a unique mechanism for coupling.

Because the phenylalanine replacement at position -4 (Y391F) apparently increased hLHR efficacy, the hydroxyl residue at this position may participate in a hydrogen-bonding interaction that restricts full hLHR/ $G_s$  activity. Again, the low expression of this mutant compromises a firm interpretation of the results. A less dramatic but similar effect was seen with this mutant in the  $\beta_2$ -AR system; however, an Ala substitution decreased both hLHR and  $\beta_2$ -AR efficacy. Therefore, this position may be a determinant of receptor/ $G_s$  signaling and may require a residue containing a phenyl ring.

Both the Q390A and R389A substitutions increased efficacy for both receptors, so the polarity of Q390 and the positive charge at R389 may restrict the activity of the two receptors. Because the loss of the positive charge at position -6 does not impair receptor signaling, the R389P mutation likely kinks the end of the  $G\alpha_s$   $\alpha 5$  helix and places the extreme C-terminus into an unfavorable conformation for receptor coupling. The results from the R389 mutations suggest that the maintenance of the helical backbone is important for  $G_s$ -receptor coupling.

*E392 restricts basal activity.*

Cell lines with any substitution at the -3 position (#392) exhibited a significant increase of basal cAMP levels, although the basal level of the 392 truncation line ( $\Delta 392$ -394) was similar to that of the hLHR<sup>+</sup>/mock cell line. This suggests that the Glu at position -3 is important for maintaining the basal level of  $G\alpha_s$  activity. Perhaps the replacement of this residue may encourage a conformational change within the  $G\alpha$  subunit that alters its affinity for GDP and thereby promotes an increase in the rate of nucleotide release and the level of basal activity. (GDP release is the rate-limiting step for G protein activation (65).) Or, if a receptor and G protein are pre-coupled within a signalosome (74,281), the loss of  $G\alpha_s$  E392 may affect the conformation of the receptor and promote the conversion to an active but agonist-less receptor state that then is able to activate the altered G protein. The negative charge at this position, however, is dispensable for ligand-induced, receptor-mediated signaling.

*Manipulation of the  $G\alpha_s$  C-terminus does not abrogate  $G\alpha_s$  function.*

Perturbation of  $G\alpha_s$  may not only impact the coupling relationship with cognate receptors, but may also disturb the structure and stability of the protein and thus the manipulation of guanine nucleotides, the affinity for  $G\beta\gamma$ , localization, and association with the effector adenylate cyclase. The crystal structures of the  $G\alpha_s$  subunit suggest that the -3, -2, -1 ( $G\alpha_s$  E392, L393, L394) positions extend from the globular protein structure, and therefore these residues are not likely to influence global protein

folding. In the crystal structures, the extreme C-terminus lies ~35-40Å from the nucleotide binding pocket (220,267), and none of the C-terminal residues have been implicated in the association with Gβγ nor the effector adenylate cyclase (136,267,282-284). If Gα<sub>s</sub> retains its N-terminal palmitoylation and associates with Gβγ, it targets properly to the plasma membrane (285). Therefore, it was hypothesized that the manipulation of the extreme C-terminus is likely to only affect the receptor-coupling relationship.

Indeed, all of the Gα<sub>s</sub> variant cell lines produced cAMP upon CTX stimulation. However, the CTX-mediated activity was significantly different for all Gα<sub>s</sub> variants when compared to wild-type Gα<sub>s</sub> cells and did not correlate with total protein expression levels as measured by Western blotting (Fig. 2.3). That CTX may require the native C-terminus to efficiently modify Gα<sub>s</sub> into its ADP-ribosylated, permanently activated form cannot be ignored. Also, the Western blots only indicated an average amount of translated protein. From these results, the Gα<sub>s</sub> C-terminal truncations and mutations may have disturbed properties of the protein independent from receptor coupling; regardless, the variant proteins were functional, and when the R<sub>max</sub> values, representative of receptor efficacy, were corrected with the corresponding CTX-stimulated activity for each variant and normalized to that of the wild-type protein, the overall trends remained similar to the uncorrected data.

That some variants could not produce R<sub>max</sub> levels similar to that of wild-type Gα<sub>s</sub> suggested that the mutations may have affected properties of the proteins independent from receptor coupling, e.g. by altering kinetics of the interaction with adenylate cyclase. Many of the Gα<sub>s</sub> variants that exhibited CTX-stimulated cAMP responses significantly higher than wild-type Gα<sub>s</sub>, however, also demonstrated increased R<sub>max</sub> values upon hCG stimulation when compared to wild-type. The corrected efficacies of these variants appear comparable to hLHR signaling through wild-type Gα<sub>s</sub>. Interestingly, the same cannot be said for the efficacy of normalized β<sub>2</sub>-AR values. The two receptors responded differently to certain Gα<sub>s</sub> variants, and these differences may, again, indicate that the mechanisms for G<sub>s</sub>-coupling may be distinct for individual receptors.

## *Conclusions*

These studies in s49 ck<sup>-</sup> cells demonstrated that hLHR signaling requires amino acid residues at the extreme C-terminus of G $\alpha_s$ , excluding L394. The  $\beta_2$ -AR also couples to this region, which agrees with previous analyses. The orientation of the end of the  $\alpha 5$  helix is important for receptor recognition, and, surprisingly, many of the terminal residues tolerated point mutations. However, because the hLHR and  $\beta_2$ -AR responded differentially to some of the variant G $\alpha_s$  proteins, this work suggests that not only may the mechanisms of GPCR/G protein coupling vary between receptors that recognize different families of G proteins, the mechanisms may also vary between receptors that couple to the same isoform of G protein. The lack of primary sequence determinants for receptor/G protein coupling supports this conclusion (2-5).

A patient with Albright hereditary osteodystrophy was determined to have an Arg to His mutation within the C-terminus of G $\alpha_s$  at position 385 that impaired G $\alpha_s$  function (286). No other naturally-occurring mutations within this region have been reported which suggests that the region has experienced selective pressure during evolution. The results presented here imply that although the region may tolerate substitution during the measurement of one type of receptor-coupling event, the wild-type sequence must remain intact for recognition by all G $_s$ -coupled receptors.

The recent solution of opsin in complex with a peptide corresponding to the last eleven amino-acids of transducin (G $\alpha_t$ ) illustrates the relationships between the terminal G $\alpha_t$  residues and the G protein binding pocket of opsin. The conserved Gly at position -3 in the G $\alpha_{i/o}$  family of G proteins permits the formation of an open reverse turn, an  $\alpha_L$ -type C-capping motif (249). There is not a Gly in this position of wild-type G $\alpha_s$ , and therefore, it most likely cannot form this type of fold. Thus, G $_s$ -coupled receptors probably require a different G protein conformation at the extreme C-terminus for coupling. Peptides corresponding to the extreme C-terminus of G $\alpha_s$  form complete helices in solution without a capping motif (287). Perhaps, for effective receptor/G $_s$  coupling, the backbone of the G $\alpha_s$  C terminus should form a helix.

In crystal structures, the  $\alpha 5$  helix of  $G\alpha_s$  bends at position -17 from the C-terminus, bringing the C-terminus towards the globular protein structure—specifically, near the  $\alpha 2$ - $\beta 4$ ,  $\alpha 3$ - $\beta 5$ , and  $\alpha 4$ - $\beta 6$  loops. The  $\alpha 3$ - $\beta 5$  loop has been implicated as important for  $\beta_2$ -AR/ $G_s$  coupling (83). However, the  $\alpha 5$  helix of  $G\alpha_{i/o}$  proteins remains straight. Much evidence indicates that the extreme C-terminus of  $G\alpha_{i/o}$  proteins is sufficient for receptor coupling. A recent model of the activation of  $G\alpha_{i1}$  by rhodopsin suggests that a rigid-body rotation and translation of the  $G\alpha$   $\alpha 5$  helix destabilizes the  $\beta 6$ - $\alpha 5$  loop, and thus promotes GDP-release and G protein activation (89). Perhaps the mechanism of activation, an event initiated at the receptor-binding interface and translated to the nucleotide pocket, is conserved in general for all isoforms of  $G\alpha$  proteins, but the specific G-protein interface for each receptor is slightly different. General points of contact may be shared for GPCRs that couple to the same families of G proteins, but for each receptor/G protein pair, the precise determinants and the strength of their contributions may vary (2,226). If the coupling interface is as unique for each GPCR/G protein pair as these studies suggest, drug discovery applications could potentially target these relationships to improve the specificity of engineered therapeutics.

## CHAPTER 3

### THE HUMAN LUTEINIZING HORMONE RECEPTOR EXHIBITS PARTICULAR PHYSIOCHEMICAL PROPERTIES THAT IMPAIR THE CHARACTERIZATION OF ITS SIGNALING ENVIRONMENT

Although evolution has endowed the GPCR with the ability to regulate numerous physiological processes and has conserved many physiochemical properties throughout the large protein family, considerable variation has occurred within the GPCR structural constraint to impart a diversity that permits the recognition of dissimilar ligand types and the response of different signaling networks (1). Because the study of these dynamic membrane proteins is difficult, the characterization of a GPCR trait or behavior can be a landmark discovery that tempts researchers to designate it a conserved GPCR property that exists within other GPCR systems. Often, however, the likelihood that this feature is not conserved is overlooked.

This chapter describes the application of experimental procedures that have been used to successfully explore the molecular landscape of a few GPCRs to examine that of the hLHR. These attempts to provide novel and useful information collected some data, but the lack of sufficient positive results did not warrant further investigation. Properties acquired by the hLHR during evolution may have prevented these analyses; for example, the addition of the large, leucine-rich repeat containing extracellular ‘arm’ to the hallmark GPCR heptahelical transmembrane domain of hLHR may have mitigated the fitness of the experimental approaches. Sensitivity issues and technical challenges were also encountered.

## ***The use of Förster Resonance Energy Transfer (FRET) to probe the molecular environment proximal to the hLHR***

### ***Introduction***

The existing paradigm of GPCR activation suggests that once inactive receptors are stimulated, they bind to and translate activity to the heterotrimeric G proteins which then dissociate from the receptor and each other to mediate intracellular signaling events (252). Co-immunoprecipitation, kinetic and, more recently, resonance energy transfer (RET) experiments have suggested that the G proteins may pre-couple to inactive GPCRs and that the complex may remain associated as a 'receptosome' during stimulation (67,73-78,253,281,288,289). Also, these methods have been used to measure the self-association of many GPCRs, suggesting that this class of proteins may, at some point in their lifetimes, exist as dimers or higher-order oligomers (290,291).

RET experiments employ bioluminescent (BRET) or fluorescent molecules to probe the proximal molecular environment with a ~100 Å 'ruler' and may therefore be used to investigate relationships between proteins or other molecules within live cells (288). In live cells, most often proteins of interest are fused to bioluminescent or fluorescent proteins that are suitable RET donor/acceptor pairs. Efficient RET partners display an extensive overlap of the donor emission and acceptor excitation spectra. The variants of the *Aequorea victoria* green fluorescent protein, cyan fluorescent protein (CFP) and yellow fluorescent protein (YFP), are a commonly used FRET donor/acceptor pair because of the efficient overlap of their spectra, their photostability in live cells, and their ability to retain a separate, native fold when incorporated as fusions with other proteins (292-294).

To better understand the molecular environment of the hLHR, FRET experiments were designed to examine its relationship with the stimulatory G protein ( $G_s$ ), its cognate signaling partner, as well as any predisposition of the receptor to dimerize. Fusions with both CFP and YFP were made at the C-terminus of hLHR, and because both the N- and C-termini of  $G\alpha_s$  are important for its function, internal fusions of CFP and YFP were made that did not affect its activity (97). With this approach, once associations between wild-type proteins are established, the application of site-directed mutagenesis may



implicate residues that mediate the interaction between these proteins and thus the molecular map of the hLHR 'receptosome' should expand.

### *Experimental Procedures*

#### *i. Materials*

HEK-293 cells were cultured according to ATCC standards with 10% newborn calf serum (Invitrogen) instead of 10% fetal bovine serum. Transfections were performed with Lipofectamine 2000 as per manufacturer's instructions (Invitrogen). Lab-Tek II four-chambered coverglasses and 96-well plates coated with poly-D-lysine were purchased from Fisher (Pittsburgh, PA).

#### *ii. cDNA plasmids*

An internal, in-frame fusion of human  $G\alpha_s$  cDNA with CFP cDNA (h $G\alpha_s$ -iCFP) was designed as described in (97) except with the method of overlap PCR (263) and cloned into pcDNA6.2Topo (Invitrogen). The cDNA for hLHR and the  $\beta_2$ -AR were amplified and each was cloned into Vivid Colors pcDNA6.2/C-YFP-GW/TOPO (Invitrogen) to create receptor-YFP fusions or were fused to CFP via the method of overlap PCR and cloned into pcDNA6.2Topo to create receptor-CFP fusions. An in-frame, N-terminal fusion of YFP with the human  $G\beta_1$  was created with the method of overlap PCR and cloned into pcDNA6.2Topo. CFP and YFP cDNA were amplified and cloned into pcDNA6.2Topo. CFP cDNA was cloned into the Vivid Colors vector to produce a cytosolic CFP-link-YFP fusion connected by a 17 amino acid residue linker. The cDNA for the transmembrane domain of CD8 was cloned into the Vivid Colors vector to create a truncated CD8-YFP fusion as in (73).

For bimolecular fluorescence complementation (BiFC) experiments, portions of the cDNA encoding YFP were fused internally to  $G\alpha_s$  (in the manner described for the CFP internal insertion) and C-terminally to hLHR and  $\beta_2$ -AR. Three different pairs of complements were designed. The first was an N-terminal YFP fragment consisting of residues 1-158 paired with a YFP fragment consisting of residues

159-238, the second was N-YFP 1-172/C-YFP 155-238, and the third was N-YFP 1-172/C-YFP 173-238 (295-297).

The cDNA for CD8 was purchased from ATCC, (Manassas, VA), the cDNA for the  $\beta_2$ -AR was purchased from the Missouri S&T cDNA Resource Center (Rolla, MO), the cDNAs for  $G\beta_1$  and  $G\beta_2$  were a generous donation from Dr. S. Hooks (UGA, Athens, GA), the cDNA for the CFP- $G\gamma_2$  was from Dr. S. R. Ikeda (NIH, Bethesda, MD), and the cDNAs for the rat  $G\alpha_s$ -iCFP, r $G\alpha_s$ -iYFP, and the BiFC pair YFP-N- $G\beta_1$ /YFP-C- $G\gamma_2$  were from Dr. C. H. Berlot (Geisinger Clinic, Danville, PA).

### *iii. Transfection of HEK-293 and HEK-293FT cells*

$2.5 \times 10^5$  cells were transiently-transfected with various levels of receptor and heterotrimeric G protein cDNA and Lipofectamine 2000 at a ratio of 3:1 (105 ng combined cDNA:315 nL Lipofectamine 2000) in a total volume of 500  $\mu$ L and plated into each well of a Lab-Tek II four-chambered coverglass coated with 0.02% gelatin. The various ratios of  $G\alpha$ : $G\beta$ : $G\gamma$  were 2:1:1 (97), 1:1:1, 3:1:1, 1:2:2, and 1:3:3. Phenol red-free DMEM was used during the transfection and visualization of the cells. For transfections with G protein-fluorescent fusions, cDNA encoding the other subunits of the G proteins was always included to promote plasma membrane localization (285,298). When receptor cDNA was transfected in conjunction with G proteins, the ratio was 2:6:3:3 (97), or was adjusted as necessary to fulfill a 105 ng total mass of cDNA/transfection. For the creation of stable lines, HEK-293 cells expressing h $G\alpha_s$ -iCFP or hLHR-CFP were selected after a period of two weeks post-transfection with the addition of 10  $\mu$ g/mL blasticidin to the complete growth medium.

For the transient transfection of GPCR-fluorescent protein fusions, a 1:1 cDNA ratio of receptor-CFP and receptor-YFP proteins was used, and a total of 50 ng plasmid and 150 nL of Lipofectamine 2000 were added to the transfection reaction unless indicated otherwise.

#### *iv. Confocal imaging and FRET analysis*

Single cells were imaged either 24 or 48 hours after transfection with a Zeiss LSM 510Meta Axiovert 200 confocal microscope with an apochromat 100x/1.46NA oil objective. The argon laser was tuned to 458 nm for CFP excitation and 514 nm for YFP excitation. CFP emission was monitored with a BP filter between 475 nm and 525 nm and YFP emission was monitored with a LP filter of 530 nm. Single-cell images were analyzed with the method of sensitized emission using the FRET macro v.4.1 based upon the method of Xia and Liu (299). Bleed-through of the fluorescent emissions was corrected with samples that contained only CFP or YFP alone, and background signal was subtracted from areas of cells that did not express the fluorescent proteins. Regions of interest (ROIs) were created to analyze the appropriate areas of cells expressing the fluorescent proteins. For the analysis of cytosolic proteins, the ROIs did not include the plasma membranes. For the analysis of GPCRs, care was taken to create ROIs that only included plasma membranes.

#### *v. Multi-cell measurements of fluorescence*

Cells were transfected as above and plated into triplicate wells of a 96-well plate coated with poly-D-lysine and after 48 hours were imaged in a Gemini EM microplate spectrofluorometer (Molecular Devices, Sunnyvale, CA). For CFP excitation the monochromator was set between 430 and 440 nm, for YFP excitation it was set between 510 and 520 nm, for CFP emission it was set between 490 and 500 nm, and for YFP emission it was set between 525 and 535 nm. Bleed-through was corrected for with samples expressing either the CFP or YFP fusions, and background was subtracted from mock-transfected samples that did not express fluorescent proteins. Three replicates of each sample were measured and the data were analyzed with Excel.

## Results

### *i. FRET was detected between a cytosolic CFP-link-YFP fusion protein*

To measure whether FRET was detectable using the chosen fluorescent donor/acceptor pair and imaging system, a control experiment was performed with cytosolic CFP and YFP proteins and a cytosolic fusion protein that contained both YFP and CFP separated by a 17 amino acid residue linker (Figure 3.1). No FRET was detected between co-expressed CFP and YFP proteins, but, as expected, a significant increase in FRET was measured in cells expressing the CFP-link-YFP fusion protein (Fig. 3.1, 3.2) (300). Therefore, the experimental design was adequate to detect FRET between the CFP/YFP pair.

### *ii. Proper plasma membrane localization of the heterotrimeric G protein-fluorescent fusions was not always observed*

To confirm that FRET can be measured between associated proteins at the plasma membrane, three different donor/acceptor pairs of G protein fluorescent fusions were analyzed with CD8-YFP as a negative control: hG $\alpha_s$ -iCFP/YFP-G $\beta_1$ , rG $\alpha_s$ -iYFP/CFP-G $\gamma_2$ , and YFP-G $\beta_1$ /CFP-G $\gamma_2$ . In cells expressing hG $\alpha_s$ -iCFP, little plasma membrane expression was detected; rather, a diffuse pattern of fluorescence was seen (Fig. 3.3A). Because G $\beta\gamma$  is necessary to target G $\alpha$  to the plasma membrane (285,298), the ratios of G $\alpha_s$ : $\beta_1$ : $\gamma_2$  cDNA were varied during transfection to optimize expression of hG $\alpha_s$ -iCFP at the plasma membrane (see *Experimental procedures*). None of the ratios rescued the appropriate localization of hG $\alpha_s$ -iCFP (Fig. 3.3A and data not shown). HEK-293 cells stably expressing hG $\alpha_s$ -iCFP exhibited no measurable CFP signal (data not shown). YFP-G $\beta_1$  was expressed at the plasma membrane (Fig. 3.3B). Because proper membrane localization of hG $\alpha_s$ -iCFP was never observed, rG $\alpha_s$ -iYFP was used as an acceptor for a CFP-G $\gamma_2$  donor. rG $\alpha_s$ -iYFP localized to the plasma membrane of some but not all transfected cells (Fig. 3.3C), indicating that proper localization of exogenous G $\alpha_s$ -fluorescent protein

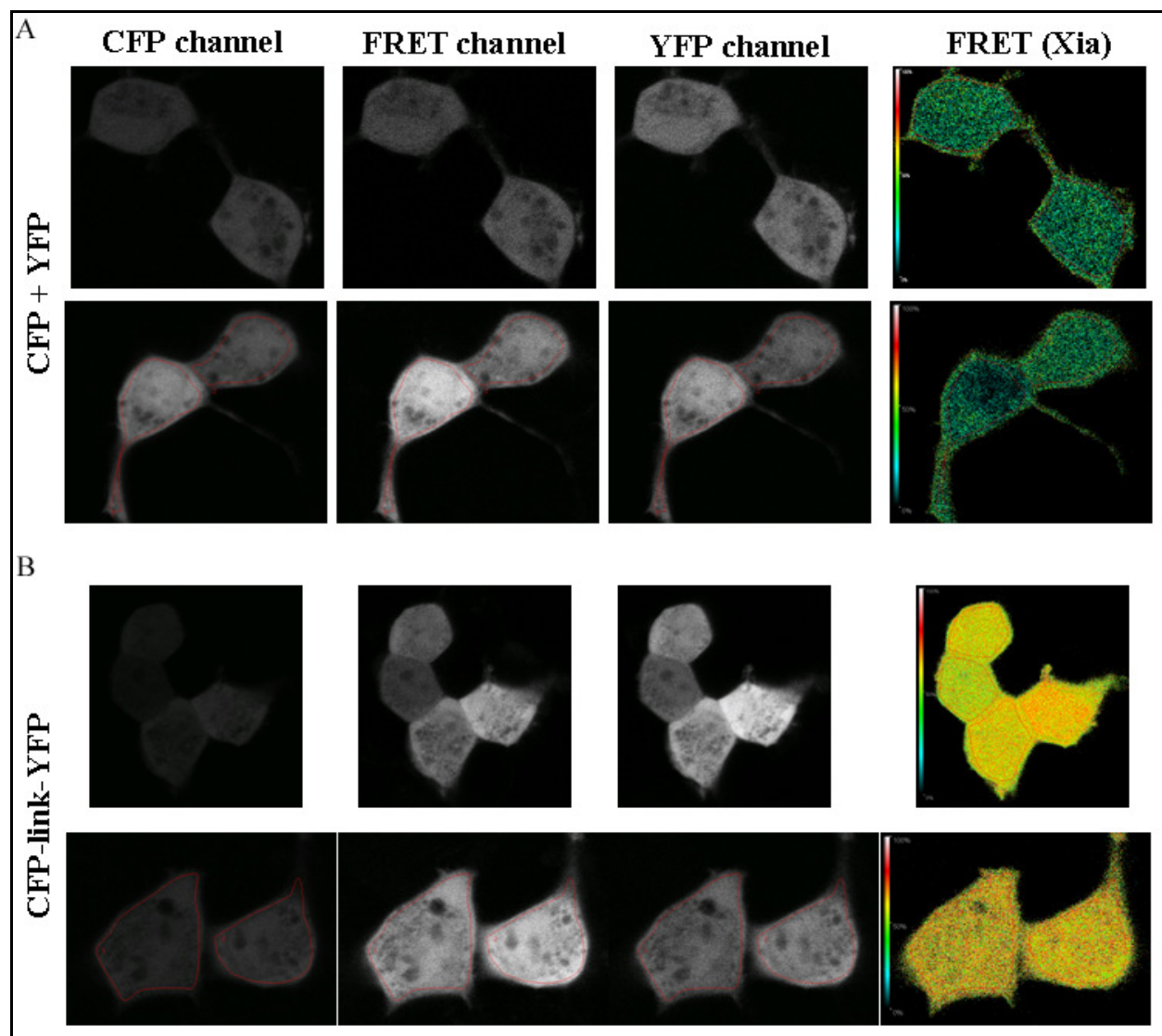


**Figure 3.1.** Images from representative FRET experiments with co-expressed cytosolic CFP and YFP (A) and the fusion CFP-link-YFP protein (B). Settings for excitation and emission for each of the channels were described in *Experimental procedures*. ROIs are indicated by the red lines in the N-FRET images. An increase in FRET is represented qualitatively by a color change from blue to red.

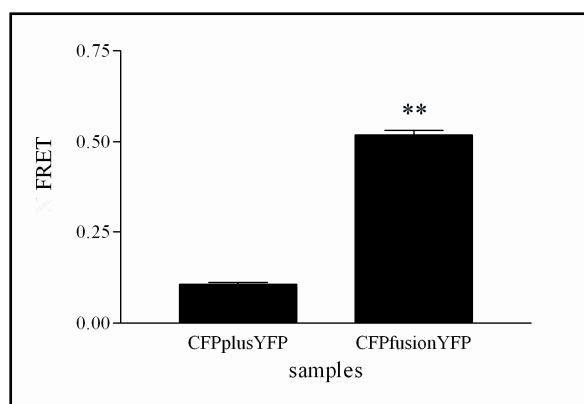


**Figure 3.2.** Quantitative analysis of FRET experiments with co-expressed cytosolic CFP and YFP (CFPplusYFP) and the CFP-link-YFP fusion (CFPfusionYFP) protein. An unpaired t-test was used for the statistical analysis (\*\*  $p < 0.0001$ );  $n = 31$ .

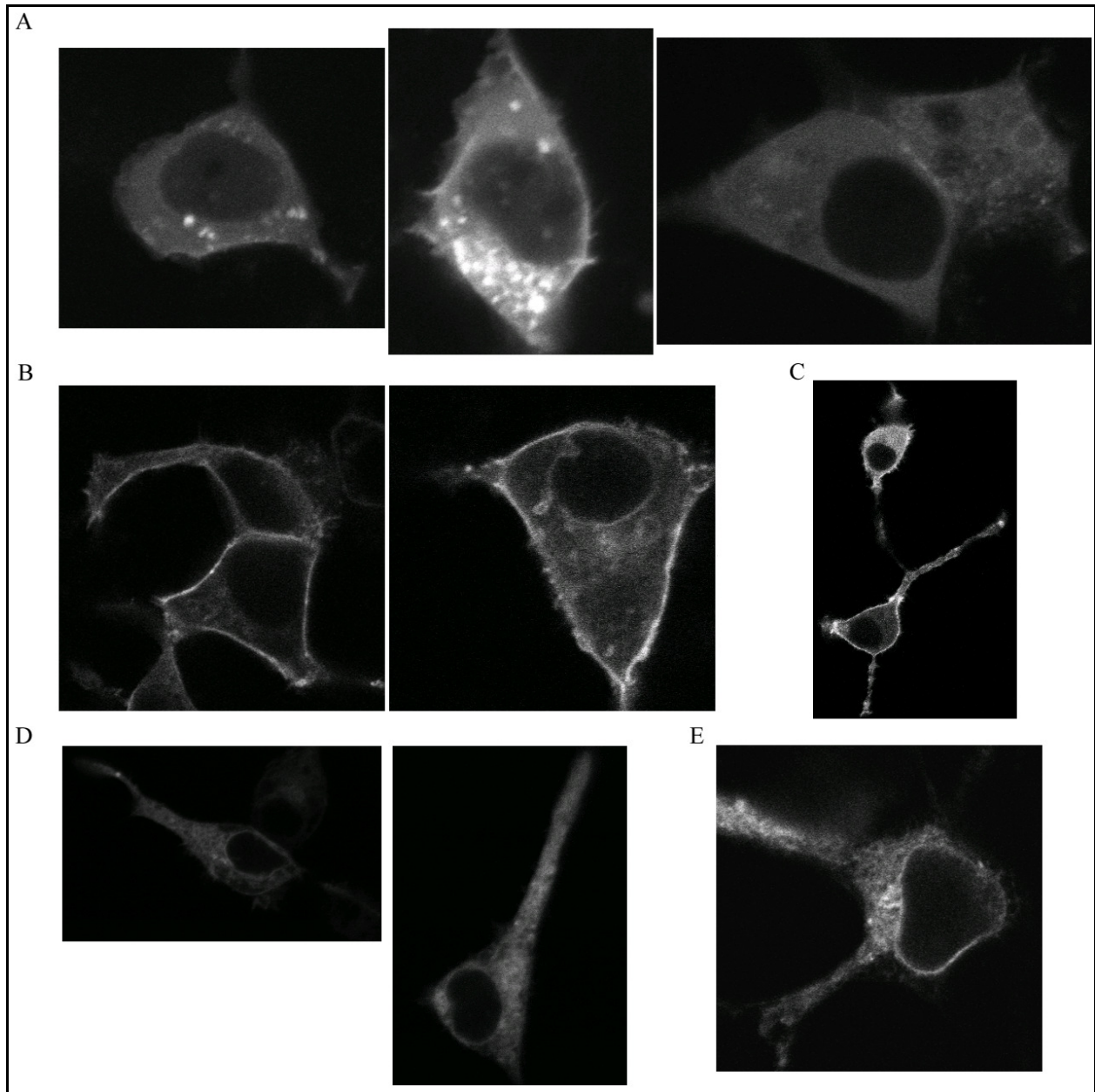


**Figure 3.3.** Images of cells expressing fusions of heterotrimeric G proteins and CFP or YFP. *A.* Three representative images of non-plasma membrane expression of hG $\alpha_s$ -iCFP. *B.* YFP-G $\beta_1$  localizes to the plasma membrane of cells. *C.* rG $\alpha_s$ -iYFP localizes to the plasma membrane of one transfected cell but not in the adjacent cell. Neither CFP-G $\gamma_2$  (*D*) nor CD8-YFP (*E*) localize to the plasma membrane. All samples were co-expressed with non-fluorescent heterotrimeric G protein partners to promote plasma membrane localization as described in *Experimental Procedures*.

fusions may correlate with expression levels. The expression of CFP-G $\gamma_2$  is depicted in Figure 3.3D.

Also, the expression of CD8-YFP was not seen exclusively at the plasma membrane as expected (Fig.

3.3E). Therefore, none of these protein pairs are acceptable for FRET analysis in this experimental design.

When a GPCR was added to the transfection mix at a ratio of 6:2:3:3 (97), proper hG $\alpha_s$ -iCFP localization was also not observed (data not shown). Switching the FRET acceptor to the G $\alpha$  subunit to (rG $\alpha_s$ -iYFP) for an hLHR-CFP donor was problematic because the hLHR-CFP plasma membrane signal was also very weak (see the following discussion).

*iii. Proper plasma membrane localization of the hLHR-CFP fusion protein was not observed*

To measure GPCR dimerization at the plasma membrane, C-terminal CFP and YFP fusions of the  $\beta_2$ -AR were expressed in HEK-293 cells. No increase in FRET was observed over a negative control (hLHR) in these samples although RET has been measured for this receptor in other reports (Fig. 3.4 and data not shown) (98). To test if hLHR-CFP and hLHR-YFP demonstrate FRET, the fusion proteins were expressed, but only a very faint hLHR-CFP signal was measured at the plasma membrane (Fig. 3.5). The ratio of hLHR-CFP:hLHR-YFP was increased to 3:1, but no difference was seen (data not shown). If the total amount of receptor cDNA was increased in the transfection reaction (to a maximum limit of 100 ng), the receptors did not properly localize to the plasma membrane (data not shown). Cells stably expressing the hLHR-CFP construct did not exhibit a CFP signal although the cells were resistant to antibiotic selection and specifically bound  $^{125}$ I-hCG (data not shown). Following procedures with BRET constructs, a variant of HEK-293T cells were transfected at the reported levels with the hLHR fusion constructs (73,76). Very little plasma membrane localization can be visualized although the fluorescent signal is quite strong in the cellular interior (Fig. 3.6).



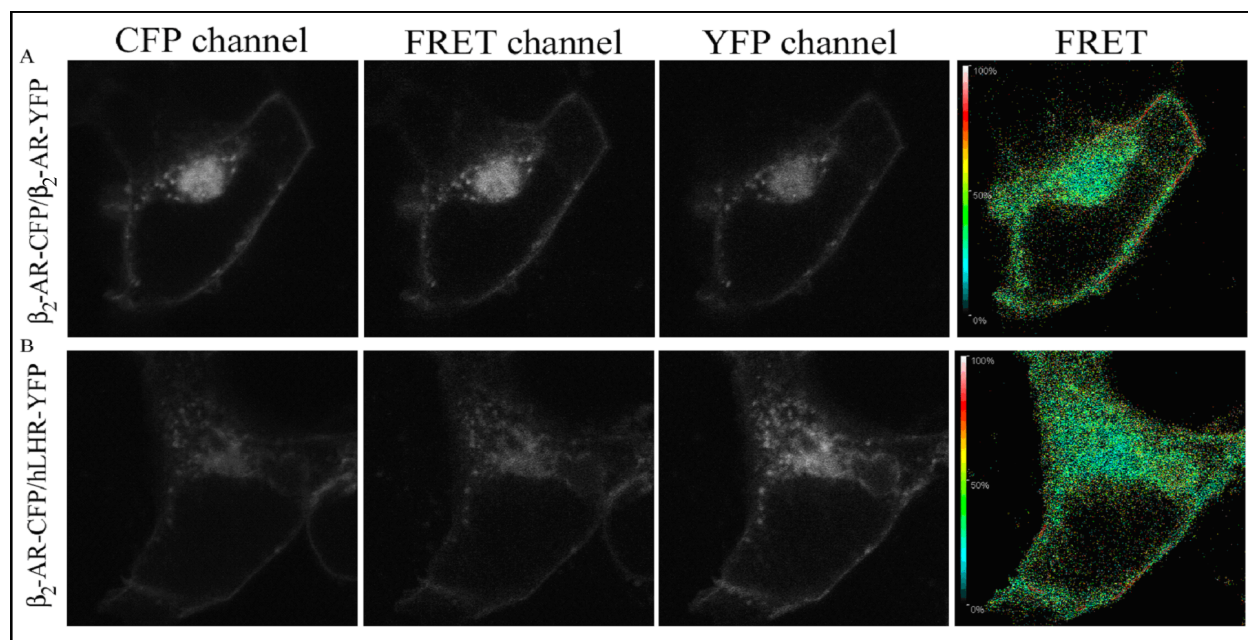


**Figure 3.4.** Representative FRET analysis of the  $\beta_2$ -AR. No difference in the FRET calculations was observed between samples expressing CFP and YFP C-terminal fusions with  $\beta_2$ -AR (A) and  $\beta_2$ -AR-CFP and hLHR-YFP (B).

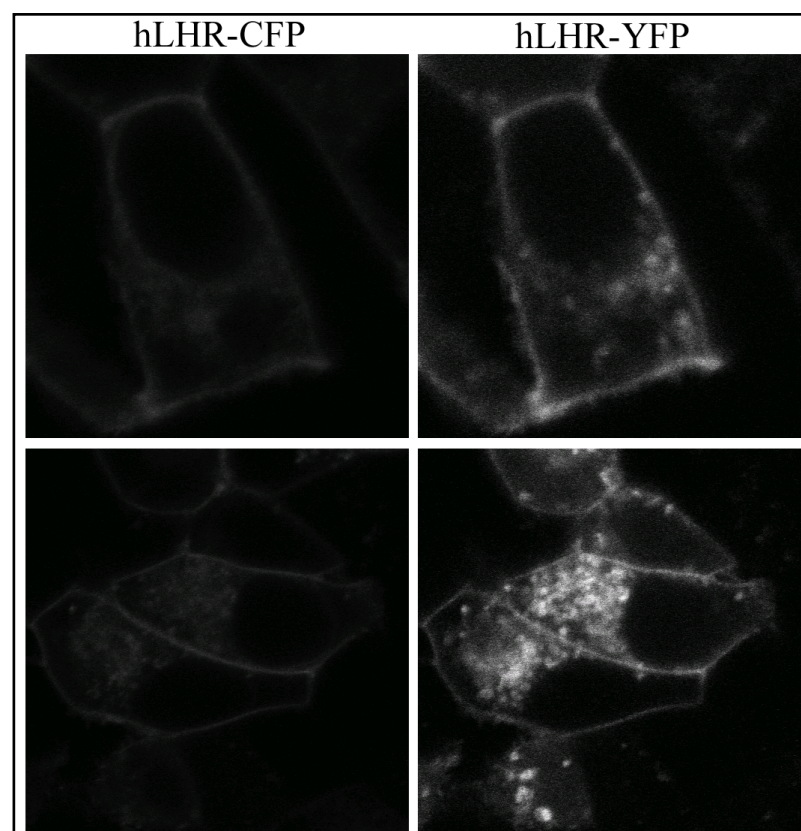


**Figure 3.5.** The signal of hLHR-CFP (left column) is less intense than that of hLHR-YFP (right column) when an equimolar ratio of the two fluorescent fusion proteins is expressed in HEK-293 cells.

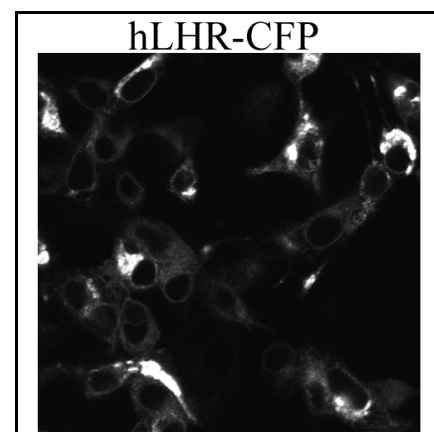


**Figure 3.6.** Expression pattern of hLHR-CFP in a variant of HEK-293T cells.



*iv. FRET was not observed in a multi-cellular measurement of heterotrimeric G protein-fluorescent fusions or between GPCR-fluorescent fusion proteins*

To better approximate the conditions of the published BRET experiments with heterotrimeric G proteins and GPCRs, the fluorescent protein fusions were transfected into HEK-293T cells, plated in 96-well plates, and observed with a microplate spectrofluorometer. Again, FRET was measured between the CFP-YFP fusion protein but not between co-expressed CFP and YFP. None of the other pairs of fusion proteins demonstrated measurable FRET in this experimental design (data not shown).

*v. BiFC was not measured between heterotrimeric G proteins, between  $G\alpha_s$  and GPCRs, nor between  $\beta_2$ -AR dimers*

Because  $G\beta\gamma$  and a few GPCRs exhibit bimolecular fluorescence complementation (BiFC) (295-297), BiFC pairs of fusion proteins with heterotrimeric G proteins and GPCRs were created as described in *Experimental procedures*. Although the BiFC pair YFP-N- $G\beta_1$ /YFP-C- $G\gamma_2$  exhibited a strong plasma membrane signal, none of the other BiFC pairs (of heterotrimeric G protein partners, GPCR partners, and G protein/GPCR partners) that were tested fluoresced (data not shown).

## *Discussion*

*i. Differences exist between BRET and FRET approaches for G protein and GPCR analysis*

Most reports of RET between G proteins and receptors or between GPCR dimers use a BRET approach with *Renilla* luciferase/YFP as the donor/acceptor pair and measure an average fluorescent signal from  $10^5$  detached (albeit live) HEK-293T cells (73,76,301,302). FRET analyses that measure the signal derived from the plasma membrane of individual cells are much less common (253,254,303,304), and very few analyze the relationships of  $G\alpha_s$  with either  $G\beta\gamma$  or with GPCRs (305). The advantage of the experimental design described herein is the measurement of appropriate microenvironments within single, live, adherent cells. The apparent disadvantage, however, is a weak or mislocalized CFP signal.

*ii. The flaws of the CFP/YFP donor/acceptor pair*

The CFP/YFP donor/acceptor pair and the single-cell confocal-LSM approach were suitable to measure FRET (Figure 3.1). However, the fluorescent fusions of hG $\alpha_s$ -iCFP, hLHR-CFP, and CFP-G $\gamma_2$  did not express well at the plasma membrane under these conditions, which rendered FRET analysis between both the set of heterotrimeric G proteins as well as G $\alpha_s$  and a GPCR (such as hLHR) impossible. Therefore, the impact of mutations within the G $\alpha_s$  subunit on its relationship with hLHR as well as G $\beta\gamma$  could not be determined with this approach.

The quantum yield of the CFP fluorescent signal is approximately half that of YFP and the signal is less photostable *in vivo* than other GFP-variant proteins (292,306). Also, the argon laser line available with most LSM systems excites CFP at 458 nm, but the excitation maximum for CFP is 433 nm. Therefore, many researchers have turned to later-generation versions of CFP and YFP such as Cerulean and Venus for more efficient FRET analysis *in vivo* (292,307,308). A better choice, however, for a fluorescent donor for YFP/Venus may be the engineered protein monomeric Teal Fluorescent Protein (mTFP). Its quantum yield approximates that of Venus and its intense signal (with minimal spectral bleed-through and increased photostability *in vivo*) is optimally excited at 458 nm, a wavelength that is commonly available to researchers (309). The emission of mTFP is red-shifted compared to that of CFP or Cerulean and is therefore an even more efficient donor for the YFP/Venus acceptor. The use of the mTFP donor may overcome the limitations of this experimental approach to i) effectively examine the relationships between hLHR and G $\alpha_s$  to more precisely define the translation of activation of hLHR to G $\alpha_s$  and ii) measure hLHR dimerization.

*iii. The manner of G $\alpha_s$  association with G $\beta\gamma$  and GPCRs may impair RET measurements*

When G $\alpha_s$  is studied in RET experiments, the RET measured between G $\alpha_s$  and G $\beta$  or G $\gamma$  is less than that between G $\alpha_{i/o}$ /G $\alpha_q$  with G $\beta$ /G $\gamma$  or than that between the G $\beta$  and G $\gamma$  pair. Similar results are seen in RET experiments measuring G $\alpha$  association with GPCRs, and thus the preference is to measure

either a  $G\beta$  or  $G\gamma$  interaction with GPCRs (73,76). Importantly, the placement of the internal fluorescent fusion within  $G\alpha_{i/o}$  appears to affect the RET measured (76). Perhaps the association of  $G\alpha_s$  with  $G\beta\gamma$  is not as similar to that of other  $G\alpha$  isoforms with  $G\beta\gamma$  as has been inferred from the crystal structures of heterotrimeric G proteins—no crystal structure  $G\alpha_s$  in complex with  $G\beta\gamma$  exists—which may explain the difference in RET measured between  $G\alpha_s$  and  $G\beta\gamma$ .

### *iii. FRET analyses with hLHR*

The problems with the current studies appear to have originated with the CFP fusion proteins. When the transfected cells synthesized  $hG\alpha_s$ -iCFP, hLHR-CFP, and CFP- $G\gamma_2$ , the CMV-driven over-expression appeared to overwhelm the cellular machinery and the proteins subsequently mislocalized. If the transfection reactions included a smaller amount of cDNA or if stable transformants were selected, the resulting CFP signal was either too weak for FRET analysis or disappeared entirely. HEK-293 cells may not appropriately manage the additional production of the exogenous G proteins at the levels necessary to use CFP as a donor for FRET in this experimental design because they express endogenous  $G\alpha_s$ ,  $G\beta_1$ , and  $G\gamma_2$ . Indeed, most reports of RET analysis with G proteins (including this one) incorporate the co-expression of non-labeled heterotrimeric G protein partners to ensure proper expression of the exogenous G proteins. The substitution of mTFP for CFP in the hLHR and  $hG\alpha_s$  fusion constructs may balance the experimental requirements for both measurable signal strength and appropriate cellular localization.

Interestingly, although the expression of hLHR-CFP was problematic, the expression of the  $\beta_2$ -AR-CFP fusion protein was not; therefore, a physiochemical property of the hLHR appears to have prevented its expression at appropriate levels for FRET with CFP as a donor. When hLHR-CFP was expressed within a variant of HEK-293T cells, the CFP fluorescence was extremely intense but very little signal was found at the plasma membrane (Fig. 3.6). Most BRET analyses of GPCR dimerization express receptors at a high level in HEK-293T cells and measure the average intensities from millions of cells. Although these studies are careful to measure a signal that most likely represents a specific interaction

rather than one due to molecular ‘crowding’, the biological relevance of such a signal is highly questionable (288,291).

This is not the first study to employ RET to measure the capacity of LHR to self-associate. The BRET experiments from one set of authors (214-216) have been complemented with a photobleaching FRET approach from another (210,212,310); both methods, however, are vulnerable to criticism. This work attempted to confirm their results with FRET experiments that were designed to minimize the introduction of experimental artifact. Its failure to do so may reflect unresolved technical problems or may indicate that LHR dimerizes when the research model imposes artificial conditions that favor self-association.

### ***G $\alpha_s$ does not specifically co-immunoprecipitate with hLHR from HEK-293 cells***

#### *Introduction*

The co-immunoprecipitation of heterotrimeric G proteins with GPCRs and effector molecules has been documented, suggesting that G proteins may pre-bind to inactive GPCRs and may not dissociate from receptors after activation (77,78,253,281,311-314). To examine more closely the nature of the association between human G $\alpha_s$  and hLHR, a co-immunoprecipitation experiment was designed. If G $\alpha_s$  is found associated with hLHR either before or after receptor activation, the hLHR residues important for the interaction of hLHR with G $\alpha_s$  could then be identified using site-directed mutagenesis. This experimental approach would thus be a powerful tool to dissect the molecular landscape of hLHR/G $\alpha_s$  signaling and any results would complement the existing functional studies that have implicated particular hLHR residues as important for the coupling relationship with G $\alpha_s$ .

## *Experimental procedures*

### *i. Materials*

Reagents used for cell culture, transfection, and membrane isolation were as described in Chapter 2 and previously. Normal mouse IgG (sc-2025), Protein G PLUS-agarose (sc-2002), anti-G $\alpha_{s/olf}$  (sc-383), and RIPA buffer were from Santa Cruz, and anti-FLAG M2affinity agarose gel (A2220) and anti-FLAG M2 monoclonal antibody (F1804) were from Sigma. The rabbit anti-mouse and sheep anti-rabbit antibodies were from Amersham (25009601 and 25007106, respectively, not replaced after transition to GE Lifesciences).

### *ii. cDNA plasmid*

To create the FLAG-hLHR cDNA construct, a FLAG epitope tag (DYKDDDDK) was inserted C-terminal to the signal sequence of hLHR after codon 24 via the method of overlap PCR (263). The final PCR product was cloned into pcDNA6.2Topo.

### *iii. Transient and stable transfection of HEK-293 cells with hLHR and FLAG-hLHR*

HEK-293 cells were transfected with Lipofectamine 2000 as per manufacturer's instructions. 400  $\mu$ g/mL of G418 was used for the maintenance of stable, clonal hLHR<sup>+</sup>/HEK-293 cells. Selection for a stable, clonal FLAG-hLHR<sup>+</sup>/HEK-293 line of cells was performed with the addition of 10  $\mu$ g/mL blasticidin to complete growth medium over two weeks. Colonies were isolated, expanded, and tested for cell-surface FLAG-hLHR expression with a <sup>125</sup>I-hCG binding assay (performed on intact cells as described in Chapter 2). The line expressing the highest concentration of cell-surface FLAG-hLHR was chosen for analysis.

#### *iv. Immunoprecipitation, SDS-PAGE, and Western Blotting*

Crude membranes were isolated from transiently-transfected or stably-expressing hLHR<sup>+</sup>/ or FLAG-hLHR<sup>+</sup>/HEK-293 cells as described in Chapter 2. 100 µg of membranes were resuspended in PBS or RIPA buffer and hCG stimulation of membranes was performed at 37°C for 30 min. Samples were pre-cleared with normal mouse IgG and Protein G-PLUS agarose as per manufacturer's instructions. Incubation of samples with anti-FLAG M2 agarose occurred overnight at 4°C. Samples were washed twice with PBS, eluted with 1X SDS sample buffer supplemented with β-mercaptoethanol, and boiled for 5 minutes before resolution on 12% SDS-polyacrylamide gels as described in Chapter 2. Western blotting against Gα<sub>s</sub> was performed as described in Chapter 2 with a 300x dilution of the primary antibody followed by a secondary antibody (sheep anti-rabbit) dilution of 5000x. The primary anti-FLAG M2 antibody was diluted 1000x and the secondary rabbit anti-mouse antibody was diluted 5000x for Western blotting towards the anti-FLAG epitope.

#### *v. Immunocytochemistry*

HEK-293 cells expressing FLAG-hLHR were washed twice with PBS, fixed in 4% formalin at room temperature for 10 minutes, and probed for FLAG expression with the anti-M2 FLAG antibody as per the manufacturer's instructions for immunocytochemistry with the Histostain-*Plus* DAB Broad Spectrum kit (Zymed Laboratories, San Francisco, CA).

### *Results*

#### *hGα<sub>s</sub> did not specifically co-immunoprecipitate with FLAG-hLHR*

Membranes from cells expressing hLHR and FLAG-hLHR proteins were probed for FLAG expression before and after anti-FLAG immunoprecipitation. FLAG-hLHR was detected by anti-FLAG Western blotting but the band was detected in only the concentrated eluate from the immunoprecipitation with an extremely high molecular weight (~250 kDa), and not with the expected molecular weight of 85-

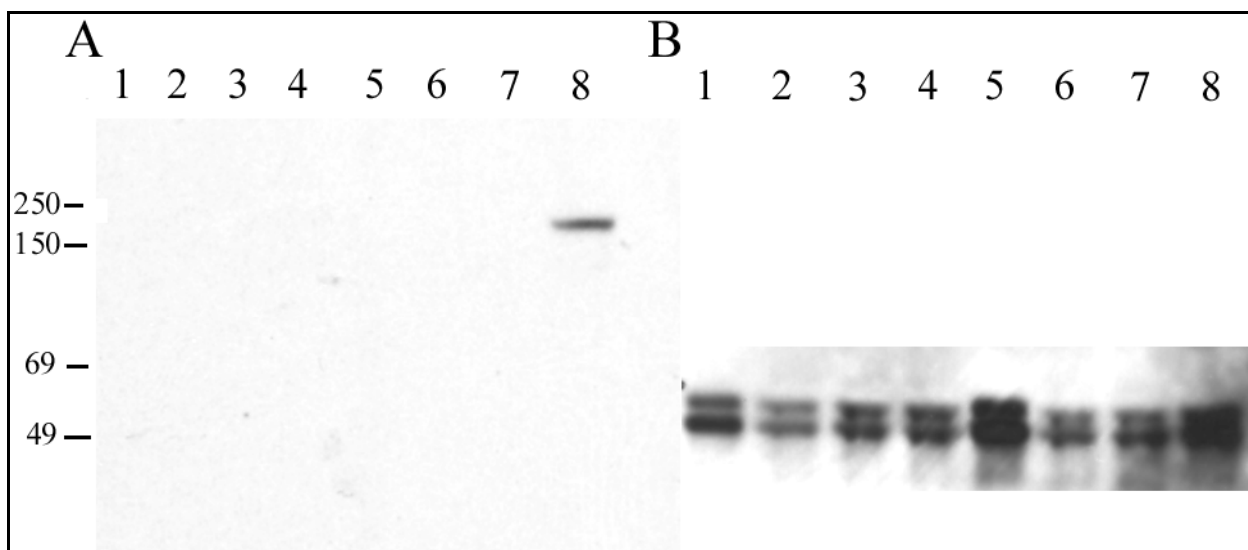


**Figure 3.7.** Western blots of hLHR<sup>+</sup> or FLAG-hLHR<sup>+</sup>/HEK-293 membranes pre- and post-immunoprecipitation with anti-FLAG conjugated agarose. (A) represents an anti-FLAG Western blot and (B) is an anti-Gα<sub>s</sub> Western blot. In both panels, lanes 1-4 contain membranes from hLHR<sup>+</sup> cells and lanes 5-8 contain membranes from FLAG-hLHR<sup>+</sup> cells. Lanes 1 and 5 depict the samples before pre-clearing, lanes 2 and 6 depict the samples after pre-clearing, lanes 3 and 7 exhibit the samples after the removal of the anti-FLAG agarose, and lanes 4 and 8 exhibit the eluate from the anti-FLAG agarose. Molecular weight markers in kDa are indicated on the left of the figure.

95 kDa (Fig. 3.7A, lane 8). The samples were then probed for the co-immunoprecipitation of hGα<sub>s</sub> with FLAG-hLHR (Fig. 3.7B). Gα<sub>s</sub> was identified in all pre- and post-immunoprecipitation samples of membranes expressing either hLHR or FLAG-hLHR and therefore was not co-immunoprecipitated specifically with FLAG-hLHR. No difference was seen between membranes of transient or stable hLHR/FLAG-hLHR transformants, after co-immunoprecipitation in two different buffers (PBS and RIPA), or after ligand stimulation (data not shown).

## Discussion

### *i. Aggregation of the hLHR ECD may impair in vitro manipulation*

FLAG-hLHR membrane expression was detected with an anti-FLAG Western blot but the protein appeared aggregated, even under reducing conditions and after boiling and SDS-PAGE. In ref. (213), co-immunoprecipitation studies of FLAG-hLHR and myc-hLHR expressed in HEK-293 cells were performed to examine hLHR dimerization. The authors reported the detection of high molecular weight

species of hLHR on Western blots; these studies did, however, identify bands at the expected molecular weights of mature and immature monomeric hLHR proteins. After personal communication with the authors, it was revealed that a different anti-FLAG antibody other than the one reported was used in the published experiments. This antibody is no longer commercially available (315).

Interestingly, 90% of the purified product of both the LHR and FSHR extracellular domains (ECDs) expressed in insect (LHR) and mammalian (FSHR) cells was reported as highly aggregated (119,120). The LHR ECD aggregate dissociated to a monomeric species after the application of both reducing agents and detergents, which suggests that non-native disulfide bonding as well as hydrophobic interactions fuel the artificial accumulation of purified ECD molecules. Perhaps the disruption of the hLHR<sup>+</sup> cells in the co-immunoprecipitation experiment encouraged the formation of receptor aggregates through inappropriate, intermolecular associations of LHR ECDs. This aggregation may have influenced the native relationship between hLHR and G<sub>s</sub>, and therefore, may have interfered with the co-immunoprecipitation results.

*ii. Signal sequence processing may remove part of the N-terminal hLHR FLAG tag*

Because the FLAG tag was inserted into the hLHR cDNA after the signal sequence, imprecise cleavage of the membrane-targeting sequence may have altered the fidelity of the N-terminal FLAG-tag. Therefore, immunocytochemistry of transfected FLAG-hLHR<sup>+</sup> cells was performed with the same anti-FLAG M2 antibody used in the co-immunoprecipitation experiments to detect cell-surface expression of FLAG-hLHR. No difference was seen between FLAG-hLHR<sup>+</sup> and hLHR<sup>+</sup> cells (data not shown).

Although the manufacturer claims the antibody is suitable for immunoprecipitation, immunoblotting, and immunocytochemistry, perhaps the conditions used were not optimal for FLAG immunocytochemical detection. Or, perhaps the antibody was unable to recognize the epitope due to aberrant processing of the upstream hLHR signal sequence. The results cannot distinguish between these two possibilities. The epitope was inserted as others have reported (213), but again, a different antibody was used in this report



for FLAG detection. Notably, the signal sequence for the human LHR is predicted from studies of the rat LHR isoform and has not been measured experimentally (10).

### *iii. Conclusions*

In these experiments, the specific co-immunoprecipitation of hG $\alpha_s$  with hLHR was not measured. The detection of hG $\alpha_s$  in the eluate from anti-FLAG immunoprecipitation of hLHR<sup>+</sup> membranes (Fig. 3.7B, lane 4) indicated that hG $\alpha_s$  non-specifically associated with the anti-FLAG agarose under the experimental conditions. Therefore, the co-immunoprecipitation of this protein with FLAG-hLHR<sup>+</sup> membranes (Fig. 3.7B, lane 8) is not specific. Although this result may reflect the character of the native hLHR/G $\alpha_s$  relationship, technical difficulties most likely influenced the experimental results.

A monomeric species of FLAG-hLHR was not detected after FLAG-immunoprecipitation on Western blots probed for FLAG expression, although a high-molecular aggregation of the protein was observed. This aggregation, likely due to artificial intermolecular interactions between hLHR extracellular domains, may have reflected an experimental artifact that disrupted a native hLHR/hG $\alpha_s$  interaction and/or prevented the specific detection of co-immunoprecipitated hG $\alpha_s$ . The anti-FLAG antibody successfully used for hLHR co-immunoprecipitation studies in the same target cell line is no longer available for use.

Although the high molecular weight, aggregated species of FLAG-hLHR was detected with the anti-FLAG M2 antibody in the eluate from anti-FLAG immunoprecipitation, incorrect cleavage of the hLHR signal sequence may have diminished the specificity of the antibody/epitope relationship and therefore may have allowed a monomeric FLAG-hLHR species to escape immunoprecipitation and/or immunodetection. The incorporation of a different epitope tag, such as a c-myc or HA tag, may resolve these issues. Also, the method of membrane collection and the co-immunoprecipitation conditions may have negatively influenced the endogenous relationship between hLHR and G $\alpha_s$ , and therefore further manipulation of these experimental variables may decrease the amount of non-specifically associated G $\alpha_s$ .

with the anti-FLAG M2 agarose. Or, perhaps the physiochemical properties of hLHR, in particular the predisposition of the LHR ECD to aggregate upon the disruption of the native environment, impair the analysis of the receptor by co-immunoprecipitation. Regardless, although potentially insightful, this biochemical approach is inferior to the observation of hLHR/G<sub>s</sub> coupling in a native environment that does not introduce the possibility of as much experimental artifact.

### ***The expression of G $\alpha_s$ C-terminal minigenes does not diminish the hLHR signaling response in HEK-293 cells***

#### *Introduction*

The C-termini of G $\alpha$  isoforms are necessary for the recognition of heterotrimeric G proteins by their cognate receptors (2). Often, peptides (or “minigenes”) corresponding to the C-termini (CT) of G $\alpha$  isoforms are sufficient to act as inhibitors to attenuate the activity of certain GPCRs. For the receptors that couple to the family of G $\alpha_{i/o}$  proteins, small peptides that comprise the C-terminal eleven amino acids are adequate to impose signaling inhibition (244-247). For G<sub>s</sub>-coupled GPCRs, longer peptides are necessary to impose the effect (274,275,280,287,316). To measure the contribution of G $\alpha_s$  residues to hLHR/G<sub>s</sub> coupling, an assay was developed to monitor the signaling inhibition of hLHR by the expression of peptides that contain the CT of G $\alpha_s$ . Six peptides of various lengths were designed and expressed in hLHR<sup>+</sup>/HEK-293 cells. If the peptides were to diminish the hLHR signaling response, then site-directed mutagenesis could be applied to identify residues important for hLHR/G<sub>s</sub> coupling.

#### *Experimental procedures*

##### *i. Materials*

Cell culture and transfection reagents were as described previously.

### ii. cDNA plasmids

G $\alpha_s$  minigene constructs were designed as listed in Table 3.1. The name of the construct represents the salient features contained within the peptide. When possible, the N-terminal amino acid residue was chosen to be A, G, H, L, T, or V according to the “N-end rule” to promote stability and increase half-life *in vivo* (317). For the very short CT and CTR constructs, oligonucleotides corresponding to the insertion sequences were synthesized (Integrated DNA Technologies, Coralville, IA) and the single-stranded DNA was annealed as described (246) to produce double-stranded products with 5'- and 3'-overhangs that were inserted into pre-digested HindIII/XhoI pcDNA3.1(Zeo/-). All other constructs were amplified with appropriate oligonucleotide primers and cloned into the HindIII and XhoI restriction sites of pcDNA3.1(Zeo/-).

**Table 3.1 Description of G $\alpha_s$  minigene constructs.**

name of construct	number of amino acid residues	location within G $\alpha_s$ (long-splice variant)
CT	11	384-394
CTR	11	**
$\alpha 5$	26	369-394
$\alpha 4\beta 6\alpha 5$	61	334-394
94	94	301-394
$\alpha 3\beta 5\alpha 4\beta 6\alpha 5$	132	263-394
Ras-like	202	193-394

\*\*A randomized, scrambled version of the CT peptide.

### iii. Cell culture and transfection

Cell culture and transfection procedures were as described previously. The cDNA ratios of hLHR to G $\alpha_s$  minigene construct in co-transfections were varied from a 1:1, 1:2, 1:4, and 1:9 in transfection mixes. For stable selection of G $\alpha_s$  minigenes in hLHR<sup>+</sup>/HEK-293 cells, the addition of 400  $\mu$ g/mL Zeocin (Invitrogen) to complete growth medium with G418 was performed for two weeks.

*iv. RT-PCR, HPLC and ion-spray mass spectrometry, Western blotting, and cAMP measurement*

RT-PCR was used to determine mRNA expression of the  $G\alpha_s$  minigenes in HEK-293 cells. Intracellular RNA was collected from  $1 \times 10^6$  HEK-293 cells with the RLN buffer of the RNeasy kit (Qiagen, Valencia, CA). RNA integrity was verified with formaldehyde agarose gel electrophoresis and the visualization of intact 28S and 18S rRNA molecules. cDNA was then generated with the iScript cDNA Synthesis Kit (BioRad, Hercules, CA) as per manufacturer's instructions. RT-PCR was performed per manufacturer's instructions with iTaq (Bio-Rad). The upstream oligonucleotide primers were designed to recognize the individual constructs and the downstream primer targeted a short sequence in the mRNA polyA tail that was common for all of the constructs (246). Products were visualized with standard DNA agarose gel electrophoresis. Cytosolic extracts underwent HPLC analysis and peaks were analyzed by ion-spray mass spectrometry as described (246). Western blotting was performed as detailed in the previous section and the measurement of cAMP production was performed as in Chapter 2.

*Results*

*i. Expression of  $G\alpha_s$  minigene constructs*

RT-PCR was performed to detect expression of  $G\alpha_s$  mRNA expression (Fig. 3.8). All of the constructs were expressed at the mRNA level except for Ras-like. To detect protein expression, ion spray mass spectrometry of HPLC peaks from cytosolic extracts was used for the small CT and CTR peptides, and the larger constructs that contained the C-terminus of  $G\alpha_s$  (the epitope recognized by the monoclonal  $G\alpha_s$  antibody) were detected by Western blotting. Neither the CT nor the CTR peptide were detected by LC-MS (data not shown), and only the expression of the  $\alpha 3\beta 5\alpha 4\beta 6\alpha 5$  protein was detected with Western blot (Figure 3.9).

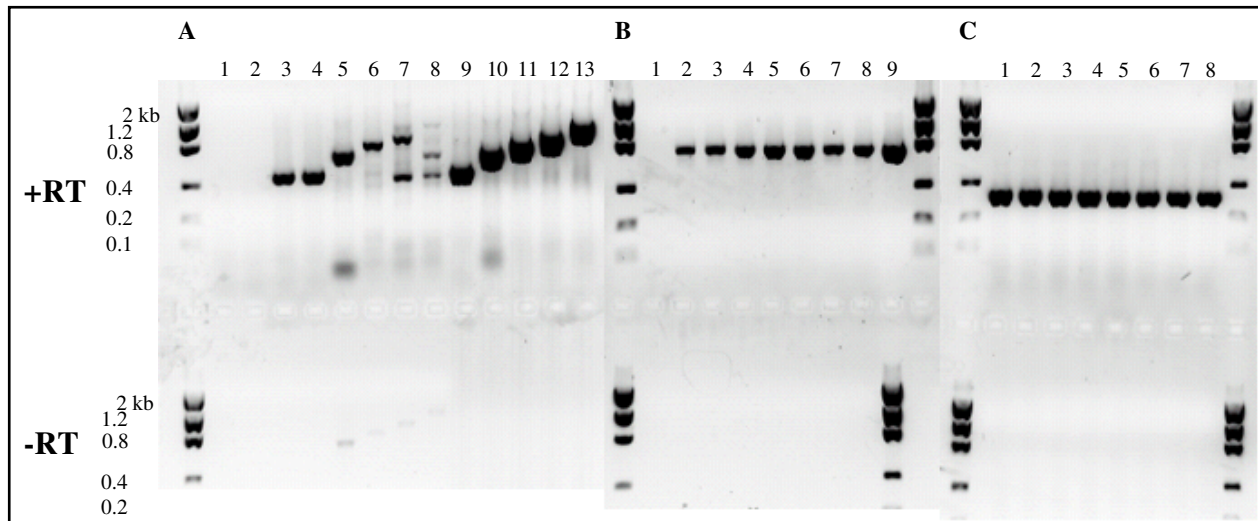


**Figure 3.8.** RT-PCR analyses of HEK-293 cells co-transfected with hLHR and  $G\alpha_s$  minigene constructs. The top panels are samples that included reverse transcriptase (RT) and the bottom panels lacked RT. **A.** RT-PCR analysis of  $G\alpha_s$  minigene expression. Lane 1: mock-transfected/mock-transfected. Lane 2: hLHR/mock-transfected. Lane 3-8: hLHR/CT, /CTR, / $\alpha 5$ , / $\alpha 4\beta 6\alpha 5$ , /94, / $\alpha 3\beta 5\alpha 4\beta 6\alpha 5$ , and /Ras-like, respectively. Lanes 9-13: Positive PCR controls with  $G\alpha_s$  minigene plasmid DNA corresponding to lanes 3-8, respectively. **B.** RT-PCR analysis of hLHR expression. Lanes 1-8 as in (A). Lane 9: Positive PCR control with hLHR plasmid DNA. **C.** GAPDH RT-PCR analysis of samples. Lanes 1-8 as in (A) and (B).

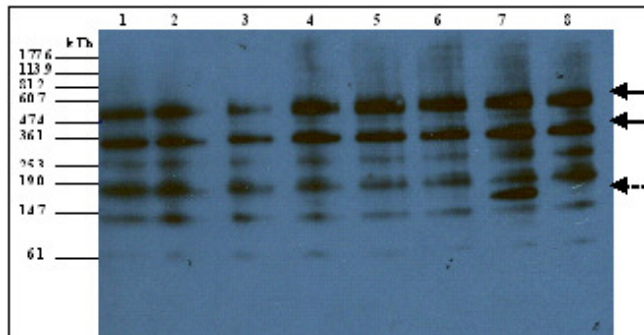
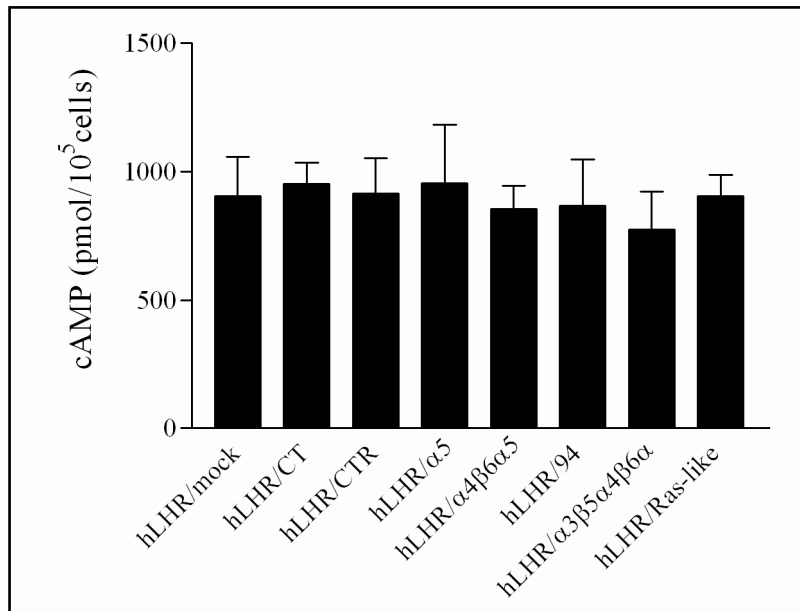


**Figure 3.9.** Anti- $G\alpha_s$  Western analysis of HEK-293 cells co-transfected with hLHR and  $G\alpha_s$  minigene constructs. Lane 1: mock transfected/mock-transfected. Lane 2: hLHR/mock-transfected. Lanes 3-8: hLHR/CT, /CTR, / $\alpha 5$ , / $\alpha 4\beta 6\alpha 5$ , /94, / $\alpha 3\beta 5\alpha 4\beta 6\alpha 5$ , and /Ras-like, respectively. Solid arrows indicate the two endogenous isoforms of  $G\alpha_s$  (long and short splice variants). Dotted arrow indicates expression of the  $\alpha 3\beta 5\alpha 4\beta 6\alpha 5$  protein.

ii. *hCG-stimulated cAMP production was not impaired by  $G\alpha_s$  C-terminal minigenes in HEK-293 cells*

After stimulation with hCG, there was no difference between the cAMP production of hLHR<sup>+</sup>/HEK-293 cells expressing the  $G\alpha_s$  minigenes and those that were mock-transfected. Maximum

**Figure 3.10.** Maximum cAMP response of HEK-293 cells co-transfected with hLHR and  $G\alpha_s$  minigene constructs. There is no significant difference between the samples and the hLHR/mock control when analyzed with One-way ANOVA followed by Dunnett's post-test ( $p > 0.05$ ). Experiments were performed in triplicate,  $n=3$ .



cAMP responses (Fig. 3.10) as well as  $EC_{50}$ s (data not shown) were compared. Decreasing the ratio of hLHR to  $G\alpha_s$  minigene (which decreases the amount of expressed receptor and increases the amount of  $G\alpha_s$  minigene) did not affect the results (data not shown). HEK-293 cells stably-expressing  $G\alpha_s$  minigenes were transfected with hLHR and similar expression and signaling results were seen (data not shown).

### Discussion

Reports agree that the C-terminus of  $G\alpha$  is necessary for effective GPCR/G protein coupling. A peptide corresponding to the extreme CT of  $G\alpha_i$  is sufficient to stabilize an activated form of rhodopsin as well as to block rhodopsin activation through transducin (87,249,318). The activities of other  $G\alpha_{i/o}$ -coupled receptors are also sensitive to the expression of  $G\alpha$  CT peptides (244-247). Studies with  $G\alpha_s$  CT peptides suggest that the expression of the  $G\alpha_s$  extreme CT is not sufficient to impair  $G_s$ -coupled GPCR activity and that longer peptides that include other  $G\alpha_s$  sequence motifs, such as the  $\alpha 3$ - $\beta 5$  and  $\alpha 4$ - $\beta 6$  loops, are necessary to reduce GPCR-mediated cAMP production (274,275,280,287,316).

This work is predominantly inconclusive because protein expression could not be verified for all  $G\alpha_s$  minigene constructs. The results for the  $\alpha 3\beta 5\alpha 4\beta 6\alpha 5$  protein may indicate, however, that truncations of  $G\alpha_s$  may be insufficient to diminish the hLHR signaling response, although the  $\alpha 3\beta 5\alpha 4\beta 6\alpha 5$  may not have assumed a fold representative of the native  $G\alpha_s$  tertiary structure and therefore may have lost the capacity to recognize hLHR to act as an inhibitor.

The transfection efficiency of HEK-293 cells is high, and the signaling response of LH receptors expressed in this model is strong. Therefore, any potential impact of the  $G\alpha_s$  constructs on the system may have been obscured and thus beyond measure. The manipulation of cDNA ratios during co-transfection and thus the relative expression levels of hLHR to  $G\alpha_s$  minigene construct did not, however, affect the cAMP production after ligand stimulation. Also, stably-transformed cells expressing the  $G\alpha_s$  CT constructs that were transiently transfected with hLHR did not exhibit any difference from the results of the experiments with transient co-transfections.

The peptides in this study were not constructed arbitrarily but were designed with parameters that would most likely promote native-like folding, increase protein stability, and lengthen *in vivo* half-life. The N-terminal amino-acids were chosen according to the 'N-end' rule, and the secondary structural elements were completely included rather than truncated where possible. Perhaps the expression of peptides shown to successfully reduce the  $G_s$ -coupled activity of other GPCRs in the hLHR system would inhibit hLHR activity, although their design appears arbitrary (275). The addition of a synthetic peptide corresponding to the C-terminal  $G\alpha_s$  21 residues to cellular membranes reduced  $A_{2A}$ -adenosine receptor activity by ~25% (274,280). Perhaps the addition of synthetic versions of  $G\alpha_s$  constructs to hLHR<sup>+</sup> membranes would overcome the problems with the described model system if the *in vivo* expression of the constructs somehow impaired their use as inhibitors. Also, the conjugation of a membrane-permeable motif to these synthetic  $G\alpha_s$  peptides could enhance the delivery of the inhibitors to the hLHR for a robust inhibition of signaling response (273,319).

If peptides corresponding to  $G\alpha_s$  could inhibit hLHR activity, not only would they be suitable tools to analyze the coupling relationship between hLHR and  $G_s$ , they may be potential therapeutic agents for the selective inhibition of constitutively-active mutant hLHR activity.

### ***A peptide corresponding to the second intracellular loop of hLHR does not inhibit hLHR activity***

#### *Introduction*

Site-directed mutagenesis and molecular modeling approaches identified amino acid residues within the cytosolic extensions of helices III and VI as well as the second intracellular loop (ICL2) of the hLHR as important for coupling to  $G_s$ . Some residues were proposed to directly interact with areas of  $G\alpha_s$  to translate activation while others were thought to coordinate the appropriate architecture for receptor/ $G\alpha_s$  association and thus indirectly support the coupling event (144). To further examine the roles of these residues in within the hLHR/ $G_s$  relationship, an *in vitro* assay was designed to measure the association of a peptide corresponding to residues 459-482 of hLHR (hLHRICL2) and  $G\alpha_s$  with a surface plasmon resonance (SPR) approach. To complement the SPR work with a supportive biological study, a similar experimental approach as described in the previous section was developed to determine if the hLHRICL2 peptide could exert a functional effect upon hLHR activity and act as an inhibitor of  $G_s$ -mediated signaling. If an association of the peptide and  $G\alpha_s$  could be measured and the peptide could inhibit hLHR signaling, the mutagenesis of implicated residues within the peptide as well as  $G\alpha_s$  would investigate the contribution of these residues to the hLHR/ $G_s$  molecular interface.

#### *Experimental procedures*

##### *i. Materials*

A 24-amino acid peptide representing residues 459–482 of hLHR was synthesized to >95% purity (verified with HPLC) by QCB (Hopkinton, MA; formerly Biosource) with a C-terminal amidation to neutralize the carboxy-charge. Lyophilized peptide was reconstituted with ddH<sub>2</sub>O, dried (to remove



residual TFA), resuspended in 10mM HEPES pH8.0 at a final concentration of 1 – 5 mg/mL, and used immediately for SPR immobilization. The cDNA for the long splice-variant of the human  $G\alpha_s$  isoform was purchased from the ATCC (Manassas, VA). The pQE-30Xa expression vector, M15 *E. coli* cells, and  $Ni^{++}$ /NTA resin were from Qiagen. The CM5 sensor chip and BIAcore 3000 machine were from BIAcore (GE Lifesciences, Piscataway, NJ). Cell culture and transfection materials were as described in Chapter 2.

*ii. Recombinant expression and purification of human  $G\alpha_s$  ( $hG\alpha_s$ )*

PCR amplification of the coding sequence of  $hG\alpha_s$  introduced 5' *NaeI* and a 3' *SacI* restriction-digestion sites for cloning into the pQE-30Xa expression vector. The clone was transformed into *E. coli* M15 cells containing the pREP4 plasmid. The protein was expressed and purified with  $Ni^{++}$ /NTA resin as described elsewhere (320).

*iii. hLHRICL2 peptide immobilization*

After equilibration of the chip to a running buffer of 10mM HEPES pH 8.0, 50mM NaCl at 25°C, a 200 mM EDC/50 mM NHS mix was injected for 7 min. to activate the surface. A 10  $\mu$ g/mL solution of hLHRICL2 peptide (3.3 mM) was injected for 2 min and was followed by a 7 min injection of 1 M ethanolamine pH 8.5 “quencher”. The flow rate at all times was 5  $\mu$ L/min. Because the hLHRICL2 peptide exhibits an unusual amount of non-specific association with the surface of the chip, a “clearing” solution (50 mM NaOH, 0.1% SDS) was injected (2 x 30  $\mu$ L @ 30  $\mu$ L/min. for 30ses) to remove any remaining peptide non-covalently associated with the chip after “quenching”. A control channel was generated in the exact same manner with the exclusion of injected peptide, and any signal from this blank channel was subtracted from the peptide-immobilized channel.

#### *iv. SPR experiments*

Five serial dilutions of the partially-purified hG $\alpha_s$  eluate were injected (7 min at a flow rate of 5  $\mu$ L/min in a running buffer of the same composition as the hG $\alpha_s$  elution buffer) across the control channel as well as the hLHR ICL2 peptide channel and the response was measured. The clearing solution was used to regenerate the surface between analyte injections.

#### *v. Cell culture, transfection, and cAMP measurement*

Cell culture and transfection were as described in Chapter 2. HEK-293 cells were co-transfected with hLHR and the hLHRICL2/pcDNA3.1(-) cDNA vector (created as described for the G $\alpha_s$  minigene constructs in the previous section). Measurement of cAMP after stimulation with hCG was performed as described in Chapter 2. The selection of HEK-293 cells stably-expressing the hLHRICL2 peptide was performed as described for the G $\alpha_s$  minigene constructs in the previous section.

### *Results*

The long splice variant of hG $\alpha_s$  was recombinantly expressed and partially purified for use as the analyte of the SPR experiment with immobilized hLHRICL2 peptide (Fig. 3.11). Figure 3.12 depicts a representative immobilization of hLHRICL2 to the carboxymethylated dextran matrix of the CM5 chip surface. Optimization of this procedure resulted in an immobilization of ~15 RUs of peptide (~50  $\mu$ M). Increasing concentrations of partially-purified hG $\alpha_s$  were then applied to the hLHRICL2 chip that resulted in a concomitant increase of associated protein on the chip surface (Fig. 3.13).

No difference was seen in the hCG-stimulated cAMP response between mock-transfected and hLHRICL2-transfected cells also expressing hLHR (data not shown). Also, stably-expressing hLHRICL2<sup>+</sup> HEK-293 cells transiently-transfected with hLHR exhibited no difference in the hCG-dependent cAMP response when compared to the transiently co-transfected cells (data not shown).

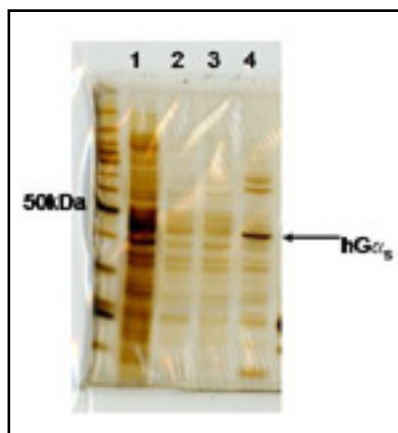


**Figure 3.11.** A silver stain of fractions collected during the purification of hG $\alpha_s$ . Far left: molecular weight markers. Lane 1: Cleared cellular lysate. Lane 2: Wash 1. Lane 3: Wash 2. Lane 4: Eluate from Ni<sup>++</sup>/NTA resin.

### Discussion

SPR, an *in vitro*, optical-based, biophysical technique that sensitively measures the physical association between untagged biomolecules, is a powerful methodology that increasingly provides novel solutions for unique applications, and because SPR experiments supply data in real-time, this technique may calculate the kinetics of binding reactions. A peptide corresponding to the second intracellular loop but not peptides comprising the sequences of the third intracellular loop and the C-tail of the

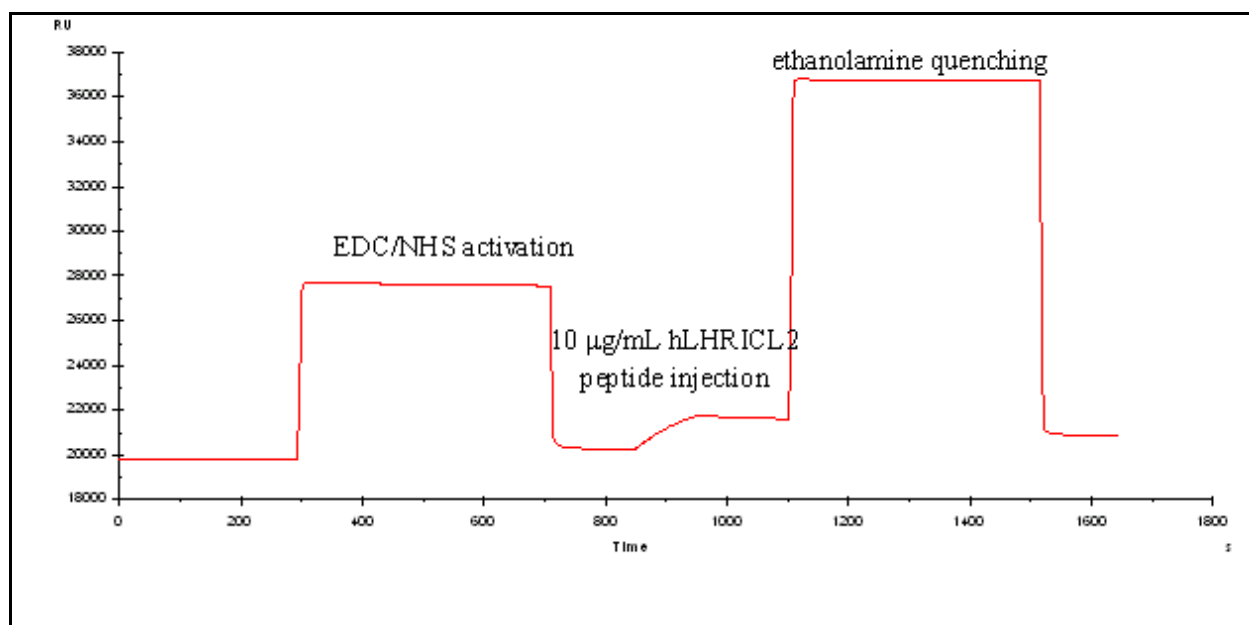


**Figure 3.12.** A representative sensorgram of hLHRICL2 peptide immobilization after EDC/NHS activation of a CM5 sensor chip.

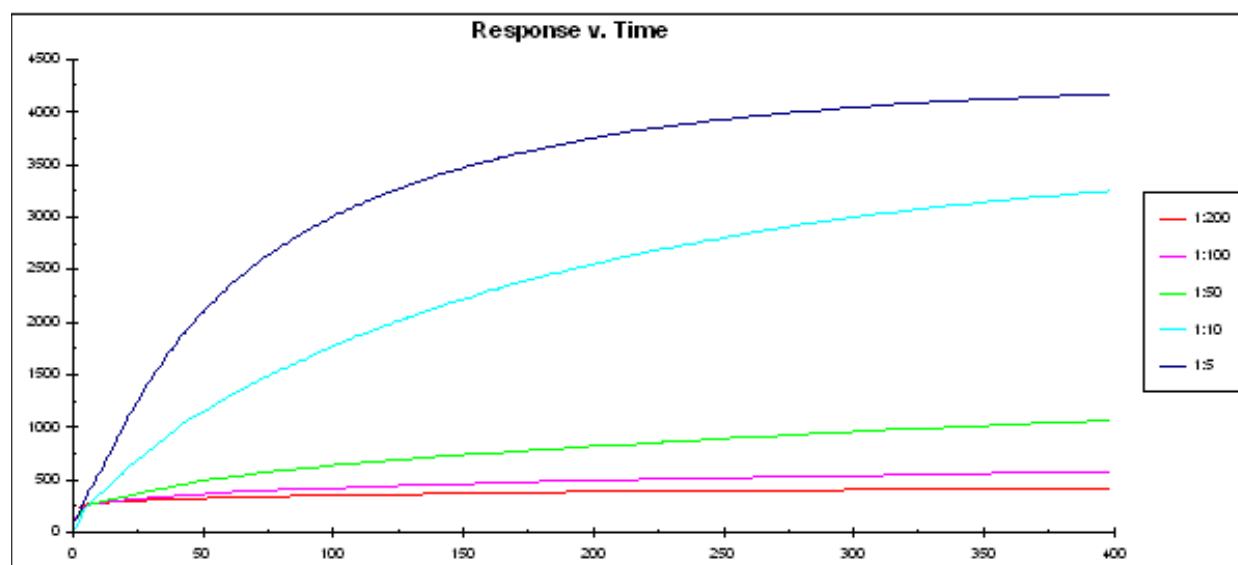


**Figure 3.13.** Sensorgram of hG $\alpha_s$  interaction with the immobilized hLHRICL2 peptide. Increasing RUs indicate an association of the serial dilutions of partially-purified hG $\alpha_s$  with the hLHRICL2 chip. may calculate the kinetics of binding reactions (321). A peptide corresponding to the third intracellular

serotonin type 6 receptor was shown, using SPR, to associate with the G $\alpha_s$  protein (322). Although the SPR work investigating the interaction between the hLHRICL2 peptide and a partial purification of G $\alpha_s$  was promising, the absence of any biological activity of the hLHRICL2 peptide *in vivo* suggested that the SPR work may lack relevance because the *in vitro* nature of the SPR methodology limits the significance of any results. As with the G $\alpha_s$  minigene peptides (discussed in the previous section), the hLHRICL2 peptide may not have exhibited sufficient intracellular stability *in vivo* to act as an inhibitor of hLHR signaling in HEK-293 cells.

SPR, and a related technology, plasmon waveguide resonance (PWR), have measured the relationship between GPCR and heterotrimeric G proteins with an insight and precision unavailable with other biophysical methods (323-327). The technical rigor and the limited availability of the dedicated PWR machines, however, restrict the use of these advanced techniques to the general population of researchers. The use of SPR to measure the relationship of artificial, representative fragments of GPCR/G protein systems is, however, accessible, although the disadvantage of this approach includes the

dissolution of the native environment which may then introduce experimental artifact as the relationships measured may not mimic an interaction that is reflective of a true *in vivo* association. The absence of a membrane-like environment, in particular, narrows the utility of the approach because the membrane environment influences the conformation of the helical extensions and cytosolic loops of GPCRs and because a post-translational S-acylation of the G $\alpha_s$  N-terminus occurs (328).

Nonetheless, the partially-purified hG $\alpha_s$  appeared to associate with the hLHRICL2 peptide, but because contaminants were present in the hG $\alpha_s$  preparation, this conclusion is unreliable. The use of a highly-purified hG $\alpha_s$  fraction as analyte would confirm the experimental results. Interestingly, other GPCRs are inhibited by the introduction of peptides that correspond to intracellular regions (329), but the hLHRICL2 peptide does not interfere with hLHR signaling. Perhaps the peptide was rapidly degraded within the *in vivo* environment and could not associate with endogenous G $\alpha_s$  and thus inhibit the association of hLHR during the G $_s$  coupling event, or perhaps the affinity of hLHR for G $\alpha_s$  exceeds that of hLHRICL2 for G $\alpha_s$  and thus the application of the hLHRICL2 peptide as an inhibitor of hLHR/G $_s$  activity is ineffectual. The described results cannot resolve these possibilities and therefore this study affords no insight into the failure of published methods to similarly affect the hLHR system.

### ***The trypsin-protection assay does not discriminate between hLHR-activated and spontaneously-active G $\alpha$ subunits***

#### ***Introduction***

The inherent plasticity within the GPCR architecture grants the receptors a selection of signaling phenotypes (36). That high levels of ligand (hCG) induce the activation of the non-cognate G $_q$  signaling pathway and that some constitutively-active versions of hLHR, such as the L457R and D578H mutants, may preferentially activate G $_q$  over G $_s$  illustrate such pleiotropy within hLHR (10). The use of alanine-scanning mutagenesis to probe the contribution of hLHR to the hLHR/G $_s$  coupling interface identified a number of key residues that mediate, either directly or indirectly, the translation of activation from

receptor to G protein (144). Many of these mutants did not produce an accumulation of cAMP upon stimulation and therefore were unable to translate activation to  $G_s$ . An assay that could determine a more precise role of for these mutations at the hLHR/ $G_s$  interface, such as the nucleotide-bound state of  $G\alpha_s$ , would complement the measurement of the downstream impact of the amino acid substitutions.

The preferred technique to analyze the nucleotide-binding state of G protein  $\alpha$  subunits is an assay that monitors the incorporation of a non-hydrolyzable GTP radionucleotide after receptor stimulation (330). This approach is limited with the LHR, however, because the measurement of radionucleotide incorporation into  $G\alpha$  after hCG stimulation has been reported to be only a few fold above background (169,171,172). An assay was developed to observe the nucleotide-binding state of  $G\alpha$

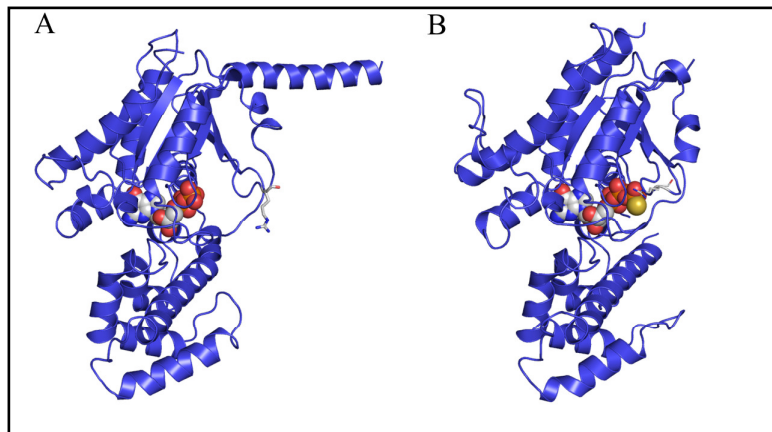


**Figure 3.14.** A highly-conserved Arg residue in the Switch II region of  $G\alpha$  isoforms is depicted in a ball-and-stick representation. *A.* The Arg extends from the globular  $G\alpha$ -GDP protein and is thus susceptible to trypsin recognition and digestion. *B.* The Arg is retracted into the  $G\alpha$ -GTP conformation and is thus protected from trypsin digestion. Images were created from PDB files 1GOT (*A*) and 1AZT (*B*) with Pymol (DeLano Scientific, LLC).

isoforms after hCG stimulation of hLHR<sup>+</sup> cellular lysate by exploiting the trypsin sensitivity of the  $G\alpha$  subunit (174). Inactive  $G\alpha$ -GDP is susceptible to trypsin degradation (Fig. 3.14A), but the conformation of  $G\alpha$  with bound GTP protects a highly-conserved arginine residue from trypsin recognition (Fig. 3.14B); therefore, only small N- and C-terminal portions of  $G\alpha$ -GTP are digested. To discern the impact of LHR mutations upon the nucleotide-binding state of  $G\alpha$ , an adaptation of this trypsin digestion assay was attempted.

## *Experimental Procedures*

### *i. Materials*

Cell culture and transfection reagents were as described in Chapter 2. Trypan blue was from Invitrogen, BSA and SLO (S5265) were from Sigma, and the C530A SLO variant was a generous donation from Dr. S. Bhakdi (University of Mainz, Germany). Purified  $G\alpha_s$  was a kind gift from Dr. P.J. Casey (Duke University Medical Center, Durham, NC).

### *ii. Cell culture and transfection*

HEK-293 cells were cultured and transfected as described in previously. MA-10 cells were cultured and transfected according to instructions from the lab of Dr. M. Ascoli (University of Iowa, Iowa City, IA). The hLHR<sup>+</sup>/HEK-293 cell line was maintained as described in earlier sections.

### *ii. Streptolysin O (SLO) permeabilization of cells*

SLO (the native or the C530A variant that exhibits the activity of wild-type SLO and possesses a longer shelf-life) was reconstituted with 100 mM DTT to a concentration of 1200 U/mL and stored at -20°C. For permeabilization, SLO was diluted to 500 U/mL in SLO buffer (25 mM MgCl<sub>2</sub>, 1 mM DTT, 100 mM HEPES pH 7.4) and kept on ice for 10 min. HEK-293 cells in 6-well plates were washed twice with PBS and then treated with vehicle or SLO on ice for 15 min. A 5X dilution in PBS of 0.4% Trypan blue was then added to parallel samples and incubated for 5 min at room temperature to determine the percentage of cells permeabilized by treatment with SLO.

### *iii. Trypsin-protection assay*

The assay was performed essentially as described (174) with the following differences. Stable hLHR<sup>+</sup>/HEK-293 cells as well as transiently-transfected HEK-293 and MA-10 cells were used for analysis of G protein activation after hCG stimulation. The cells were transiently transfected with wild-

type, D578H (a constitutively-activating mutant), and I472A (an inactive mutant) hLHR cDNA.

Experimental conditions were varied as indicated in the text.

For SLO-permeabilized cells, adherent HEK-293 cells were permeabilized and then stimulated with hCG as with the standard trypsin assay. The cells were then treated with increasing concentrations of trypsin for increasing periods of time and lysed in 1X SDS-PAGE sample buffer. SDS-PAGE and Westerns were performed as in the standard trypsin assay.

## Results

### *i. The trypsin-protection assay does not discriminate between hLHR-activated and spontaneously-active G protein subunits*

The anti-G $\alpha_s$  Western blot in Figure 3.15A depicts the treatment of purified G $\alpha_s$  with a non-hydrolyzable GTP analog, GTP $\gamma$ S, and trypsin. The addition of GTP $\gamma$ S to the assay buffer protected the protein from complete degradation by trypsin. Endogenous G $\alpha_s$  from hLHR<sup>+</sup>/HEK-293 membranes was also protected from trypsin digestion after the addition of GTP $\gamma$ S (Fig. 3.15B). No difference was seen after the stimulation of hLHR with hCG, however, indicating that the assay could not detect the nucleotide-binding state of G $\alpha$  after hLHR activation.

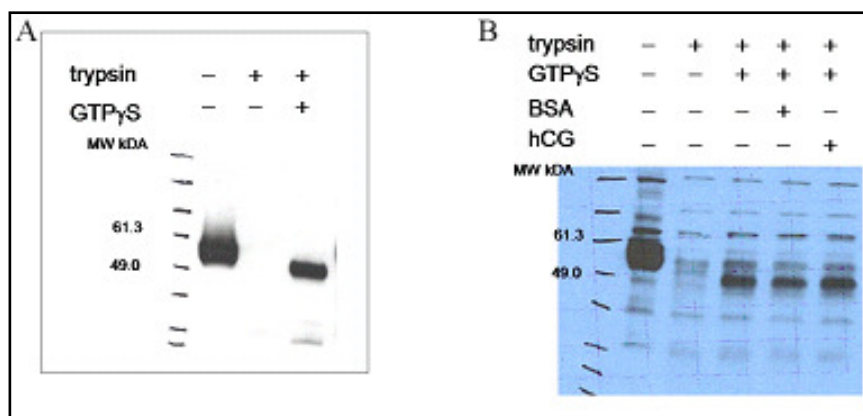


**Figure 3.15.** Trypsin digestion assay. **A.** Anti-G $\alpha_s$  Western blot of purified G $\alpha_s$  treated with GTP $\gamma$ S and trypsin. **B.** Crude membranes were collected from hLHR<sup>+</sup>/HEK-293 cells and stimulated with either BSA (negative control) or hCG then subjected to trypsin digestion.



Because the same results were collected from HEK-293 and MA-10 cells transiently-transfected with wild-type hLHR, D578H, and I472A as well as from the same samples probed for  $G\alpha_{i/o}$  and  $G\alpha_q$  (data not shown), many experimental conditions were varied to discourage the uncoupling of  $G\alpha$  from the receptors during sample preparation. These included the method of cellular disruption as well as the concentrations of GDP, GTP $\gamma$ S, trypsin, and membrane protein loaded into the gels. No difference was seen with these variations of the experimental procedure (data not shown).

*ii. Modification of the trypsin digestion assay to analyze a permeabilized cellular environment*

Presumably the  $G\alpha$  subunit uncoupled from receptor control during the preparation of samples and was therefore able to spontaneously and independently bind GTP $\gamma$ S for protection against trypsin digestion. Therefore, the assay was modified to create an intact cellular environment for the membrane proteins. Cells were permeabilized with Streptolysin O (SLO), a pore-forming toxin, to expose the  $G\alpha$  protein to trypsin in a more native-like environment. Figure 3.16 depicts the permeabilization of HEK-293 cells with the SLO toxin. Greater than 95% of cells treated with SLO (Fig. 3.16B) were stained with trypan blue whereas less than 5% of cells treated with vehicle (Fig. 3.16A) appear permeabilized.

Although cells were permeabilized with SLO, trypsin did not access the  $G\alpha$  subunit in this environment

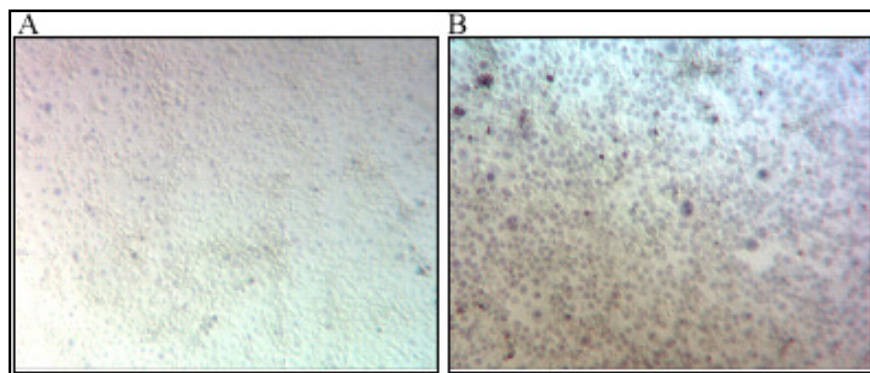


**Figure 3.16.** Trypan blue treatment of adherent HEK-293 cells permeabilized with SLO. *A.* Cells treated with vehicle. *B.* Cells treated with SLO. 10x magnification.

(Fig. 3.17C). Increasing the cellular lysate:trypsin ratio digested  $G\alpha_s$  but did not specifically identify GTP $\gamma$ S-bound  $G\alpha_s$  (Fig. 3.17A, B).

### Discussion

The adaptation of the trypsin digestion assay as it was published was unsuccessful. The method of cellular disruption appeared to uncouple the  $G\alpha$  subunit from receptor control. Different types of homogenizers and homogenization treatments in buffers containing various concentrations of detergent (CHAPS) were employed to encourage the retention of a native receptor/G protein relationship. When no difference in the results was observed, the assay was modified to retain the *in vivo* cellular environment with the application of permeabilizing agents to adherent, intact cells. The SLO toxin formed pores in the cellular membranes, theoretically providing access for trypsin to the membranes and thus,  $G\alpha_s$ . The membranes in this state were not “solubilized” as they were in the standard trypsin assay, and perhaps the  $G\alpha$  subunits and trypsin molecules were separated by different phases and trypsin was thus unable to digest the G protein and detect its nucleotide-bound state (Fig. 3.17C). When the ratio of cellular lysate

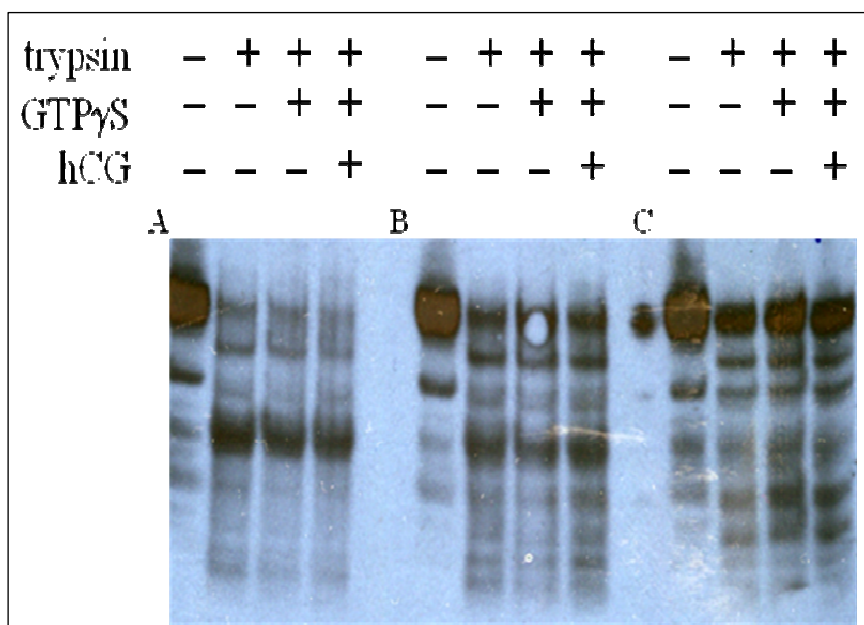


**Figure 3.17.** Western blot of SLO-permeabilized HEK-293 cells from a trypsin protection assay. 50  $\mu$ g cellular lysate was loaded per lane. Increasing amounts of cellular lysate:trypsin were applied as indicated: (A) 1:5, (B) 1:10, and (C) 1:50.

to trypsin was increased (Fig. 3.17A,B), digestion of the  $G\alpha$  subunit was observed but the addition of GTP $\gamma$ S was insufficient to protect the  $G\alpha_s$  subunit from the enzymatic digestion. The trypsin protection assay was never adapted to suit the purposes of this work. Notably, this technique is not a standard within the field, and personal communication with the authors indicated that they encountered the same problems with subsequent repetitions of the assay after publication of the initial report (331).

### ***Non-specific effects of $G\alpha$ -targeted RNAi preclude its use to dissect hLHR/ $G_s$ signaling***

#### *Introduction*

Functional studies that probe the signaling of hLHR through  $G_s$  suggest that residues within the second intracellular loop of hLHR are important for the coupling event (144). Very little is known, however, about the contribution of  $G\alpha_s$  residues to the molecular interface formed with hLHR. To effectively measure the contribution of  $G\alpha_s$  to hLHR coupling, a model system lacking the endogenous presence of  $G\alpha_s$  is necessary. A report detailing the use of RNAi to effectively knock-down expression of heterotrimeric G protein isoforms (332) prompted the design of a model system that utilized RNAi to decrease the endogenous expression and function of  $G\alpha_s$  in hLHR<sup>+</sup>/HEK-293 cells.

#### *Experimental Procedures*

##### *i. Materials*

Cell culture and transfection reagents were as listed previously. siRNAs were custom synthesized to target human  $G\alpha_s$  (h $G\alpha_s$ ) mRNA by Dharmacon as in ref. (332) and as a negative, non-specific RNAi control, a non-targeting siRNA was purchased. Oligofectamine (Invitrogen) was used as per manufacturer instructions for the transfection of siRNAs. A set of four shRNAs targeting h $G\alpha_s$  mRNA (#TR304299) were purchased from Origene (Rockville, MD), and as a negative, non-specific RNAi control, a non-targeting shRNA was included. Transfection of shRNA-containing vectors was with Lipofectamine2000 as detailed previously. RIPA buffer was from Santa Cruz.

*ii. Introduction of siRNAs and shRNAs targeting human  $G\alpha_s$  into hLHR<sup>+</sup>/HEK-293 cells*

A clonal line of HEK-293 cells stably expressing hLHR was created after transfection with hLHR cDNA in pcDNA6.2Topo (Invitrogen) and subsequent selection with 10 $\mu$ g/mL blasticidin for 2 weeks. hLHR expression was monitored with <sup>125</sup>I-hCG binding assays as described in Chapter 2. Knockdown with siRNAs was performed as described in (332) using two phases of transfection with Oligofectamine approximately 3 days apart. Cells were collected 48 hours after the second transfection and assayed for protein expression and cAMP activity. shRNAs targeting hG $\alpha_s$  in the pRS vector were transfected with Lipofectamine into hLHR<sup>+</sup>/HEK-293 cells and selection for stable lines occurred in 1  $\mu$ g/mL puromycin for 2 weeks. Cells were then assayed for protein expression via Western blotting as described previously.

*iii. Preparation of crude cellular lysate, SDS-PAGE, Western blotting, and cAMP measurement*

Cells in 10cm dishes were lysed as per manufacturer's instructions in RIPA buffer. Western blots were performed as described previously and in Chapter 2. The production of cAMP was monitored as discussed in Chapter 2.

*Results*

*i. siRNAs successfully decreased the expression of hG $\alpha_s$  in hLHR<sup>+</sup>/HEK-293 cells but a concomitant decrease in cAMP production was an off-target RNAi effect*

RNAi with siRNAs directed towards hG $\alpha_s$  decreased the expression of hG $\alpha_s$  in hLHR<sup>+</sup>/HEK-293 cells (Fig. 3.18). A decrease in cAMP production upon hCG stimulation for these cells compared to mock-transfected cells was also observed (Fig. 3.19). The non-specific RNAi-transfected control cells, however, also exhibited a similar decrease in cAMP production. Therefore, the effect upon second messenger stimulation was a result of an off-target RNAi effect and any direct effect of the hG $\alpha_s$ -targeting siRNAs could not be distinguished from the negative, non-targeting control.

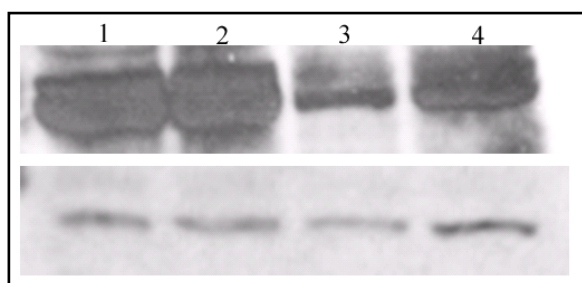
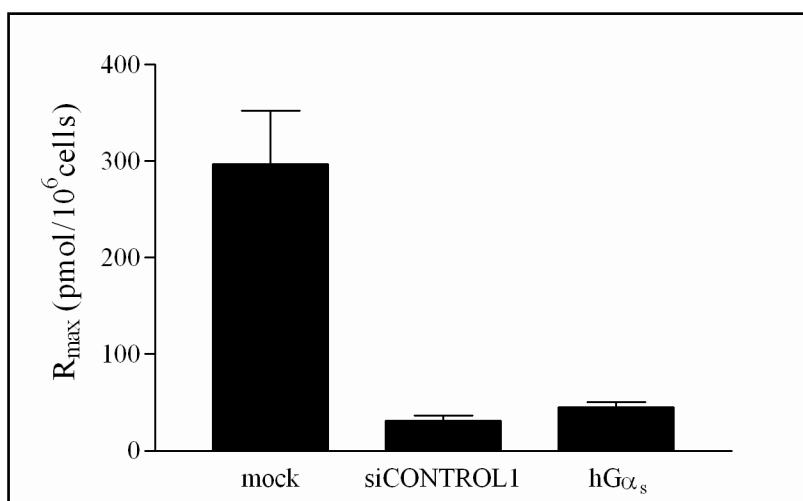


**Figure 3.18.** Protein expression of hLHR<sup>+</sup>/HEK-293 cells receiving RNAi treatment. Panel (A), anti-Gα<sub>s</sub> and (B), anti-actin Western blots. Lane 1: Mock-transfected cells, 10 μg cellular protein. Lane 2: Non-targeting siRNA-transfected control cells, 10 μg cellular protein. Lane 3 and 4: Gα<sub>s</sub> siRNA-transfected cells, 10 and 20 μg cellular protein, respectively.

**Figure 3.19.** Maximum cAMP production of hLHR<sup>+</sup>/HEK-293 cells receiving RNAi treatment and hCG stimulation.



ii. *shRNAs targeting hGα<sub>s</sub> did not successfully knock-down hGα<sub>s</sub> protein expression.*

The four shRNAs directed to knock-down hGα<sub>s</sub> protein expression had no effect upon endogenous hGα<sub>s</sub> protein levels in hLHR<sup>+</sup>/HEK-293 cells as measured by Western blotting either when transiently transfected or after selection of stable transformants (data not shown).

### Discussion

The transfection of siRNAs targeting the human isoforms of Gα<sub>s</sub> successfully reduced the amount of protein expression as measured by Western blotting. When stimulated with hCG, both sets of cells transfected with targeting and non-targeting siRNAs exhibited a decrease in cAMP production, and therefore, the decrease of cAMP synthesis cannot be attributed to the knockdown of Gα<sub>s</sub> expression and must be considered a non-specific RNAi effect (333). The report that described the procedure for Gα<sub>s</sub>

knockdown used HeLa cells that do not express endogenous hLHR, and notably, the negative control for RNAi was not precisely described (332). If the control was a sample of mock-transfected cells, the functional results of this work agree with the previous study, but if, however, the negative control was a non-targeting siRNA, a discrepancy remains. The aim of this work was to create a model cell hLHR<sup>+</sup> line that exhibited decreased expression and diminished function of G $\alpha_s$ . Neither the siRNA nor the shRNA approach generated such a model.

## ***Conclusion***

This chapter described attempts to further characterize the molecular landscape of hLHR. Specifically, the hLHR/G<sub>s</sub> coupling relationship and the capacity of hLHR to dimerize were probed with techniques that have yet to become well-established. The failure of these methods to provide reliable data may be at least somewhat attributable to the nature of hLHR, notably the capacity of its large extracellular domain to aggregate. Many of the methods required a high level of protein expression that appeared to interfere with proper trafficking and localization. This work questions some of the published results concerning the glycoprotein hormone receptors and other GPCRs, but was not undertaken to rigorously examine the experiments of others. Rather, the goal was to adapt these techniques for the exploration of the molecular relationships of hLHR and, unfortunately, success was limited. Perhaps these methods are not suitable for the examination of all members of the GPCR family, and/or perhaps the conditions of the experiments described herein were not sufficiently sensitive to provide conclusive data.

## CONCLUSIONS

The investigation of natural phenomena begins with general characterizations that define simple ‘rules’ of behavior. Once a foundation is cast, exceptions may be recognized which then prompt an amendment of the original interpretation to accommodate the newly observed complexity. The theoretical models of GPCR signaling have progressed through this cycle of discovery and revision and should continue to do so as the expanding catalogue of GIPs extends the known breadth of the GPCR ‘receptosome’. As methodologies become more sensitive and comprehensive, the reliance upon representative GPCRs, such as rhodopsin and the  $\beta_2$ -AR, to embody the principles of receptor activity will taper, and the characterization of more receptors should expose the behavioral diversity encompassed within the GPCR superfamily.

Importantly, the work described within this document led to the conclusion that the hLHR and  $\beta_2$ -AR differentially couple to  $G\alpha_s$ . This novel and valuable information revealed that the receptors as well as  $G\alpha_s$  display a distinct pattern of residues for recognition, and each unique arrangement can facilitate  $G\alpha_s$  nucleotide exchange. Therefore, the G proteins exhibit a structural plasticity that complements that of their cognate receptors. The G protein family is not as diverse as that of the GPCRs, yet they maintain the specificity of the signaling relay from each unique ligand/receptor pair. The presentation of distinct coupling interfaces, the patterning of  $G\alpha\beta\gamma$  isoform pairings, and the association of regulatory and/or scaffolding proteins may each contribute to this fidelity of G protein signaling transmission. These complexities are not addressed by current models of GPCR/G protein coupling.

Although the hLHR and other glycoprotein hormone receptors are rhodopsin-like, they do not exhibit high- and low-affinity ligand-binding states—the association with G proteins does not influence the ligand-binding capacity of GpHRs because the ECDs bind ligand and subsequently translate

activation to the transmembrane domains. The GpHRs thus demonstrate interesting mechanisms of GPCR/G protein coupling that may not fully align with the prevailing dogma.

hLHR appears to signal primarily through G protein-governed pathways, but the emergent molecular and physiological responses suggest an intricacy of signaling networks that are not explained by simple, linear receptor-G protein-effector relationships. Indeed, any model that describes hLHR activity should define its role(s) within a cellular context but must also consider its position as part of a complex tissue microenvironment.

Advances in science progress with the evolution of available tools. Many of the current methods to observe molecular environments require the use of engineered, non-native systems to attain the sensitivity and conditions necessary for data collection. Conclusions drawn from these techniques must always account for the possibility of introduced artifact. GPCR studies often utilize over-expression systems to increase signal strength, but receptors expressed at these levels may not exhibit normal behavior. Also, methods may successfully measure phenomena in one system, but even slight differences in closely-related systems may hinder their application in others. Currently, not all tools suit the analysis of all GPCRs, but the future is always promising.

This is an exciting time for research with GPCRs. The application of sophisticated technologies continues to expose the remarkable properties of these proteins that mediate much of human physiology. The study of these receptors satisfies those interested in both fundamental biochemistry as well as in clinical research, and the translation of one to the other offers significant and lucrative opportunities that will only be realized through an astute appreciation of the nuances encapsulated within this, the largest of the human gene families.



## REFERENCES

1. Lefkowitz, R. J. (2007) *Acta Physiol (Oxf)* **190**, 9-19
2. Cabrera-Vera, T. M., Vanhauwe, J., Thomas, T. O., Medkova, M., Preininger, A., Mazzoni, M. R., and Hamm, H. E. (2003) *Endocr Rev* **24**, 765-781
3. Van Tol, H. H. (1998) *Adv Pharmacol* **42**, 486-490
4. Nordhoff, V., Gromoll, J., and Simoni, M. (1999) *Arch Med Res* **30**, 501-509
5. Piersma, D., Verhoef-Post, M., Berns, E. M., and Themmen, A. P. (2007) *Mol Cell Endocrinol* **260-262**, 282-286
6. Seminara, S. B., and Crowley, W. F., Jr. (2001) *Endocrinology* **142**, 2173-2177
7. Themmen, A. P. N., and Huhtaniemi, I. T. (2000) *Endocr Rev* **21**, 551-583
8. Themmen, A. P. (2005) *Reproduction* **130**, 263-274
9. Eyssette-Guerreau, S., Pinto, G., Sultan, A., Le Merrer, M., Sultan, C., and Polak, M. (2008) *J Pediatr Endocrinol Metab* **21**, 995-1002
10. Ascoli, M., Fanelli, F., and Segaloff, D. L. (2002) *Endocr Rev* **23**, 141-174
11. Jones, R. E. (1997) *Human Reproductive Biology*, 2nd ed., Academic Press, San Diego
12. Clements, J. A., Reyes, F. I., Winter, J. S., and Faiman, C. (1976) *J Clin Endocrinol Metab* **42**, 9-19
13. Molsberry, R. L., Carr, B. R., Mendelson, C. R., and Simpson, E. R. (1982) *J Clin Endocrinol Metab* **55**, 791-794
14. Huhtaniemi, I. (2006) *Mol Cell Endocrinol* **254-255**, 84-90
15. Banerjee, I., and Clayton, P. (2007) *J Neuroendocrinol* **19**, 831-838
16. DiVall, S. A., and Radovick, S. (2008) *Ann N Y Acad Sci* **1135**, 19-28
17. Matthiesson, K. L., McLachlan, R. I., O'Donnell, L., Frydenberg, M., Robertson, D. M., Stanton, P. G., and Meachem, S. J. (2006) *J Clin Endocrinol Metab* **91**, 3962-3969
18. Filicori, M. (1999) *Fertil Steril* **71**, 405-414
19. Hillier, S. G. (2001) *Mol Cell Endocrinol* **179**, 39-46
20. Richards, J. S. (2001) *Endocrinology* **142**, 2184-2193
21. Stocco, C., Telleria, C., and Gibori, G. (2007) *Endocr Rev* **28**, 117-149
22. Oon, V. J., and Johnson, M. R. (2000) *Hum Reprod Update* **6**, 519-529
23. Chakravarti, S., Collins, W. P., Forecast, J. D., Newton, J. R., Oram, D. H., and Studd, J. W. (1976) *Br Med J* **2**, 784-787
24. Choi, J. H., Wong, A. S., Huang, H. F., and Leung, P. C. (2007) *Endocr Rev* **28**, 440-461
25. Cramer, D. W., and Welch, W. R. (1983) *J Natl Cancer Inst* **71**, 717-721
26. Ozols, R. F., Bookman, M. A., Connolly, D. C., Daly, M. B., Godwin, A. K., Schilder, R. J., Xu, X., and Hamilton, T. C. (2004) *Cancer Cell* **5**, 19-24
27. Ichikawa, Y., Yoshida, S., Suzuki, H., Nishida, M., Tsunoda, H., Kubo, T., Miwa, M., and Uchida, K. (1996) *Jpn J Clin Oncol* **26**, 298-302
28. Lu, J. J., Zheng, Y., Kang, X., Yuan, J. M., Lauchlan, S. C., Pike, M. C., and Zheng, W. (2000) *Gynecol Oncol* **79**, 158-168
29. Fredriksson, R., Lagerstrom, M. C., Lundin, L. G., and Schioth, H. B. (2003) *Mol Pharmacol* **63**, 1256-1272
30. Gether, U. (2000) *Endocr Rev* **21**, 90-113
31. Gurevich, V. V., and Gurevich, E. V. (2008) *Trends Pharmacol Sci* **29**, 234-240
32. Muller, G. (2000) *Curr Med Chem* **7**, 861-888

33. Tao, Y. X. (2006) *Pharmacol Ther* **111**, 949-973
34. Schoneberg, T., Schulz, A., Biebermann, H., Hermsdorf, T., Rompler, H., and Sangkuhl, K. (2004) *Pharmacol Ther* **104**, 173-206
35. Drews, J. (1996) *Nat Biotechnol* **14**, 1516-1518
36. Maudsley, S., Martin, B., and Luttrell, L. M. (2005) *J Pharmacol Exp Ther* **314**, 485-494
37. Kenakin, T. (1995) *Trends Pharmacol Sci* **16**, 232-238
38. Kenakin, T. (1995) *Trends Pharmacol Sci* **16**, 188-192
39. Kenakin, T. (2007) *Mol Pharmacol* **72**, 1393-1401
40. Luttrell, L. M. (2006) *Methods Mol Biol* **332**, 3-49
41. Jacoby, E., Bouhelal, R., Gerspacher, M., and Seuwen, K. (2006) *ChemMedChem* **1**, 761-782
42. Bockaert, J., Roussignol, G., Becamel, C., Gavarini, S., Joubert, L., Dumuis, A., Fagni, L., and Marin, P. (2004) *Biochem Soc Trans* **32**, 851-855
43. Bockaert, J., Fagni, L., Dumuis, A., and Marin, P. (2004) *Pharmacol Ther* **103**, 203-221
44. Sun, Y., McGarrigle, D., and Huang, X. Y. (2007) *Mol Biosyst* **3**, 849-854
45. Schioth, H. B., and Fredriksson, R. (2005) *Gen Comp Endocrinol* **142**, 94-101
46. Hall, R. A., Premont, R. T., and Lefkowitz, R. J. (1999) *J Cell Biol* **145**, 927-932
47. Gurevich, V. V., and Gurevich, E. V. (2008) *Trends Neurosci* **31**, 74-81
48. Kenakin, T. (2004) *Trends Pharmacol Sci* **25**, 186-192
49. Onaran, H. O., and Costa, T. (1997) *Ann N Y Acad Sci* **812**, 98-115
50. De Lean, A., Stadel, J. M., and Lefkowitz, R. J. (1980) *J Biol Chem* **255**, 7108-7117
51. Kenakin, T. P. (1997) *Pharmacologic analysis of drug-receptor interaction*, 3rd ed., Lippincott-Raven Publishers, Philadelphia
52. Samama, P., Cotecchia, S., Costa, T., and Lefkowitz, R. J. (1993) *J Biol Chem* **268**, 4625-4636
53. Weiss, J. M., Morgan, P. H., Lutz, M. W., and Kenakin, T. P. (1996) *J Theor Biol* **181**, 381-397
54. Kobilka, B. K., and Deupi, X. (2007) *Trends Pharmacol Sci* **28**, 397-406
55. Roberts, D. J., and Waelbroeck, M. (2004) *Biochem Pharmacol* **68**, 799-806
56. Birnbaumer, L. (2007) *Biochim Biophys Acta* **1768**, 756-771
57. Mustafi, D., and Palczewski, K. (2009) *Mol Pharmacol* **75**, 1-12
58. Fanelli, F., Verhoef-Post, M., Timmerman, M., Zeilemaker, A., Martens, J. W., and Themmen, A. P. (2004) *Mol Endocrinol* **18**, 1499-1508
59. Fanelli, F., and Puett, D. (2002) *Endocrine* **18**, 285-293
60. Filipek, S., Teller, D. C., Palczewski, K., and Stenkamp, R. (2003) *Annu Rev Biophys Biomol Struct* **32**, 375-397
61. Fotiadis, D., Jastrzebska, B., Philippsen, A., Muller, D. J., Palczewski, K., and Engel, A. (2006) *Curr Opin Struct Biol* **16**, 252-259
62. Bhattacharya, S., Hall, S. E., and Vaidehi, N. (2008) *J Mol Biol* **382**, 539-555
63. Worth, C. L., Kleinau, G., and Krause, G. (2009) *PLoS One* **4**, e7011
64. Fung, B. K. (1983) *J Biol Chem* **258**, 10495-10502
65. Gilman, A. G. (1987) *Annu Rev Biochem* **56**, 615-649
66. Levitzki, A., and Klein, S. (2002) *Chembiochem* **3**, 815-818
67. Rebois, R. V., Warner, D. R., and Basi, N. S. (1997) *Cell Signal* **9**, 141-151
68. Feder, D., Im, M. J., Klein, H. W., Hekman, M., Holzhofer, A., Dees, C., Levitzki, A., Helmreich, E. J., and Pfeuffer, T. (1986) *EMBO J* **5**, 1509-1514
69. Hekman, M., Feder, D., Keenan, A. K., Gal, A., Klein, H. W., Pfeuffer, T., Levitzki, A., and Helmreich, E. J. (1984) *EMBO J* **3**, 3339-3345
70. Tolkovsky, A. M., and Levitzki, A. (1978) *Biochemistry* **17**, 3795
71. Levitzki, A. (1986) *Physiol Rev* **66**, 819-854
72. Hein, P., Rochais, F., Hoffmann, C., Dorsch, S., Nikolaev, V. O., Engelhardt, S., Berlot, C. H., Lohse, M. J., and Bunemann, M. (2006) *J Biol Chem* **281**, 33345-33351
73. Gales, C., Rebois, R. V., Hogue, M., Trieu, P., Breit, A., Hebert, T. E., and Bouvier, M. (2005) *Nat Methods* **2**, 177-184

74. Rebois, R. V., Robitaille, M., Gales, C., Dupre, D. J., Baragli, A., Trieu, P., Ethier, N., Bouvier, M., and Hebert, T. E. (2006) *J Cell Sci* **119**, 2807-2818
75. Lohse, M. J., Hoffmann, C., Nikolaev, V. O., Vilardaga, J. P., and Bunemann, M. (2007) *Adv Protein Chem* **74**, 167-188
76. Gales, C., Van Durm, J. J., Schaak, S., Pontier, S., Percherancier, Y., Audet, M., Paris, H., and Bouvier, M. (2006) *Nat Struct Mol Biol* **13**, 778-786
77. Dowal, L., Provitera, P., and Scarlata, S. (2006) *J Biol Chem* **281**, 23999-24014
78. Benians, A., Nobles, M., Hosny, S., and Tinker, A. (2005) *J Biol Chem* **280**, 13383-13394
79. Herrmann, R., Heck, M., Henklein, P., Kleuss, C., Hofmann, K. P., and Ernst, O. P. (2004) *J Biol Chem* **279**, 24283-24290
80. Herrmann, R., Heck, M., Henklein, P., Kleuss, C., Wray, V., Hofmann, K. P., and Ernst, O. P. (2006) *Vision Res* **46**, 4582-4593
81. Johnston, C. A., and Siderovski, D. P. (2007) *Mol Pharmacol* **72**, 219-230
82. Itoh, Y., Cai, K., and Khorana, H. G. (2001) *Proc Natl Acad Sci U S A* **98**, 4883-4887
83. Grishina, G., and Berlot, C. H. (2000) *Mol Pharmacol* **57**, 1081-1092
84. Herrmann, R., Heck, M., Henklein, P., Hofmann, K. P., and Ernst, O. P. (2006) *J Biol Chem* **281**, 30234-30241
85. Rasenick, M. M., Watanabe, M., Lazarevic, M. B., Hatta, S., and Hamm, H. E. (1994) *J Biol Chem* **269**, 21519-21525
86. Onrust, R., Herzmark, P., Chi, P., Garcia, P. D., Lichtarge, O., Kingsley, C., and Bourne, H. R. (1997) *Science* **275**, 381-384
87. Hamm, H. E., Deretic, D., Arendt, A., Hargrave, P. A., Koenig, B., and Hofmann, K. P. (1988) *Science* **241**, 832-835
88. Slessareva, J. E., Ma, H., Depree, K. M., Flood, L. A., Bae, H., Cabrera-Vera, T. M., Hamm, H. E., and Graber, S. G. (2003) *J Biol Chem* **278**, 50530-50536
89. Oldham, W. M., Van Eps, N., Preininger, A. M., Hubbell, W. L., and Hamm, H. E. (2006) *Nat Struct Mol Biol* **13**, 772-777
90. Fotiadis, D., Liang, Y., Filipek, S., Saperstein, D. A., Engel, A., and Palczewski, K. (2003) *Nature* **421**, 127-128
91. Ernst, O. P., Gramse, V., Kolbe, M., Hofmann, K. P., and Heck, M. (2007) *Proc Natl Acad Sci U S A* **104**, 10859-10864
92. Chabre, M., and le Maire, M. (2005) *Biochemistry* **44**, 9395-9403
93. Filipek, S., Krzysko, K. A., Fotiadis, D., Liang, Y., Saperstein, D. A., Engel, A., and Palczewski, K. (2004) *Photochem Photobiol Sci* **3**, 628-638
94. Limbird, L. E. (1996) *Cell surface receptors : a short course on theory and methods*, 2nd ed., Kluwer Academic Publishers, Boston
95. Lefkowitz, R. J., and Shenoy, S. K. (2005) *Science* **308**, 512-517
96. Marsh, S. R., Grishina, G., Wilson, P. T., and Berlot, C. H. (1998) *Mol Pharmacol* **53**, 981-990
97. Hynes, T. R., Mervine, S. M., Yost, E. A., Sabo, J. L., and Berlot, C. H. (2004) *J Biol Chem* **279**, 44101-44112
98. Angers, S., Salahpour, A., Joly, E., Hilaiet, S., Chelsky, D., Dennis, M., and Bouvier, M. (2000) *Proc Natl Acad Sci U S A* **97**, 3684-3689
99. Hanson, M. A., and Stevens, R. C. (2009) *Structure* **17**, 8-14
100. Lundstrom, K. (2006) *Curr Protein Pept Sci* **7**, 465-470
101. Vassilatis, D. K., Hohmann, J. G., Zeng, H., Li, F., Ranchalis, J. E., Mortrud, M. T., Brown, A., Rodriguez, S. S., Weller, J. R., Wright, A. C., Bergmann, J. E., and Gaitanaris, G. A. (2003) *Proc Natl Acad Sci U S A* **100**, 4903-4908
102. Vassart, G., Pardo, L., and Costagliola, S. (2004) *Trends Biochem Sci* **29**, 119-126
103. Smits, G., Campillo, M., Govaerts, C., Janssens, V., Richter, C., Vassart, G., Pardo, L., and Costagliola, S. (2003) *EMBO J* **22**, 2692-2703
104. Vischer, H. F., Granneman, J. C., and Bogerd, J. (2003) *Mol Endocrinol* **17**, 1972-1981

105. Vischer, H. F., Granneman, J. C., Noordam, M. J., Mosselman, S., and Bogerd, J. (2003) *J Biol Chem* **278**, 15505-15513
106. Angelova, K., Puett, D., and Bogerd, J. (2010).
107. Song, Y. S., Ji, I., Beauchamp, J., Isaacs, N. W., and Ji, T. H. (2001) *J Biol Chem* **276**, 3426-3435
108. Vischer, H. F., Granneman, J. C., and Bogerd, J. (2006) *Mol Endocrinol* **20**, 1880-1893
109. Kleinau, G., and Krause, G. (2009) *Endocr Rev* **30**, 133-151
110. Ulloa-Aguirre, A., Uribe, A., Zarinan, T., Bustos-Jaimes, I., Perez-Solis, M. A., and Dias, J. A. (2007) *Mol Cell Endocrinol* **260-262**, 153-162
111. Zhang, M., Tao, Y. X., Ryan, G. L., Feng, X., Fanelli, F., and Segaloff, D. L. (2007) *J Biol Chem* **282**, 25527-25539
112. Hirsch, B., Kudo, M., Naro, F., Conti, M., and Hsueh, A. J. (1996) *Mol Endocrinol* **10**, 1127-1137
113. Kleinau, G., Brehm, M., Wiedemann, U., Labudde, D., Leser, U., and Krause, G. (2007) *Mol Endocrinol* **21**, 574-580
114. Van Loy, T., Van Hiel, M. B., Vandersmissen, H. P., Poels, J., Mendive, F., Vassart, G., and Vanden Broeck, J. (2007) *Gen Comp Endocrinol* **153**, 59-63
115. Braun, T., Schofield, P. R., and Sprengel, R. (1991) *EMBO J* **10**, 1885-1890
116. Moyle, W. R., Bernard, M. P., Myers, R. V., Marko, O. M., and Strader, C. D. (1991) *J Biol Chem* **266**, 10807-10812
117. Osuga, Y., Kudo, M., Kaipia, A., Kobilka, B., and Hsueh, A. J. (1997) *Mol Endocrinol* **11**, 1659-1668
118. Fralish, G. B., Narayan, P., and Puett, D. (2001) *Endocrinology* **142**, 1517-1524
119. Fan, Q. R., and Hendrickson, W. A. (2005) *Nature* **433**, 269-277
120. Li, Y., and Puett, D. (2006) unpublished results.
121. Bhowmick, N., Huang, J., Puett, D., Isaacs, N. W., and Laphorn, A. J. (1996) *Mol Endocrinol* **10**, 1147-1159
122. Hipkin, R. W., Sanchez-Yague, J., and Ascoli, M. (1992) *Mol Endocrinol* **6**, 2210-2218
123. Ascoli, M., and Puett, D. (2009) The Gonadotropins and Their Receptors. in *Yen and Jaffee's Reproductive Endocrinology* (Strauss III, J. F., and Barbieri, R. eds.), 6 Ed., Elsevier Publ. Co., Philadelphia, PA. pp 35-55
124. Galet, C., and Ascoli, M. (2005) *Mol Endocrinol* **19**, 1263-1276
125. Moyle, W. R., Lin, W., Myers, R. V., Cao, D., Kerrigan, J. E., and Bernard, M. P. (2005) *Endocrine* **26**, 189-205
126. Sanders, J., Chirgadze, D. Y., Sanders, P., Baker, S., Sullivan, A., Bhardwaja, A., Bolton, J., Reeve, M., Nakatake, N., Evans, M., Richards, T., Powell, M., Miguel, R. N., Blundell, T. L., Furmaniak, J., and Smith, B. R. (2007) *Thyroid* **17**, 395-410
127. Tapanainen, J. S., Lapolt, P. S., Perlas, E., and Hsueh, A. J. (1993) *Endocrinology* **133**, 2875-2880
128. Matzuk, M. M., Keene, J. L., and Boime, I. (1989) *J Biol Chem* **264**, 2409-2414
129. Sairam, M. R. (1989) *FASEB J* **3**, 1915-1926
130. Moyle, W. R., Xing, Y., Lin, W., Cao, D., Myers, R. V., Kerrigan, J. E., and Bernard, M. P. (2004) *J Biol Chem* **279**, 44442-44459
131. Bruysters, M., Verhoef-Post, M., and Themmen, A. P. (2008) *J Biol Chem* **283**, 25821-25828
132. Bonomi, M., Busnelli, M., Persani, L., Vassart, G., and Costagliola, S. (2006) *Mol Endocrinol* **20**, 3351-3363
133. Gromoll, J., Eiholzer, U., Nieschlag, E., and Simoni, M. (2000) *J Clin Endocrinol Metab* **85**, 2281-2286
134. Wu, H., Lustbader, J. W., Liu, Y., Canfield, R. E., and Hendrickson, W. A. (1994) *Structure* **2**, 545-558
135. Okada, T., Sugihara, M., Bondar, A. N., Elstner, M., Entel, P., and Buss, V. (2004) *J Mol Biol* **342**, 571-583

136. Lambright, D. G., Sondek, J., Bohm, A., Skiba, N. P., Hamm, H. E., and Sigler, P. B. (1996) *Nature* **379**, 311-319
137. Nurwakagari, P., Breit, A., Hess, C., Salman-Livny, H., Ben-Menahem, D., and Gudermann, T. (2007) *J Mol Endocrinol* **38**, 259-275
138. Ji, I., Lee, C., Song, Y., Conn, P. M., and Ji, T. H. (2002) *Mol Endocrinol* **16**, 1299-1308
139. Lee, C., Ji, I., Ryu, K., Song, Y., Conn, P. M., and Ji, T. H. (2002) *J Biol Chem* **277**, 15795-15800
140. Kristiansen, K. (2004) *Pharmacol Ther* **103**, 21-80
141. Angelova, K., Fanelli, F., and Puett, D. (2002) *J Biol Chem* **277**, 32202-32213
142. Zhang, M., Mizrachi, D., Fanelli, F., and Segaloff, D. L. (2005) *J Biol Chem* **280**, 26169-26176
143. Schulz, A., Schoneberg, T., Paschke, R., Schultz, G., and Gudermann, T. (1999) *Mol Endocrinol* **13**, 181-190
144. Angelova, K., Fanelli, F., and Puett, D. (2008) *Mol Endocrinol* **22**, 126-138
145. Fernandez, L. M., and Puett, D. (1997) *Mol Cell Endocrinol* **128**, 161-169
146. Kudo, M., Osuga, Y., Kobilka, B. K., and Hsueh, A. J. (1996) *J Biol Chem* **271**, 22470-22478
147. Abell, A. N., McCormick, D. J., and Segaloff, D. L. (1998) *Mol Endocrinol* **12**, 1857-1869
148. Palczewski, K., Kumasaka, T., Hori, T., Behnke, C. A., Motoshima, H., Fox, B. A., Le Trong, I., Teller, D. C., Okada, T., Stenkamp, R. E., Yamamoto, M., and Miyano, M. (2000) *Science* **289**, 739-745
149. Meng, E. C., and Bourne, H. R. (2001) *Trends Pharmacol Sci* **22**, 587-593
150. Greasley, P. J., Fanelli, F., Rossier, O., Abuin, L., and Cotecchia, S. (2002) *Mol Pharmacol* **61**, 1025-1032
151. Ballesteros, J. A., Jensen, A. D., Liapakis, G., Rasmussen, S. G., Shi, L., Gether, U., and Javitch, J. A. (2001) *J Biol Chem* **276**, 29171-29177
152. Shapiro, D. A., Kristiansen, K., Weiner, D. M., Kroeze, W. K., and Roth, B. L. (2002) *J Biol Chem* **277**, 11441-11449
153. Visiers, I., Ballesteros, J. A., and Weinstein, H. (2002) *Methods Enzymol* **343**, 329-371
154. Hirakawa, T., Galet, C., and Ascoli, M. (2002) *Endocrinology* **143**, 1026-1035
155. Bhaskaran, R. S., Min, L., Krishnamurthy, H., and Ascoli, M. (2003) *Biochemistry* **42**, 13950-13959
156. Hipkin, R. W., Liu, X., and Ascoli, M. (1995) *J Biol Chem* **270**, 26683-26689
157. Min, L., Galet, C., and Ascoli, M. (2002) *J Biol Chem* **277**, 702-710
158. Wang, Z., Liu, X., and Ascoli, M. (1997) *Mol Endocrinol* **11**, 183-192
159. Galet, C., Hirakawa, T., and Ascoli, M. (2004) *Mol Endocrinol* **18**, 434-446
160. Hirakawa, T., Galet, C., Kishi, M., and Ascoli, M. (2003) *J Biol Chem* **278**, 49348-49357
161. Latronico, A. C., Anasti, J., Arnhold, I. J., Rapaport, R., Mendonca, B. B., Bloise, W., Castro, M., Tsigos, C., and Chrousos, G. P. (1996) *N Engl J Med* **334**, 507-512
162. Laue, L. L., Wu, S. M., Kudo, M., Bourdony, C. J., Cutler, G. B., Jr., Hsueh, A. J., and Chan, W. Y. (1996) *Mol Endocrinol* **10**, 987-997
163. Kosugi, S., Mori, T., and Shenker, A. (1996) *J Biol Chem* **271**, 31813-31817
164. Angelova, K., Narayan, P., Simon, J. P., and Puett, D. (2000) *Mol Endocrinol* **14**, 459-471
165. Kosugi, S., Mori, T., and Shenker, A. (1998) *Mol Pharmacol* **53**, 894-901
166. Zhu, X., Gilbert, S., Birnbaumer, M., and Birnbaumer, L. (1994) *Mol Pharmacol* **46**, 460-469
167. Van Durme, J., Horn, F., Costagliola, S., Vriend, G., and Vassart, G. (2006) *Mol Endocrinol* **20**, 2247-2255
168. Kuhn, B., and Gudermann, T. (1999) *Biochemistry* **38**, 12490-12498
169. Herrlich, A., Kuhn, B., Grosse, R., Schmid, A., Schultz, G., and Gudermann, T. (1996) *J Biol Chem* **271**, 16764-16772
170. Liu, G., Duranteau, L., Carel, J. C., Monroe, J., Doyle, D. A., and Shenker, A. (1999) *N Engl J Med* **341**, 1731-1736

171. Rajagopalan-Gupta, R. M., Rasenick, M. M., and Hunzicker-Dunn, M. (1997) *Mol Endocrinol* **11**, 538-549
172. Rajagopalan-Gupta, R. M., Lamm, M. L., Mukherjee, S., Rasenick, M. M., and Hunzicker-Dunn, M. (1998) *Endocrinology* **139**, 4547-4555
173. Shinozaki, H., Fanelli, F., Liu, X., Jaquette, J., Nakamura, K., and Segaloff, D. L. (2001) *Mol Endocrinol* **15**, 972-984
174. Hirakawa, T., and Ascoli, M. (2003) *Endocrinology* **144**, 3872-3878
175. Donadeu, F. X., and Ascoli, M. (2005) *Endocrinology* **146**, 3907-3916
176. Uilenbroek, J. T., and Richards, J. S. (1979) *Biol Reprod* **20**, 1159-1165
177. Muller, J., Gondos, B., Kosugi, S., Mori, T., and Shenker, A. (1998) *J Med Genet* **35**, 340-341
178. Martinelle, N., Holst, M., Soder, O., and Svechnikov, K. (2004) *Endocrinology* **145**, 4629-4634
179. Salvador, L. M., Maizels, E., Hales, D. B., Miyamoto, E., Yamamoto, H., and Hunzicker-Dunn, M. (2002) *Endocrinology* **143**, 2986-2994
180. Dewi, D. A., Abayasekara, D. R., and Wheeler-Jones, C. P. (2002) *Endocrinology* **143**, 877-888
181. Faure, M., Voyno-Yasenetskaya, T. A., and Bourne, H. R. (1994) *J Biol Chem* **269**, 7851-7854
182. Hirakawa, T., and Ascoli, M. (2003) *Mol Endocrinol* **17**, 2189-2200
183. Cameron, M. R., Foster, J. S., Bukovsky, A., and Wimalasena, J. (1996) *Biol Reprod* **55**, 111-119
184. Shiraishi, K., and Ascoli, M. (2007) *Endocrinology* **148**, 3214-3225
185. Shiraishi, K., and Ascoli, M. (2008) *Exp Cell Res* **314**, 25-37
186. Luttrell, D. K., and Luttrell, L. M. (2004) *Oncogene* **23**, 7969-7978
187. Luttrell, L. M., Daaka, Y., and Lefkowitz, R. J. (1999) *Curr Opin Cell Biol* **11**, 177-183
188. Roskoski, R., Jr. (2005) *Biochem Biophys Res Commun* **331**, 1-14
189. Ma, Y. C., Huang, J., Ali, S., Lowry, W., and Huang, X. Y. (2000) *Cell* **102**, 635-646
190. Gu, C., Ma, Y. C., Benjamin, J., Littman, D., Chao, M. V., and Huang, X. Y. (2000) *J Biol Chem* **275**, 20726-20733
191. Yaciuk, P., Choi, J. K., and Shalloway, D. (1989) *Mol Cell Biol* **9**, 2453-2463
192. Schmitt, J. M., and Stork, P. J. (2002) *Mol Cell* **9**, 85-94
193. Obara, Y., Labudda, K., Dillon, T. J., and Stork, P. J. (2004) *J Cell Sci* **117**, 6085-6094
194. Shiraishi, K., and Ascoli, M. (2006) *Endocrinology* **147**, 3419-3427
195. Andric, N., and Ascoli, M. (2008) *Mol Cell Endocrinol* **285**, 62-72
196. Galet, C., and Ascoli, M. (2008) *Cell Signal* **20**, 1822-1829
197. Mizutani, T., Shiraishi, K., Welsh, T., and Ascoli, M. (2006) *Mol Endocrinol* **20**, 619-630
198. Tai, P., Shiraishi, K., and Ascoli, M. (2009) *Endocrinology* **150**, 3766-3773
199. Andric, N., and Ascoli, M. (2008) *Endocrinology* **149**, 5549-5556
200. Carvalho, C. R., Carnevalheira, J. B., Lima, M. H., Zimmerman, S. F., Caperuto, L. C., Amanso, A., Gasparetti, A. L., Meneghetti, V., Zimmerman, L. F., Velloso, L. A., and Saad, M. J. (2003) *Endocrinology* **144**, 638-647
201. Park, J. Y., Su, Y. Q., Ariga, M., Law, E., Jin, S. L., and Conti, M. (2004) *Science* **303**, 682-684
202. Panigone, S., Hsieh, M., Fu, M., Persani, L., and Conti, M. (2008) *Mol Endocrinol* **22**, 924-936
203. Harrison, C., and van der Graaf, P. H. (2006) *J Pharmacol Toxicol Methods* **54**, 26-35
204. Salahpour, A., and Masri, B. (2007) *Nat Methods* **4**, 599-600; author reply 601
205. DeMars, G. (2004) Lipid Raft Mediated Signaling, or How I Learned to Stop Worrying and Love the Controversy. The University of Georgia, Athens, GA
206. Lingwood, D., and Simons, K. (2010) *Science* **327**, 46-50
207. Pin, J. P., Galvez, T., and Prezeau, L. (2003) *Pharmacol Ther* **98**, 325-354
208. Kusuda, S., and Dufau, M. L. (1988) *J Biol Chem* **263**, 3046-3049
209. Crine, P., Aubry, M., and Potier, M. (1984) *Ann N Y Acad Sci* **438**, 224-236
210. Roess, D. A., Horvat, R. D., Munnelly, H., and Barisas, B. G. (2000) *Endocrinology* **141**, 4518-4523
211. Hunzicker-Dunn, M., Barisas, G., Song, J., and Roess, D. A. (2003) *J Biol Chem* **278**, 42744-42749

212. Lei, Y., Hagen, G. M., Smith, S. M., Liu, J., Barisas, G., and Roess, D. A. (2007) *Mol Cell Endocrinol* **260-262**, 65-72
213. Tao, Y. X., Johnson, N. B., and Segaloff, D. L. (2004) *J Biol Chem* **279**, 5904-5914
214. Urizar, E., Montanelli, L., Loy, T., Bonomi, M., Swillens, S., Gales, C., Bouvier, M., Smits, G., Vassart, G., and Costagliola, S. (2005) *EMBO J* **24**, 1954-1964
215. Guan, R., Feng, X., Wu, X., Zhang, M., Zhang, X., Hebert, T. E., and Segaloff, D. L. (2009) *J Biol Chem* **284**, 7483-7494
216. Zhang, M., Feng, X., Guan, R., Hebert, T. E., and Segaloff, D. L. (2009) *Cell Signal* **21**, 1663-1671
217. Fanelli, F. (2007) *Mol Cell Endocrinol* **260-262**, 59-64
218. Guan, R., Wu, X., Feng, X., Zhang, M., Hebert, T. E., and Segaloff, D. L. (2010) *Cell Signal* **22**, 247-256
219. Gesty-Palmer, D., and Luttrell, L. M. (2008) *J Recept Signal Transduct Res* **28**, 39-58
220. Sunahara, R. K., Tesmer, J. J., Gilman, A. G., and Sprang, S. R. (1997) *Science* **278**, 1943-1947
221. Casey, P. J. (1995) *Biochem Soc Trans* **23**, 161-166
222. Ross, E. M. (1995) *Curr Biol* **5**, 107-109
223. Wedegaertner, P. B., Wilson, P. T., and Bourne, H. R. (1995) *J Biol Chem* **270**, 503-506
224. Schoneberg, T., Schultz, G., and Gudermann, T. (1999) *Mol Cell Endocrinol* **151**, 181-193
225. LeVine, H., 3rd. (1999) *Mol Neurobiol* **19**, 111-149
226. Blahos, J., 2nd, Mary, S., Perroy, J., de Colle, C., Brabet, I., Bockaert, J., and Pin, J. P. (1998) *J Biol Chem* **273**, 25765-25769
227. McFadzean, I., Mullaney, I., Brown, D. A., and Milligan, G. (1989) *Neuron* **3**, 177-182
228. Taylor, J. M., Jacob-Mosier, G. G., Lawton, R. G., Remmers, A. E., and Neubig, R. R. (1994) *J Biol Chem* **269**, 27618-27624
229. Lee, C. H., Katz, A., and Simon, M. I. (1995) *Mol Pharmacol* **47**, 218-223
230. Bae, H., Anderson, K., Flood, L. A., Skiba, N. P., Hamm, H. E., and Graber, S. G. (1997) *J Biol Chem* **272**, 32071-32077
231. Bae, H., Cabrera-Vera, T. M., Depree, K. M., Graber, S. G., and Hamm, H. E. (1999) *J Biol Chem* **274**, 14963-14971
232. Krieger-Brauer, H. I., Medda, P. K., Sattel, B., and Kather, H. (2000) *J Biol Chem* **275**, 2486-2490
233. Conklin, B. R., Herzmark, P., Ishida, S., Voyno-Yasenetskaya, T. A., Sun, Y., Farfel, Z., and Bourne, H. R. (1996) *Mol Pharmacol* **50**, 885-890
234. Kostenis, E., Gomeza, J., Lerche, C., and Wess, J. (1997) *J Biol Chem* **272**, 23675-23681
235. Kostenis, E., Degtyarev, M. Y., Conklin, B. R., and Wess, J. (1997) *J Biol Chem* **272**, 19107-19110
236. Kisselev, O., Ermolaeva, M., and Gautam, N. (1995) *J Biol Chem* **270**, 25356-25358
237. Kisselev, O., Pronin, A., Ermolaeva, M., and Gautam, N. (1995) *Proc Natl Acad Sci U S A* **92**, 9102-9106
238. McIntire, W. E., MacCleery, G., and Garrison, J. C. (2001) *J Biol Chem* **276**, 15801-15809
239. Yasuda, H., Lindorfer, M. A., Woodfork, K. A., Fletcher, J. E., and Garrison, J. C. (1996) *J Biol Chem* **271**, 18588-18595
240. West, R. E., Jr., Moss, J., Vaughan, M., Liu, T., and Liu, T. Y. (1985) *J Biol Chem* **260**, 14428-14430
241. Hirsch, J. P., Dietzel, C., and Kurjan, J. (1991) *Genes Dev* **5**, 467-474
242. Kallal, L., and Kurjan, J. (1997) *Mol Cell Biol* **17**, 2897-2907
243. Gilchrist, A., Mazzoni, M. R., Dineen, B., Dice, A., Linden, J., Proctor, W. R., Lupica, C. R., Dunwiddie, T. V., and Hamm, H. E. (1998) *J Biol Chem* **273**, 14912-14919
244. Gilchrist, A., Bunemann, M., Li, A., Hosey, M. M., and Hamm, H. E. (1999) *J Biol Chem* **274**, 6610-6616
245. Gilchrist, A., Li, A., and Hamm, H. E. (2002) *Sci STKE* **2002**, PL1

246. Gilchrist, A., Li, A., and Hamm, H. E. (2002) *Methods Enzymol* **344**, 58-69
247. Gilchrist, A., Vanhauwe, J. F., Li, A., Thomas, T. O., Voyno-Yasenetskaya, T., and Hamm, H. E. (2001) *J Biol Chem* **276**, 25672-25679
248. Dratz, E. A., Furstenau, J. E., Lambert, C. G., Thireault, D. L., Rarick, H., Schepers, T., Pakhlevanians, S., and Hamm, H. E. (1993) *Nature* **363**, 276-281
249. Scheerer, P., Park, J. H., Hildebrand, P. W., Kim, Y. J., Krauss, N., Choe, H. W., Hofmann, K. P., and Ernst, O. P. (2008) *Nature* **455**, 497-502
250. Baneres, J. L., and Parello, J. (2003) *J Mol Biol* **329**, 815-829
251. Digby, G. J., Lober, R. M., Sethi, P. R., and Lambert, N. A. (2006) *Proc Natl Acad Sci U S A* **103**, 17789-17794
252. Bourne, H. R. (1997) *Curr Opin Cell Biol* **9**, 134-142
253. Nobles, M., Benians, A., and Tinker, A. (2005) *Proc Natl Acad Sci U S A* **102**, 18706-18711
254. Bunemann, M., Frank, M., and Lohse, M. J. (2003) *Proc Natl Acad Sci U S A* **100**, 16077-16082
255. Oldham, W. M., Van Eps, N., Preininger, A. M., Hubbell, W. L., and Hamm, H. E. (2007) *Proc Natl Acad Sci U S A* **104**, 7927-7932
256. Iiri, T., Herzmark, P., Nakamoto, J. M., van Dop, C., and Bourne, H. R. (1994) *Nature* **371**, 164-168
257. Cherfils, J., and Chabre, M. (2003) *Trends Biochem Sci* **28**, 13-17
258. Iiri, T., Farfel, Z., and Bourne, H. R. (1998) *Nature* **394**, 35-38
259. Nanoff, C., Koppensteiner, R., Yang, Q., Fuerst, E., Ahorn, H., and Freissmuth, M. (2006) *Mol Pharmacol* **69**, 397-405
260. Cao, J., Panetta, R., Yue, S., Steyaert, A., Young-Bellido, M., and Ahmad, S. (2003) *Bioinformatics* **19**, 234-240
261. Sgourakis, N. G., Bagos, P. G., and Hamodrakas, S. J. (2005) *Bioinformatics* **21**, 4101-4106
262. Insel, P. A., Bourne, H. R., Coffino, P., and Tomkins, G. M. (1975) *Science* **190**, 896-898
263. Horton, R. M., Hunt, H. D., Ho, S. N., Pullen, J. K., and Pease, L. R. (1989) *Gene* **77**, 61-68
264. Bourne, H. R., Coffino, P., and Tomkins, G. M. (1975) *Science* **187**, 750-752
265. Berlot, C. H. (2002) *Methods in Enzymology* **344**, 261-277
266. Wu, C., Narayan, P., and Puett, D. (1996) *J Biol Chem* **271**, 31638-31642
267. Tesmer, J. J., Sunahara, R. K., Gilman, A. G., and Sprang, S. R. (1997) *Science* **278**, 1907-1916
268. Sullivan, K. A., Miller, R. T., Masters, S. B., Beiderman, B., Heideman, W., and Bourne, H. R. (1987) *Nature* **330**, 758-760
269. Lambright, D. G., Noel, J. P., Hamm, H. E., and Sigler, P. B. (1994) *Nature* **369**, 621-628
270. Tesmer, V. M., Kawano, T., Shankaranarayanan, A., Kozasa, T., and Tesmer, J. J. (2005) *Science* **310**, 1686-1690
271. Conklin, B. R., Farfel, Z., Lustig, K. D., Julius, D., and Bourne, H. R. (1993) *Nature* **363**, 274-276
272. Palm, D., Munch, G., Malek, D., Dees, C., and Hekman, M. (1990) *FEBS Lett* **261**, 294-298
273. D'Ursi, A. M., Giusti, L., Albrizio, S., Porchia, F., Esposito, C., Caliendo, G., Gargini, C., Novellino, E., Lucacchini, A., Rovero, P., and Mazzoni, M. R. (2006) *Mol Pharmacol* **69**, 727-736
274. Mazzoni, M. R., Taddei, S., Giusti, L., Rovero, P., Galoppini, C., D'Ursi, A., Albrizio, S., Triolo, A., Novellino, E., Greco, G., Lucacchini, A., and Hamm, H. E. (2000) *Mol Pharmacol* **58**, 226-236
275. Feldman, D. S., Zamah, A. M., Pierce, K. L., Miller, W. E., Kelly, F., Rapacciuolo, A., Rockman, H. A., Koch, W. J., and Luttrell, L. M. (2002) *J Biol Chem* **277**, 28631-28640
276. Angelova, K., Narayan, P., and Puett, D. (2003) *Mol Cell Endocrinol* **204**, 1-9
277. Thompson, J. D., Higgins, D. G., and Gibson, T. J. (1994) *Nucleic Acids Res* **22**, 4673-4680
278. Larkin, M. A., Blackshields, G., Brown, N. P., Chenna, R., McGettigan, P. A., McWilliam, H., Valentin, F., Wallace, I. M., Wilm, A., Lopez, R., Thompson, J. D., Gibson, T. J., and Higgins, D. G. (2007) *Bioinformatics* **23**, 2947-2948



279. Pantaloni, C., and Audigier, Y. (1993) *J Recept Res* **13**, 591-608
280. Grieco, P., Albrizio, S., D'Ursi, A. M., Giusti, L., Mazzoni, M. R., Novellino, E., and Rovero, P. (2003) *Eur J Med Chem* **38**, 13-18
281. Dupre, D. J., Robitaille, M., Ethier, N., Villeneuve, L. R., Mamarbachi, A. M., and Hebert, T. E. (2006) *J Biol Chem* **281**, 34561-34573
282. Wall, M. A., Coleman, D. E., Lee, E., Iniguez-Lluhi, J. A., Posner, B. A., Gilman, A. G., and Sprang, S. R. (1995) *Cell* **83**, 1047-1058
283. Grishina, G., and Berlot, C. H. (1997) *J Biol Chem* **272**, 20619-20626
284. Berlot, C. H., and Bourne, H. R. (1992) *Cell* **68**, 911-922
285. Evanko, D. S., Thiagarajan, M. M., and Wedegaertner, P. B. (2000) *J Biol Chem* **275**, 1327-1336
286. Schwindinger, W. F., Miric, A., Zimmerman, D., and Levine, M. A. (1994) *J Biol Chem* **269**, 25387-25391
287. D'Ursi, A. M., Albrizio, S., Greco, G., Mazzeo, S., Mazzoni, M. R., Novellino, E., and Rovero, P. (2002) *Journal of Peptide Science* **8**, 476-488
288. Hebert, T. E., Gales, C., and Rebois, R. V. (2006) *Cell Biochem Biophys* **45**, 85-109
289. Rebois, R. V., and Hebert, T. E. (2003) *Receptors Channels* **9**, 169-194
290. Terrillon, S., and Bouvier, M. (2004) *EMBO Rep* **5**, 30-34
291. Lohse, M. J. (2006) *Nat Methods* **3**, 972-973
292. Rizzo, M. A., Springer, G. H., Granada, B., and Piston, D. W. (2004) *Nat Biotechnol* **22**, 445-449
293. Mitra, R. D., Silva, C. M., and Youvan, D. C. (1996) *Gene* **173**, 13-17
294. Tsien, R. Y. (1998) *Annu Rev Biochem* **67**, 509-544
295. Vidi, P. A., Chen, J., Irudayaraj, J. M., and Watts, V. J. (2008) *FEBS Lett* **582**, 3985-3990
296. Vidi, P. A., Chemel, B. R., Hu, C. D., and Watts, V. J. (2008) *Mol Pharmacol* **74**, 544-551
297. Hynes, T. R., Tang, L., Mervine, S. M., Sabo, J. L., Yost, E. A., Devreotes, P. N., and Berlot, C. H. (2004) *J Biol Chem* **279**, 30279-30286
298. Takida, S., and Wedegaertner, P. B. (2003) *J Biol Chem* **278**, 17284-17290
299. Xia, Z., and Liu, Y. (2001) *Biophys J* **81**, 2395-2402
300. Shimosono, S., and Miyawaki, A. (2008) *Methods Cell Biol* **85**, 381-393
301. Audet, N., Gales, C., Archer-Lahlou, E., Vallieres, M., Schiller, P. W., Bouvier, M., and Pineyro, G. (2008) *J Biol Chem* **283**, 15078-15088
302. Milligan, G., and Bouvier, M. (2005) *FEBS J* **272**, 2914-2925
303. Azpiazu, I., and Gautam, N. (2004) *J Biol Chem* **279**, 27709-27718
304. Philip, F., Sengupta, P., and Scarlata, S. (2007) *J Biol Chem* **282**, 19203-19216
305. Ganpat, M. M., Nishimura, M., Toyoshige, M., Okuya, S., Pointer, R. H., and Rebois, R. V. (2000) *Cell Signal* **12**, 113-122
306. Kremers, G. J., Goedhart, J., van Munster, E. B., and Gadella, T. W., Jr. (2006) *Biochemistry* **45**, 6570-6580
307. Koushik, S. V., Chen, H., Thaler, C., Puhl, H. L., 3rd, and Vogel, S. S. (2006) *Biophys J* **91**, L99-L101
308. Nagai, T., Ibata, K., Park, E. S., Kubota, M., Mikoshiba, K., and Miyawaki, A. (2002) *Nat Biotechnol* **20**, 87-90
309. Day, R. N., Booker, C. F., and Periasamy, A. (2008) *J Biomed Opt* **13**, 031203
310. Roess, D. A., and Smith, S. M. (2003) *Biol Reprod* **69**, 1765-1770
311. Damaj, B. B., McColl, S. R., Mahana, W., Crouch, M. F., and Naccache, P. H. (1996) *J Biol Chem* **271**, 12783-12789
312. Gu, Y. Z., and Schonbrunn, A. (1997) *Mol Endocrinol* **11**, 527-537
313. Mukhopadhyay, S., McIntosh, H. H., Houston, D. B., and Howlett, A. C. (2000) *Mol Pharmacol* **57**, 162-170
314. Shraga-Levine, Z., and Sokolovsky, M. (2000) *Cell Mol Neurobiol* **20**, 305-317
315. Segaloff, D. L. (2007).

316. Albrizio, S., Caliendo, G., D'Errico, G., Novellino, E., Rovero, P., and D'Ursi, A. M. (2005) *J Pept Sci* **11**, 617-626
317. Varshavsky, A. (1997) *Genes Cells* **2**, 13-28
318. Garcia, P. D., Onrust, R., Bell, S. M., Sakmar, T. P., and Bourne, H. R. (1995) *EMBO J* **14**, 4460-4469
319. Chang, M., Zhang, L., Tam, J. P., and Sanders-Bush, E. (2000) *J Biol Chem* **275**, 7021-7029
320. Linder, M. E. (1999) Expression and Purification of G Protein Alpha Subunits in *Escherichia Coli*. in *G Proteins: Techniques of Analysis* (Manning, D. R. ed.), CRC Press, Boca Raton, FL. pp 1-22
321. Homola, J. (2003) *Anal Bioanal Chem* **377**, 528-539
322. Kang, H., Lee, W. K., Choi, Y. H., Vukoti, K. M., Bang, W. G., and Yu, Y. G. (2005) *Biochem Biophys Res Commun* **329**, 684-692
323. Hruby, V. J., and Tollin, G. (2007) *Curr Opin Pharmacol* **7**, 507-514
324. Tollin, G., Salamon, Z., Cowell, S., and Hruby, V. J. (2003) *Life Sci* **73**, 3307-3311
325. Tollin, G., Salamon, Z., and Hruby, V. J. (2003) *Trends Pharmacol Sci* **24**, 655-659
326. Komolov, K. E., Senin, II, Philippov, P. P., and Koch, K. W. (2006) *Anal Chem* **78**, 1228-1234
327. Northup, J. (2004) *Methods Mol Biol* **261**, 93-112
328. Linder, M. E., Middleton, P., Hepler, J. R., Taussig, R., Gilman, A. G., and Mumby, S. M. (1993) *Proc Natl Acad Sci U S A* **90**, 3675-3679
329. Kuliopulos, A., and Covic, L. (2003) *Life Sci* **74**, 255-262
330. Harrison, C., and Traynor, J. R. (2003) *Life Sci* **74**, 489-508
331. Ascoli, M. (2003).
332. Krumins, A. M., and Gilman, A. G. (2006) *J Biol Chem* **281**, 10250-10262
333. Svoboda, P. (2007) *Curr Opin Mol Ther* **9**, 248-257

## APPENDIX

The following poster, submitted to the 18<sup>th</sup> Annual Symposium of the Protein Society, San Diego, CA, August 2004, represents original work that was begun as a requirement for the admission to Doctoral Candidacy in the Spring of 2004. Novel models of the human leucine-rich repeat-containing G Protein Coupled Receptors extracellular domains were created after sequence alignment, protein threading, and homology modeling were performed as described.

